Identification of Regions Required for CDCA7 Interaction with DNA Damage Repair Machinery

Shaina Jaff

A thesis submitted to the Faculty of Graduate Studies

In partial fulfillment of the requirements for the degree of

Master of Science

Graduate Program in Biology

York University

Toronto, Ontario

August, 2023

© Shaina Jaff, 2023

Abstract

CDCA7 (Cell Division Cycle Associated Protein 7) is a transcription factor protein that binds to DNA and histone modifying enzymes supporting DNA methylation and contributes to repair of double stranded breaks in DNA. Mutations of the *cdca7* gene cause ICF (Immunodeficiency, centromeric instability, and facial abnormalities) syndrome. CDCA7 has been shown to bind with HELLS (Helicase, lymphoid specific) as a bipartite nucleosome remodeller to allow for *de novo* methylation by DNMT3b (DNA methyl transferase 3b). Additionally, CDCA7 associates with Ku70 and Ku80, proteins essential for DNA damage repair via the Non-Homologous End Joining (NHEJ) pathway, and γ-H2AX, whose accumulation is facilitated by Ku proteins and is a biomarker of DNA damage. I show here that CDCA7 requires a putative leucine zipper for association with HELLS, while the binding of 14-3-3 at a phosphorylated residue in CDCA7 regulates Ku70/80 and γ-H2AX association. This study further elucidates the mechanism of how CDCA7 plays a crucial role in maintaining genomic stability by participating in various DNA repair processes and DNA methylation.

Dedication and Acknowledgements

This work would not have been possible without the help of so many people, who all deserve more than just slight acknowledgement at the start of my thesis, but for now this will have to suffice. First and foremost, I must acknowledge Dr. Michael Scheid who has spent tireless and endless days and nights supporting me from the beginning of the summer before my honour's thesis experience, up until now. I have always felt I can reach out to you for help in any and all crises, and you have taught me to troubleshoot with kindness and generosity. You made a mediocre student become deserving of recommendation of distinction, and I cannot thank you enough for the opportunity you gave me.

Thank you to Dr. Mark Bayfield, for all of your time and energy spent as my co-supervisor on my committee. I really took all of your kind feedback and used it to improve from early amateur work to become deserving of your high praise at the culmination of this project, which will fuel me and motivate me in my studies for years to come.

Secondly, I must thank Baodong Wu, David Miller, Ghazal Nehemi, and Rachel Corridore. Baodong for teaching everything to me, for David for reminding me and teaching me protocols and techniques, for Ghazal for filling in the gaps, and to Rachel for reteaching me everything when I returned from maternity leave. I could not have gotten to this milestone without you.

To Gagan and Becky! I could not have made it through the hard parts without your motivation and fun. You made my last year in Dr. Scheid's lab better than I ever expected. I loved tennis Tuesdays that became Wednesdays, and I loved our fan fiction talks that kept me motivated through my writing.

And finally, I must thank my family. To my sister, Ashira Perez for motivating me forever, I loved learning sciences with you. To my parents, Dr. Paul and Dr. Leandra Forman, for helping and supporting my dreams and listening whenever I talked your ear off about my science. To my loving and supportive husband Uriel Jaff, who supported me not only financially but also emotionally all these years, who still has no idea what I did for three years on those late nights you supported me from afar and close, but perhaps now will know a little bit more if you read this. And to my son, Benny, for who everything I do is to make the world a better place for you.

Table of Contents

List of Tables

List of Figures

List of Abbreviations

AKT	Also known as protein kinase B
ATM	Ataxia telangiectasia mutated
CDCA7	Cell division associated protein 7
DDR	DNA damage response
DNA	Deoxyribonucleic acid
DNMT	DNA methyl transferase
DSB's	Double stranded breaks
HELLS	Helicase, lymphoid specific
HR	Homologous recombination
IP	Immunoprecipitation
ICF Syndrome	Immunodeficiency, centromeric abnormalities, facial anomalies syndrome
Ku80/70	Ku protein 80 and 70 complex
mRNA	Messenger RNA (ribonucleic acid)
Myc	Myelocytomatosis, also known as c-Myc
NHEJ	Non homologous end-joining
γ-H2AX	phosphorylated-Histone 2AX
14-3-3	Name of protein "14-3-3"

Chapter 1: Introduction and Research Objectives

Cancer.

Cancer is a debilitating disease characterized by cells acquiring genetic mutations resulting in dysregulated growth and metastasis. Cancer is the second most common cause of death in children and adults in the world (Mattiuzzi et al., 2019). Its epidemiology, pathology, and morphology, usually resembling the original mutated tissue, has been studied immensely (Barletta, 2014; Miwa et al., 2023; Tomoka et al., 2018). Advances in cancer detection has allowed for diagnosis and identification of specific types and stages to predict prognoses and different treatment outcomes (Carriaga et al., 1995; Mobadersany et al., 2018; Woo et al., 2022; Avery et al., 2022). However, the underlying molecular basis and origins of various cancer types is complex. Even though cancers present morphologically similar in the same tissue types, the underlying cause can be different. Investigating the basis of different cancer genetics as well as epigenetics will allow for improved treatments and outcomes to specific cancers.

Signaling pathways critical for human development contain many components including tumour suppressors and oncogenes, genes that are required for regular cell division and maintenance but are genetically modified in cancer. Elucidating these key components is key to understanding the molecular basis of cancers. The Wnt, TFGB, Notch, and RTK pathways among others contain many signaling proteins. These proteins include but are not limited to genes such as Ras, p53, and Myc that are genetically mutated as either overstimulated or show diminished activity in a multitude of cancers and provide a heterogeneous molecular basis for cancers that look similar histologically and pathologically (Malone et al., 2020). These genes are critical for cell cycle control and progression from one stage of the cell cycle to the next, and

when they are disrupted or misregulated, cause cancer (Kumar et al., 2023). Genomic profiles using microarray technologies correlate with vastly studied pathological and epidemiological studies of cancers and may provide a route to understand the molecular and genetic basis of different cancers (Gilbertson, 2011; Malone et al., 2020).

PI3K/AKT Pathway.

The PI3K/AKT/MTOR (Phosphatidylinositol 3-kinase/protein kinase B/mechanistic target of rapamycin) pathway is a transduction cell signaling pathway in the human cell (Hemmings et al., 2012; Gill et al., 2013). This pathway is critical for growth, apoptosis, maintenance, proliferation, cell cycle progression, apoptosis and inhibition, and other regulatory cell processes (Hemmings et al., 2012). It is particularly involved in regulation, growth, and differentiation of adult stem cells. Overexpression of growth factor stimulants or mutation of components of this pathway results in various cancers (Liang et al., 2003). Several inhibitors of components of this pathway have been supported by the FDA and dozens of proteins in this pathway have been assessed in clinical trials and applied as anticancer agents (Li et al., 2022).

In the PI3K pathway, growth factors or oncogenes such as the insulin receptor tyrosine kinase (InsR), the related insulin-like growth factor 1 receptor (IGF-1R), Epidermal growth factor (EGF), or Platelet-derived growth factor receptors (PDGF-R), bind to receptor tyrosine kinases (RTKs) that dimerize and autophosphorylate themselves at their cytoplasmic domains, causing a cell-signaling cascade (Gill et al., 2013; Hemmings et al., 2012; Li et al., 2022). These phosphorylated residues recruit PI3K to the cell membrane, converting phosphatidylinositol-4,5-biphosphase (PIP2) to phosphatidylinositol-3,4,5-triphosphase (PIP3) (Hemmings et al., 2012; Gill et al., 2013). PIP3 recruits phosphoinositide-dependent kinase 1 (PDK1) (Hemmings et al., 2012; Gill et al., 2013).

Recruitment of AKT to the plasma membrane by PIP3 leads to its phosphorylation on two key sites, Thr308 in AKT's activation loop by PDK1 and Ser473 in the regulatory C-tail by mTORC2 (Alessi et al., 1997). The Thr308 and Ser473 phosphorylation events (pT308 and pS473) stimulate Akt kinase activity by relieving autoinhibition (Manning et al., 2017). Activated AKT then translocates to the nucleus and phosphorylates target proteins (Cohen et al., 1997).

AKT.

The ser/thr protein kinase AKT is involved in many of the biological effects of the PI3K pathway including cell proliferation, survival, and cellular responses to insulin and nutrients. Mutated oncogene AKT is frequently hyperactivated in human cancers and is therefore a potential anticancer and therapeutic target as a downstream target of the PI3K pathway (Bae et al., 2022; Li et al., 2022). AKT phosphorylates its substrates at serine/threonine residues residing in the consensus motif RXRXXS/T. Phosphorylation and dephosphorylation of AKT regulates AKT-dependent behaviour and subsequent affects (Lorusso et al., 2016). AKT regulates MYC, an important tumour suppressor.

MYC.

A protooncogene myelocytomatosis (Myc) gene, known as cellular-Myc (c-Myc) encodes the Myc protein. MYC is a transcription factor highly regulated by various epigenetic factors and pathways and is implicated in more than 70% of known cancers. MYC is known to participate in various cellular processes such as cytoskeletal regulation, DNA replication, DNA transcription, protein synthesis, angiogenesis, immune response, cell metabolism, cell growth,

and apoptosis (Dang et al., 2012). In non-cancerous cells, MYC expression is activated by growth factors through activation of enhancers.

The MYC protein, whose translation is enhanced by activated mTOR, a component of the PI3K pathway, dimerizes with transcription factor MAX through a basic helix loop helix domain to form a heterodimer (Blackwood et al., 1991). This complex then binds directly to DNA and activates transcription of genes containing high affinity E-boxes. Upon nutrient shortage or hypoxia, MYC translation, protein stability, and MYC/MAX dimerization is inhibited. As a downstream target of AKT, FOXO3a proteins counteract MYC activation (Amati et al., 1993; Coller et al., 2000; Dang et al., 2012).

Microarray analysis was used to identify novel targets of MYC, however their function remains to be understood (Dang et al., 2012). Candidate genes were subjected to chromatin immunoprecipitation (ChIP) to determine which gene promoters were enriched with MYC. 89 genes were identified, and 27 of those were of unknown function. The most differentially expressed gene was named *JP01* (Prescott et al., 2001).

CDCA7.

CDCA7 was originally discovered as *JP01* as a direct target gene of MYC that does not require an intermediate protein (Prescott et al., 2001), and is a downstream target of the PI3K (Phosphatidylinositol 3-kinase) pathway (Figure 2.1.). The nomenclature committee adopted the name of CDCA7 for JP01 since its expression peaks around the G1/S transition of the cell cycle and will be referred to as CDCA7 hereafter (Whitfield, et al., 2002).

The CDCA7 (Cell division cycle associated protein 7) gene consists of nine exons encoding a 47 kilo-Dalton (kDa) and 371 amino acid protein shown in Figure 2.1 (Gill et al., 2013). The expressed protein contains a putative N-terminal Leucine Zipper domain, a Nuclear

Localization Site, a highly acidic "E" region, and a C-terminal domain containing four CXXC-type zinc finger motifs known as the Zinc Finger domain (Gill et al., 2013). The nuclear localization site is bound by 14-3-3 when CDCA7 is phosphorylated by AKT (Gill et al., 2013). The "E region" of CDCA7 is critical for interaction with the microtubule spindle assembly protein TPX2 (Pariel, et al., 2018). The C-terminal domain containing a "Zinc Finger" is necessary for CDCA7 to bind to DNA, and is common to transcription factors (Laity et al., 2001). The N-terminal domain contains a coiled coil leucine region with multiple leucines or isoleucines spaced at 7 amino acids intervals through an alpha helix, suggesting the ability for CDCA7 to homo or heterodimerize (O'Neil et al., 1990). This gene was observed as participating in c-Myc responsive neoplastic transformation and tumorigenesis in Rat1a cells (Prescott et al., 2001).

CDCA7 is a gene involved in causing tumorigenesis through various cell signaling pathways. It has been implicated in many cancers including but not limited to esophageal squamous cell carcinoma, hepatocellular carcinoma, and ovarian cancer (Li et al., 2023; Tian et al., 2023; Cai et al., 2021). This novel target offers a promising avenue for therapeutically addressing distinct cancer types.

14-3-3 Adapter Proteins.

14-3-3 adapter protein is a 30 kDa protein involved in protein trafficking, cell-cycle control, apoptosis, autophagy and other cell signal transduction pathways, as well as innate immunity and viral infection. These proteins are highly conserved in mammals, and there are 7 subtypes ((α/β, γ, ε, η, σ, τ [also called θ] and ζ/δ)) (Chaudri et al., 2003). The N-terminal domain binds to membranes, while the C-terminal domain binds to other proteins (Fu et al., 2000). Several hundred proteins have been identified as binding to 14-3-3 adapter proteins. (Ballone et

al., 2018). Their recognition sequences are diverse, indicating their diverse role in the cell, however most ligands have conserved phosphorylated serine (Ser)/threonine (Thr) sequence motifs (Coblitz et al., 2006).

The 14-3-3 phospho adapter proteins have many different capabilities. They can regulate transcription factors in cell cycle, for example FOXO. FOXO is a transcription factor belonging to the forkhead family with characteristic pterygoid spiral DNA-binding domains (Kloet et al., 2015). The PI3K/AKT pathway is the main upstream pathway that regulates FOXO1. Binding of FOXO to 14-3-3 results in loss of FOXO's transcriptional activity and its role in regulating the cell cycle (Tzivion et al., 2011).

Furthermore, 14-3-3 proteins can control cell division related proteins' activity. For example, they bind to cell division cycle 25A (CDC25A) at Ser178 and Thr507, which are phosphorylated by CHK1 to block the interaction between CDC25A and cyclin-dependent kinase 2 (CDK2), and then retard entry of cells into S phase (Furnari et al., 1997).

Additionally, 14-3-3 proteins regulate nuclear–cytoplasm protein shuttling. The nuclear export signal is highly conserved in 14-3-3 sequences. Binding with 14-3-3 proteins will hide the nuclear localization sequence (NLS) in the ligands and then regulate their function (Liu et al., 2021). For example, Caspase-2 is an apical protease involved in proteolysis of the cell substrate and is directly involved in the apoptosis signaling cascade, and is the only known caspase to shuttle through the nucleus, and this shuttling is facilitated by 14-3-3 (Kalabova et al., 2017). When Caspase-2 is phosphorylated, its NLS signal is obscured by its rigid binding by 14-3-3 and prevents Caspase-2 activity (Kalabova et al., 2017).

These are just some of the many examples of how 14-3-3 functions to control and regulate various processes in the cell by binding with various factors to regulate their activity.

This published literature describing the role of 14-3-3 binding to phosphorylated Serine or Threonine sites to regulate the cell cycle and activity of cell division related proteins, membrane trafficking of various proteins, and regulate transcription factor activity led to the investigation of potential interaction with *CDCA7*, a cell division cycle associated transcription factor protein.

AKT and 14-3-3 regulate CDCA7 interaction with MYC.

The MYC binding region on CDCA7 was mapped to Threonine 163 on CDCA7 and was established as critical for CDCA7-MYC mediated apoptosis (Gill et al., 2013). Knockdown of CDCA7 rescued cells from MYC-dependent apoptosis following removal from serum (Gill et al., 2013). Using immunoprecipitation experiments, it was determined expressed CDCA7 coimmunoprecipitates with endogenous 14-3-3 when phosphorylated at this same T163 site by AKT. These results indicated a feed-forward loop; MYC activation upregulates CDCA7, with AKT phosphorylation activity controlling the accessibility of CDCA7 to nuclear MYC via 14-3-3 binding to phosphorylated T163 on CDCA7 (Gill et al., 2013).

MYC binds to CDCA7 in the nucleus at the threonine 163 site. When the PI3K pathway is activated and AKT translocates into the cell phosphorylating CDCA7 at T163, CDCA7 is bound by 14-3-3 masking CDCA7's NLS (nuclear localization signal). CDCA7 is sequestered by 14-3-3 from the nucleus to the cytoplasm, and therefore disassociated from MYC (Johnson et al., 2010; Gill et al., 2013). This AKT phosphorylation T163 site of CDCA7 therefore regulates MYC-dependent apoptosis and determines whether CDCA7 will bind to MYC or to 14-3-3, regulating its transcriptional activity at the level of the nucleus and MYC-dependent apoptosis (Gill et al., 2013). MYC activation upregulates CDCA7, with AKT phosphorylation activity

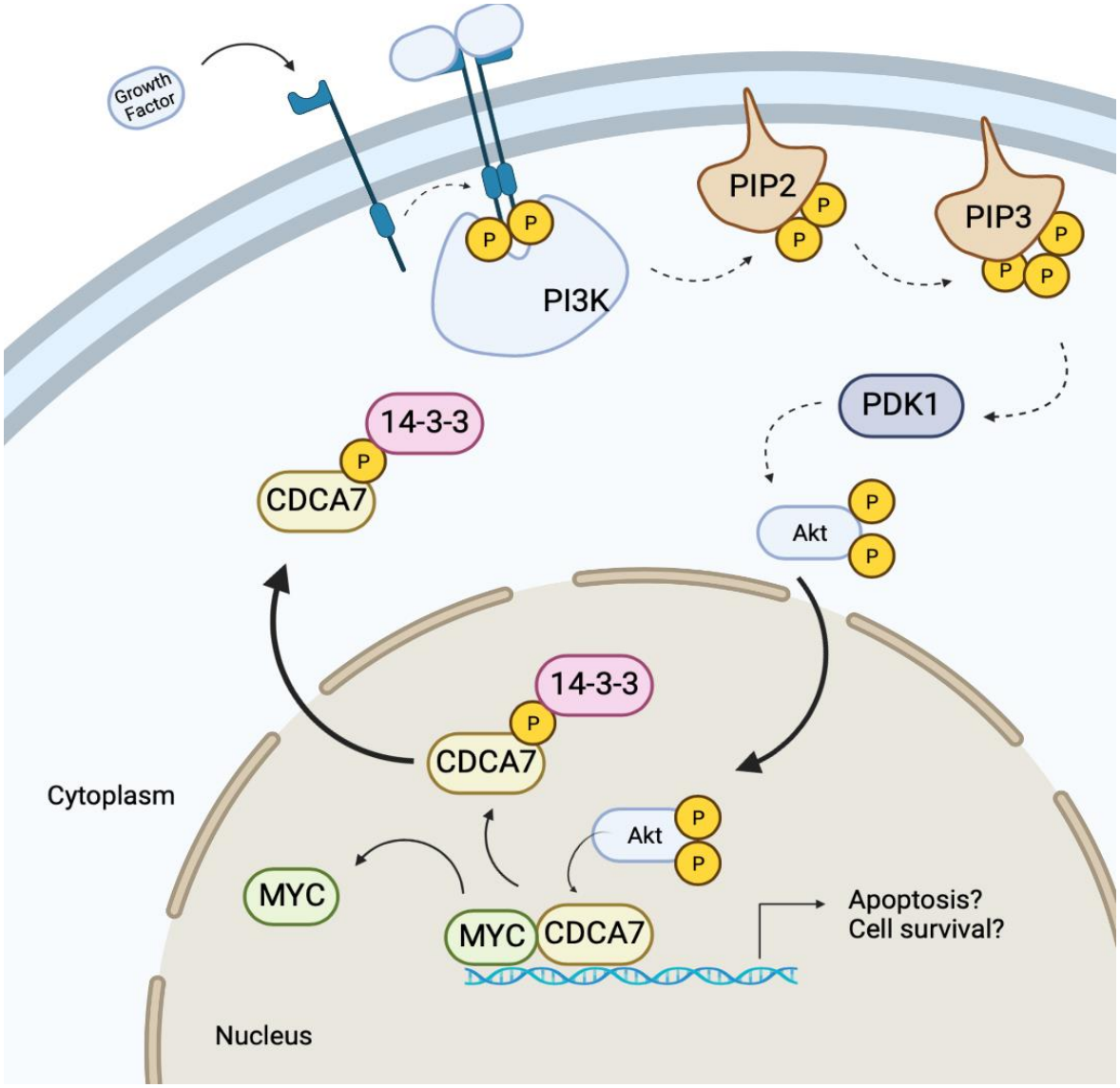

Figure 1.1. The PI3K (Phosphatidylinositol 3-kinase) pathway is a transduction cell signaling pathway. This pathway is critical for growth, apoptosis, maintenance, proliferation, and other regulatory cell processes, and disruptions of this pathway result in cancers (Hemmings et al., 2012). In the PI3K pathway, growth factors bind to receptor tyrosine kinases (RTKs) that dimerize and autophosphorylate themselves at their cytoplasmic domains, causing a cell-signaling cascade (Gill et al., 2013; Hemmings et al., 2012). These phosphorylated residues recruit PI3K to the cell membrane, converting phosphatidylinositol-4,5-biphosphase (PIP2) to phosphatidylinositol-3,4,5-triphosphase (PIP3) (Hemmings et al., 2012; Gill et al., 2013). PIP3 recruits phosphoinositide-dependent kinase 1 (PDK1) activating AKT (Hemmings et al., 2012; Gill et al., 2013). Activated AKT then translocates to the nucleus and phosphorylates target proteins, including CDCA7 (Cohen et al., 1997; Gill et al., 2013).MYC, an important transcription factor and proto-oncogene, binds to CDCA7 in the nucleus at the threonine 163 site, but when the PI3K pathway is activated and AKT translocates into the cell phosphorylating CDCA7 at T163, CDCA7 and MYC disassociate (Gill et al., 2013). Phosphorylated CDCA7 is instead bound at the phosphorylated T163 site by 14-3-3 masking CDCA7's NLS (nuclear localization signal), resulting in the translocation of CDCA7 from the nucleus to the cytoplasm (Johnson et al., 2010; Gill et al., 2013). This AKT phosphorylation T163 site of CDCA7 therefore regulates MYC-dependent apoptosis and determines whether CDCA7 will bind to MYC or to 14-3-3 (Gill et al., 2013).

controlling the accessibility of CDCA7 to nuclear MYC via 14-3-3 binding to phosphorylated T163 on CDCA7 (Gill et al., 2013) (Figure 1).

ZBTB24.

CDCA7 is transcriptionally regulated by ZBTB24. ZBTB24 encodes a protein with a BTB (Broad-Complex, Tramtrack and Bric A Brac**)** domain, an AT hook, and eight C2H2-type zinc finger motifs (Unoki et al., 2019). A ZBTB24 BTB domain deletion mouse showed loss of functional ZBTB24 leads to early embryonic lethality (Wu et al., 2016). *Cdca7* was identified as the most negatively regulated gene in *Zbtb24* homozygous mutant mESCs. ZBTB24 was enriched at the *CDCA7* promoter showing ZBTB24 functions as a transcription factor directly controlling *Cdca7* expression (Wu et al., 2016). Further experiments showed ZBTB24 binds to the 12-bp consensus sequence [CT(G/T)CCAGGACCT] at the CDCA7 promoter to transcriptionally activate CDCA7 (Ren et al., 2019). This illustrates the relationship between ZBTB24 and CDCA7, and how it is defective in ICF syndrome. An additional protein mutated in ICF syndrome is HELLS.

HELLS.

CDCA7 recruits HELLS to chromatin to allow for methylation of the genome (Jennes et al., 2018). The HELLS (helicase, lymphoid specific) gene encodes an approximately 95 kDa protein. Four important domains include an N-terminal coiled coil region at amino acids 30-115, helicase ATP binding domain at amino acids 235-403, a DEAH box motif at aa's 354-357, and a C-terminal Helicase domain at amino acids 603-767. It functions as a helicase and Snf2-like ATP -dependent chromatin remodeling enzyme that interacts with DNMT3b to open histone H1-containing heterochromatin (Kollarovic et al., 2020).

HELLS is a SNF2 ATPase family protein, required for *de novo* DNA methylation of repetitive elements and developmentally programmed genes through interaction with DNMT3b (Zhu et al., 2006). HELLS also promotes the efficient repair of DNA double-strand breaks (DSBs) (Burrage et al., 2012). Murine embryonic fibroblasts with a *HELLS* mutation display excessive numbers of centrosomes and abnormal mitosis, and mouse mutants homozygous for a *HELLS* deletion die soon after birth while their hematopoietic cells poorly contribute to T and B cells in recipient mice (Fan et al., 2003; Geiman et al., 2001).

The literature describes how ZBTB24, CDCA7 and HELLS work together to allow for *de novo* methylation by DNMT3b. ZBTB24 binds to the promoter of *CDCA7* and transcriptionally regulates CDCA7 (Ren et al., 2019; Wu et al., 2016). CDCA7 in turn recruits HELLS, and secondly, CDCA7 acts to stimulate HELLS ATP dependent nucleosome remodeling activity. CDCA7 and HELLS together act as a bipartite nucleosome remodeling complex (Jenness et al., 2018). This allows for recruitment of and *de novo* methylation by DNMT3b at centromeric and pericentromeric repeats to provide genome stability and prevent multiradial breaks and abnormal chromosome configurations as demonstrated in ICF syndrome (Ren et al., 2019; Thijssen et al., 2015; Toubiana et al., 2018; Jenness et al., 2018).

ICF Syndrome.

ICF (immunodeficiency, centromeric instability, and facial abnormality) syndrome is a rare autosomal recessive disease characterized by facial dysmorphism, recurrent infections, centromeric instability and hypomethylation (Ehrlich et al., 2006; Unoki et al., 2019).
This disease is associated with immunodeficiency; ICF patients possess naive B cells but lack mature B cells in the peripheral blood (Blanco-betancourt et al., 2004). Serum levels of IgG,

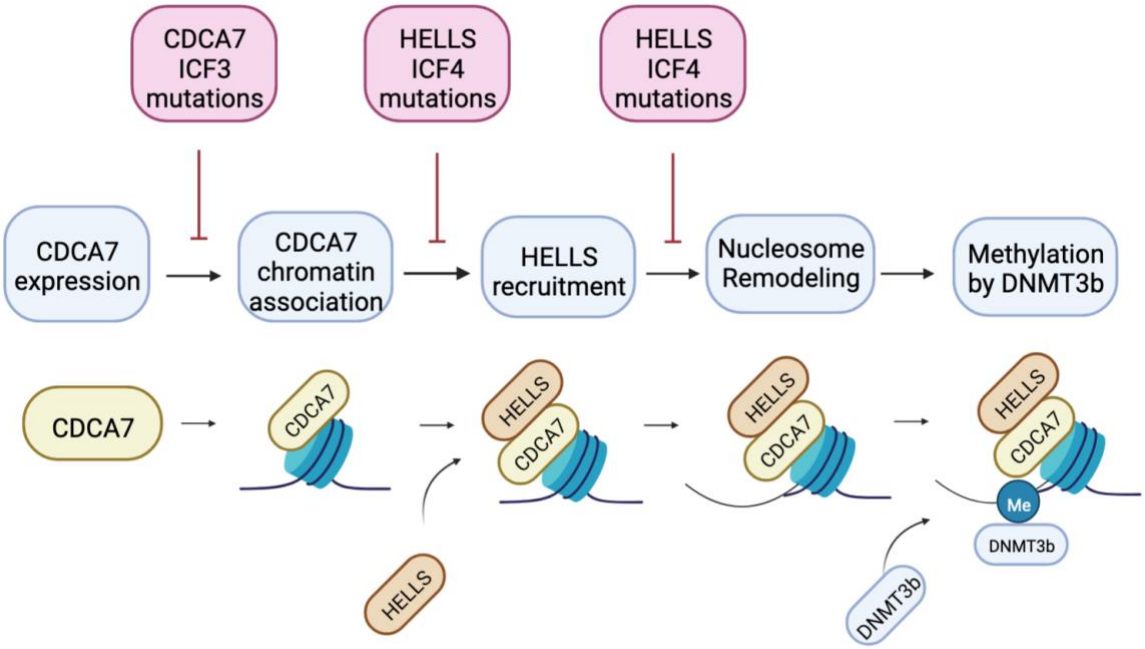

Figure 1.2. CDCA7, an important transcription factor, and HELLS, helicase lymphoid specific, SWI/snf chromatin remodeler, work together as a bipartite nucleosome remodeling complex to allow for *de novo* methylation by DNMT3b. This allows for epigenetic regulation of genes during embryonic development and provides stability to centromeric and pericentromeric regions of chromosomes. This process is misregulated when CDCA7 and HELLS are mutated causing ICF (Immunodeficiency, centromeric instability, and facial anomalies) syndromes type 3 and 4, respectively. (Adapted from Jenness et al., 2018).

IgM, IgE, and/or IgA are low, although the type of immunoglobulin deficiency is variable. Recurrent infections are the presenting symptom, usually in early childhood. Other variable symptoms of this probably under-diagnosed syndrome include mild facial dysmorphism, growth retardation, failure to thrive, and psychomotor retardation (Ehrlich et al., 2006; Unoki et al., 2019).

At the cellular level, this syndrome expresses centromeric instability manifesting as stretched heterochromatin, chromosome breaks, and multiradial configurations involving the centromeric regions of chromosomes 1, 9, and 16 in activated lymphocytes (Maraschio et al., 1988). ICF always involves limited hypomethylation of DNA (Ehrlich et al., 2006; Unoki et al., 2019).

This disease is associated with mutations in *DNMT3b* (DNA methyl transferase 3 b) in ICF1, *ZBTB24* in ICF2, *HELLS* in ICF3, in *CDCA7* in ICF4, and an unknown genetic basis for ICFX respectively (Thijssen et al., 2015; de Greef et al., 2011). In ICF type 1, DNMT3b is mutated, and in ICF1 cells, a phenotype of CG hypomethylation is observed in pericentromeric repeats and subtelomeric regions. In the remaining identified types of 2, 3, 4, and unidentified X, ICF patients show hypomethylation in pericentromeric repeats and centromeric α-satellite repeats, but not in subtelomeric regions (Jiang et al., 2005; Toubiana et al., 2018). These subtelomeric expanses are often abnormally short and susceptible to DNA damage (Smeets et al., 1994; Unoki et al., 2016; Sagie et al., 2017). The ways in which these genes relate to each other and are defective in ICF syndrome resulting in their phenotypes demonstrate their dependent relationship and how they ultimately facilitate *de novo* methylation by *DNMT3b* and their critical role in providing genome stability and gene regulation.

Epigenetics and Methylation.

Epigenetics is the study of heritable changes in gene activity or function that is not associated with any change of the DNA sequence itself (Moore et al., 2013). Any external post-translational modification (PTM) that does not involve a deletion, insertion, translocation, or substitution to the actual gene itself is an epigenetic affect. These include PTM's such as phosphorylation and methylation. PTM's are critical in regulatory proteins in cellular processes such as localization, activity, and protein-protein interactions. When these PTM's malfunction or are not present, this results in disease phenotypes (Moore et al., 2013; Wang et al., 2017).

One example is phosphorylation, which plays a critical role in many biological processes. Phosphorylation is the addition of a phosphate group by a kinase to a molecule or protein. Proteins are most generally phosphorylated at a Tyrosine, Serine, or Threonine residue. Protein kinases are characterized by their enzymatic ability to catalyze the phosphorylation reaction on proteins. This phosphorylation potentially allows for interaction or binding of another protein, or activates the activity of the phosphorylated protein (Hornbeck et al., 2015; Want et al., 2017).

In the genome, DNA methylation is an epigenetic mechanism catalyzed by a family of DNA methyl transferases (DNMT's). DNA methylation is essential for silencing retroviral elements, regulating tissue-specific gene expression, genomic imprinting, and X chromosome inactivation (Moore et al., 2013). Methylation is the process of transfer of an S-adenyl methionine (SAM) onto the C5 position of the cytosine to form 5-methylcytosine (5mC). DNMT3a and DNMT3b are known as "de novo" DNMT since they have the capacity to establish *new* methylation patterns to unmodified DNA, while DNMT1 merely copies the methylation pattern of the parental strand to the daughter strand during DNA replication. All DNMT's are intensively involved in embryonic development, and their expression falls and is

significantly reduced by terminal cell differentiation. This process is applied in the silencing of genes temporally regulated during embryonic development (Compere et al., 1981). Genes that are methylated are unable to be transcriptionally accessed. Importantly, DNA methylation in different genomic regions may exert different influences on gene activities based on the underlying genetic sequence.

When this process of methylation is misregulated, it results in the phenotype characteristically seen in pathological states such as ICF syndrome and many cancers (Gill et al., 2013; Jenness et al., 2018; Lakshminarasimhan et al., 2016). Recent next-generation sequencing studies of cancer genomes have revealed frequent and recurrent mutations in a wide variety of epigenetic modulators, including mediators of DNA methylation and genes encoding subunits of chromatin remodelers (Shen et al., 2013). A cancer epigenome is marked by genome-wide hypomethylation and site-specific CpG island promoter hypermethylation (Sharma et al., 2010). This hypomethylation results in excessively activated regulatory proteins and has been demonstrated in cancer types such as gastric cancer, colon cancer, and melanoma as well as ICF syndrome (Wilson et al., 2007; Tuck-Muller et al., 2000). This hypomethylation typically occurs at genomic sequences including repetitive elements, retrotransposons, CpG poor promoters, introns and gene deserts, indicating the importance of methylation of these areas of the genome (Rodriguez et al., 2006). A homozygous mutant DNMT3b knockout in mice is lethal in embryogenesis, demonstrating its critical role in methylation processes (Okano et al., 1999).

Epigenetic mechanisms, such as DNA methylation, have been indicated to play roles in the repair of DNA, such as in non-homologous end joining repair (NHEJ) of DNA double stranded breaks (DSBs). Upon the induction of DNA damage, the chromatin structure unwinds

to allow access to enzymes to catalyze the repair (Fig. 3) (Mao et al., 2008; Fernandez et al., 2021).

Double Stranded Breaks and DNA Repair.

Each of the cells within the human body experience many tens of thousands DNA lesions per day (Lindahl et al., 2000). The cell is constantly undergoing complex physiological processes that offer many opportunities for mismatch or aberrant DNA replication allowing for mutations to be generated. Alternatively, DNA damage may be produced by reactive-oxygen compounds arising as by-products from oxidative respiration or through redox-cycling events involving environmental toxic agents and Fenton reactions mediated by heavy metals (Valko et al., 2006). A single DSB can activate the DNA damage checkpoint, which delays cell cycle progression, and a single DSB allowed to progress with no checkpoint in mitosis resulted in aneuploidy, demonstrating the cell cycle checkpoint control's critical role in the cell in preventing single stranded breaks from happening (van den Berg et al., 2018). When single stranded breaks do occur and enter close proximity to one another, these can cause less frequently occurring yet extremely toxic double stranded breaks (DSBs) (Khanna et al., 2001).

DNA double-strand breaks (DSBs) are generated both extrinsically, for example, by chemotherapeutic agents, and physiologically, for example, during V(D)J recombination in developing B and T lymphocytes, and class switch recombination (CSR) in activated mature B cells (Kumar et al., 2014; Alt et al., 2013). There are an estimated 10 DSBs per day in a cell, and these pathological DSBs arise from ionizing radiation, reactive oxygen species, DNA replication errors and inadvertent cleavage by nuclear enzymes (Chang et al., 2017). They can occur at the termini of chromosomes due to defective metabolism of chromosome ends (telomeres). In addition, DNA DSBs are generated to initiate recombination between homologous chromosomes

during meiosis and occur as intermediates during developmentally regulated rearrangements, such as V(D)J recombination and immunoglobulin class-switch recombination. Whereas these programmed rearrangements are initiated by specific enzymes that generate DNA DSBs in the target locus (the RAG1 and RAG2 proteins in V(D)J recombination, for example) the recombination intermediates seem to be resolved by the same pathways that are used to repair IR-induced DSBs (Khanna et al., 2001).

There are two distinctly identified yet complimentary mechanisms for DNA repair, known as homologous recombination (HR) and non-homologous end-joining (NHEJ). Typically, DSBs are prevented from direct ligation since they have two incompatible DNA ends due to either chemical modifications or mismatching overhangs.

Homologous Recombination.

In homologous recombination, the DNA ends are first resected, a piece cut out while retaining some part, in the 5′ to 3′ direction by nucleases, enzymes that digest nucleic acids. The resulting 3′ single-stranded tails then invade the DNA double helix of a homologous, undamaged partner molecule, and are extended by the action of DNA polymerase, which copies information from the partner. Following branch migration, the resulting DNA crossovers (Holliday junctions) are resolved to yield two intact DNA molecules.

Non-homologous End-joining (NHEJ).

In contrast, NHEJ of two DNA ends does not require an undamaged partner and does not rely on extensive homologies between the two overhanging ends. In this process, usually after degradation at the termini, the two ends are ligated together (Khanna et al., 2001). Prior to NHEJ, short regions of the 5′ or 3′ overhangs by either exonuclease or endonuclease activity are

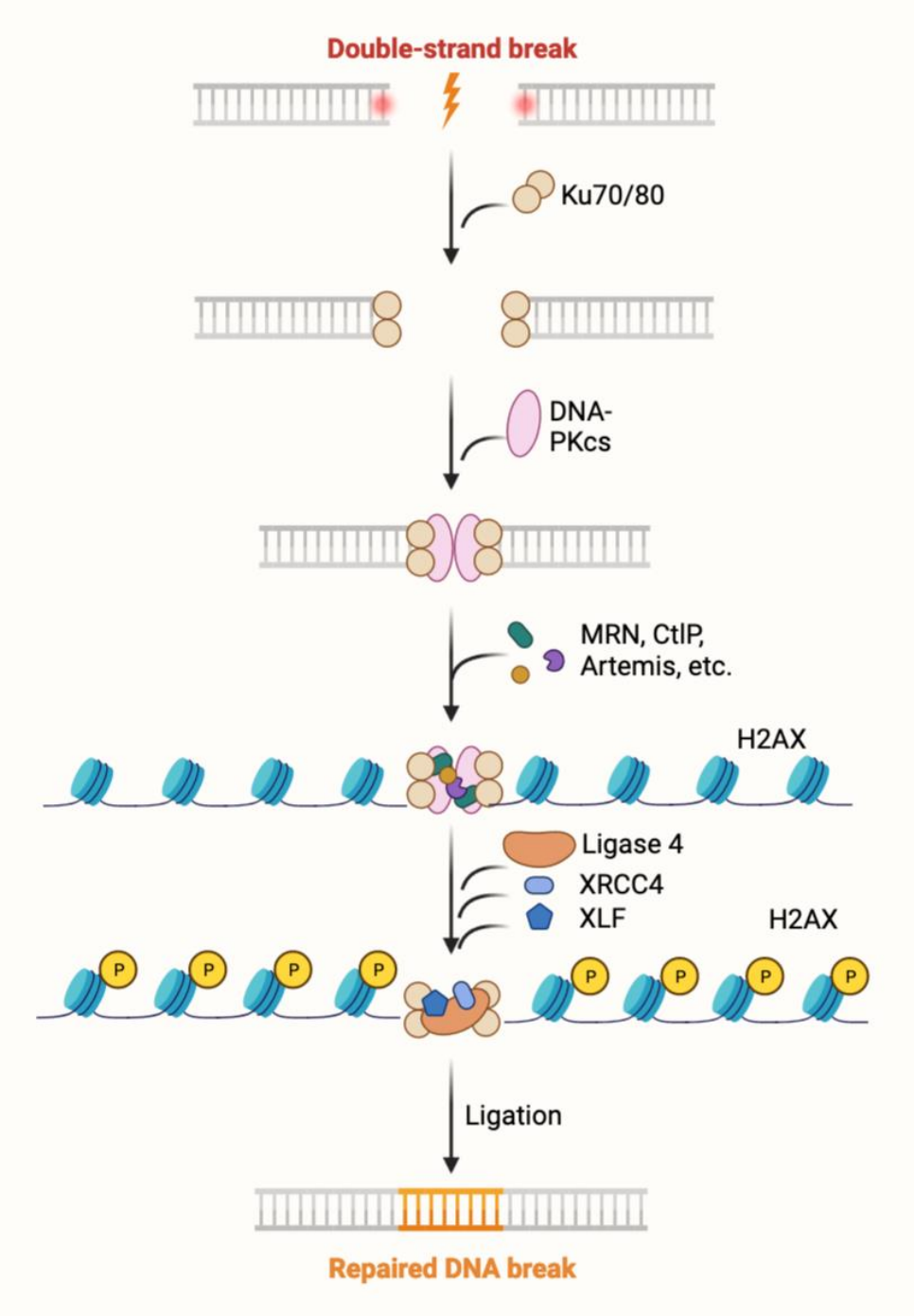

Figure 1.3. Double stranded base repair by the NHEJ (Non-homologous end-joining) pathway. Ku70 and Ku80 proteins heterodimerize to form the Ku complex. The Ku proteins detect and bind to double stranded breaks of DNA, protecting the exposed and vulnerable ends and facilitate a short resection of the DNA. They then recruit and activate DNA PKc's and other binding proteins that allow for accumulation of phosphorylation of Ser139 of Histone 2AX (γ-H2AX), a marker of DNA damage. XRCC4 directs DNA ligase IV to ligate the DNA and polymerization of new DNA. Images created using Biorender.

resected to generate small regions of microhomology (≤4 nucleotides) between the strands to allow for successful ligation and "end-joining" (Chang et al., 2017).

The general process of NHEJ requires an organized resection, protection of exposed ends, recruitment of polymerases to generate a new piece of DNA, and finally the ligation of the break. Highly characteristic of NHEJ is the protection of the exposed ends by the binding of Ku70–Ku80. Ku80 is critical in protecting the vulnerable ends of DNA exposed by a double stranded break. When the cell perceives DNA damage in the form of a double stranded break, Ku80 and Ku70 dimerize to recruit other NHEJ proteins to form DNA-PK (DNA-dependent protein kinase catalytic subunit) complexes, member of the PI3K pathway, that bind to the DSB site. These recruit X-ray cross-complementing protein 4 (XRCC4) and XRCC4-like factor (XLF), with XRCC4 recruiting DNA ligase IV (LIG4) to ligate the double stranded DNA break (Williams et al., 2014).

This DNA-PKcs is recruited in complex with the endonuclease Artemis. Autophosphorylation by DNA-PKcs activates Artemis. This endonuclease is capable of cutting multiple DNA substrates at the borders between single-strand and double-strand DNA (ss–dsDNA) (Chang et al., 2017). Artemis has intrinsic 5′ exonuclease activity on ssDNA, even without DNA-PKcs. Artemis has endonuclease activity when complexed with DNA-PKcs on double stranded DNA on both the 5′ and the 3′ DNA overhangs. These types of overhangs are often created at pathological DNA breaks and on DNA hairpins formed during V(D)J recombination in immune development. Artemis is critical for forming this DNA hairpin opening process during V(D)J recombination. Severe combined immunodeficiency (SCID) owing to a V(D)J recombination defect in antigen receptor gene assembly is clearly observed in those lacking Artemis (Moshuos et al., 2001; Ma et al., 2002). Excessive resection by Artemis

endonuclease is prevented by the Ku80/Ku70 complex, part of the DNA-PKc's, that protects the exposed ends of the double stranded DNA (Chang et al., 2017).

DNA ligase IV and XRCC4 are the most central components of NHEJ in eukaryotes (Leiber et al., 2010). This process of end resection and protection by the Artemis-DNA-PK complexes allows for subsequent ligation by Ligase IV-XRCC4 ending with DSB repair of DNA (Mao et al., 2008; Fernandez et al., 2021). XLF is a 33 kDa protein with structural similarity to XRCC4 (Dai et al., 2003). The N-terminal head domain of XLF interacts with the N-terminal head domain of XRCC4. This XRCC4–XLF complex forms a "sleeve-like" structure around a DNA duplex (Brouwer et al., 2016; Ahnesorg et al., 2006).

PAXX (paralogue of XRCC4 and XLF) is a 22 kDa protein whose C terminus (aa 199–201) interacts with Ku, and PAXX mutants are more sensitive to ionizing radiation and DSB-inducing agents (Ochi et al., 2015). The literature demonstrating DNA-PKC's, Artemis, PAXX, Ligase IV interact with Ku indicate its critical role in facilitating DNA damage repair by NHEJ of DBSs.

Ku80.

Ku80 (also known as XRCC5) and Ku70 (also known as XRCC6), heterodimerize as the Ku complex also known as Ku and bind to discontinuities in double-stranded (ds) DNA such as double-strand breaks, single-strand gaps, and noncomplementary segments (Blier et al., 1993). Eukaryotic Ku contains three distinctly identified domains: the Ku core that is conserved in eukaryotes and prokaryotes; an N-terminal von Willebrand A domain; and the C-terminal helix–extension–helix (HEH) domain (Aravind et al., 2001).

The Ku complex has many functional roles in various cell signaling processes. Ku is required to initiate the cell signaling cascade that results in c-NHEJ by various protein-protein

interactions culminating in ligation by DNA ligase IV activity stimulated by Ku (Gottlieb et al., 1993; Ramsden et al., 1998). For the joining of two blunt DNA ends, Ku and XRCC4–DNA ligase IV are sufficient, and the addition of other NHEJ proteins does not substantially improve the joining, indicating the critical and powerful response of the Ku complex in repairing DNA damage sites (Chang et al., 2017).

Ku80 has been shown by the literature to be critical for heterodimerization with Ku70 to form the Ku complex, which subsequently recruits and activates the catalytic p350 subunit of the DNA dependent protein kinase. In Ku80 null mouse lines, Ku70 mRNA is unaffected while Ku70 protein expression levels are reduced in Ku80 null mice, and while the p350 catalytic subunit protein expression was not affected, the capacity of p350 to bind to the exposed DNA ends was impaired in mutants deficient in Ku80. However, introduction of human Ku80 into Ku80 null mice lead to increased Ku70 protein production and restored Ku70 binding to DNA double stranded breaks, suggesting the critical role of Ku80 in forming the Ku heterodimer. The supplementation of Ku80 restored the capacity of p350 to find to exposed DNA ends in Ku80 null mice, and rescued the mutant phenotypes from impaired DNA break repair and decreased cell survival (Chen et al., 1996).

Additionally, Ku has been shown to be important in telomere maintenance, as it is an integral component of the telomere binding complex and is shown to be participant in facilitating the perinuclear localization of the telomere, silencing, and preventing shortening (Hsu et al., 1999; Mishra et al., 1999; Galy et al.2000). As well, Ku proteins promote accumulation of phosphorylated Histone 2AX, (γ-H2AX) an important biomarker of DNA damage (Kinner et al., 2008).

Various cytological and molecular changes that likely resulted from the defect in DNA repair were observed in *CDCA7* and *HELLS* mutant HEK293 cells and also in *DNMT3B* and *ZBTB24* mutant cells. Furthermore, CDCA7 or HELLS deficiency caused a C-NHEJ defect and delay in Ku80 accumulation at DNA damage sites. The literature shows the defect in C-NHEJ accounts for some of the common features of ICF cells, including instability of satellite repeats, abnormal chromosome configuration, reduced proliferation rate, and apoptosis (Unoki et al., 2019).

V(D)J Recombination, Class Switch Recombination and c-NHEJ.

V(D)J is the process by which genomic segments encoding the variable (V), diversity (D), and joining (J) elements of immunoglobulin Ig and T cell receptor (TCR) genes are assembled (Deriano et al., 2011; Nussenzweig, et al., 1997).The TCR β and δ chain and Ig heavy chain (IgH) variable region exons are assembled from V, D, and J segments, while TCR α and γ chain and Ig κ and λ light chain (IgL) exons are assembled from V and J segments (Bassing et al., 2002). V(D)J recombination is initiated by a double stranded break (DSB) between the V, D, and J segments and flanking RSS (recombination signal sequences). The RS ends are joined while the coding regions is potentially modified and may result in an inversion or deletion of intervening sequences (Tonegawa et al., 1983). The joining phase of the V(D)J recombination reaction is carried out principally by NHEJ proteins (Sekiguchi et al., 2001).

In early B and T cell development, NHEJ is required for V(D)J recombination. Additionally, a link between DSB repair and V(D)J recombination was discovered through study of severe combined immunodeficient (SCID) mice, which are both radiosensitive and immunodeficient (Bosma et al., 1991). A null mutation in Ku80 subunit of the DNA-PK results

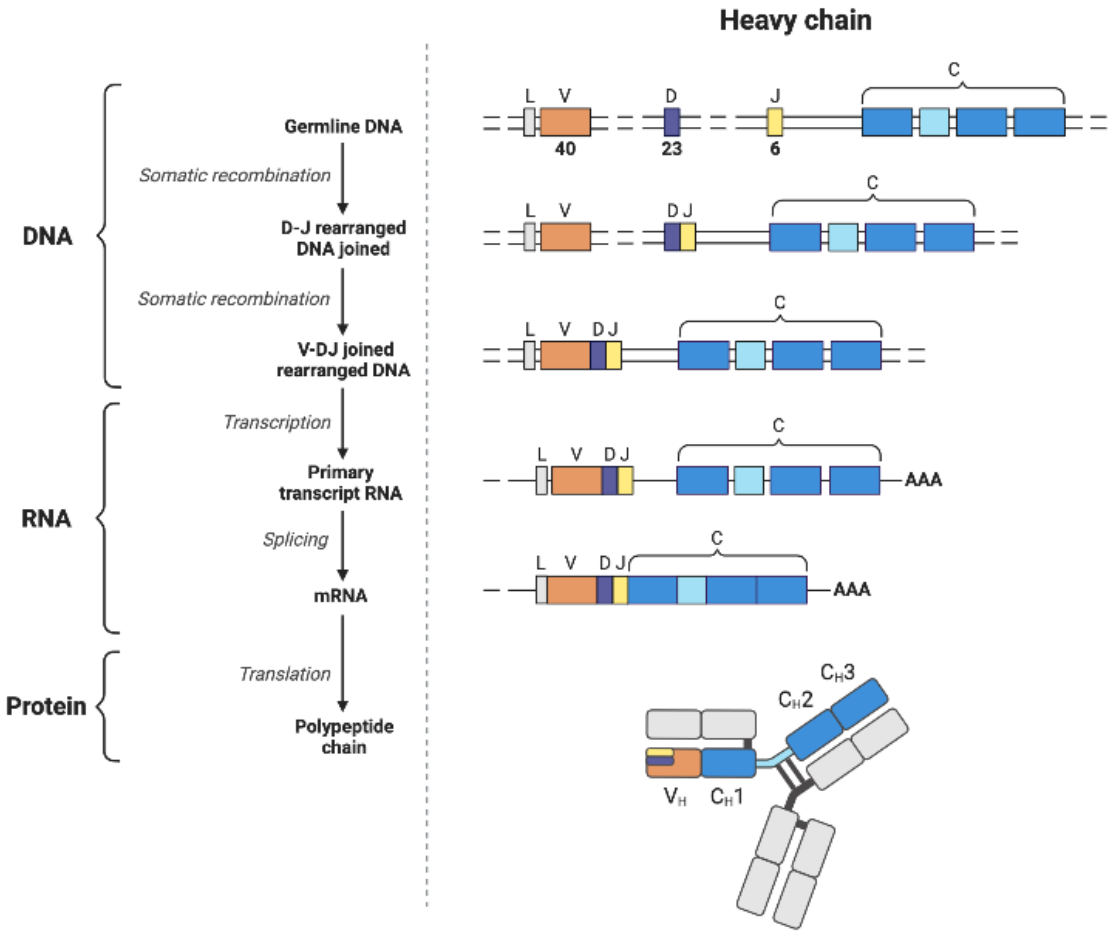

Figure 1.4. V(D)J recombination is the process by which genomic segments encoding the variable (V), diversity (D), and joining (J) elements of immunoglobulin Ig and T cell receptor (TCR) genes are assembled (Deriano et al., 2011; Nussenzweig, et al., 1997).The TCR β and δ chain and Ig heavy chain (IgH) variable region exons are assembled from V, D, and J segments, while TCR α and γ chain and Ig κ and λ light chain (IgL) exons are assembled from V and J segments (Bassing et al., 2002). V(D)J recombination is initiated by a double stranded break (DSB) between the V, D, and J segments and flanking RSS (recombination signal sequences). The RS ends are joined while the coding regions is potentially modified and may result in an inversion or deletion of intervening sequences (Tonegawa et al., 1983). The joining phase of the V(D)J recombination reaction is carried out principally by NHEJ proteins (Sekiguchi et al., 2001).

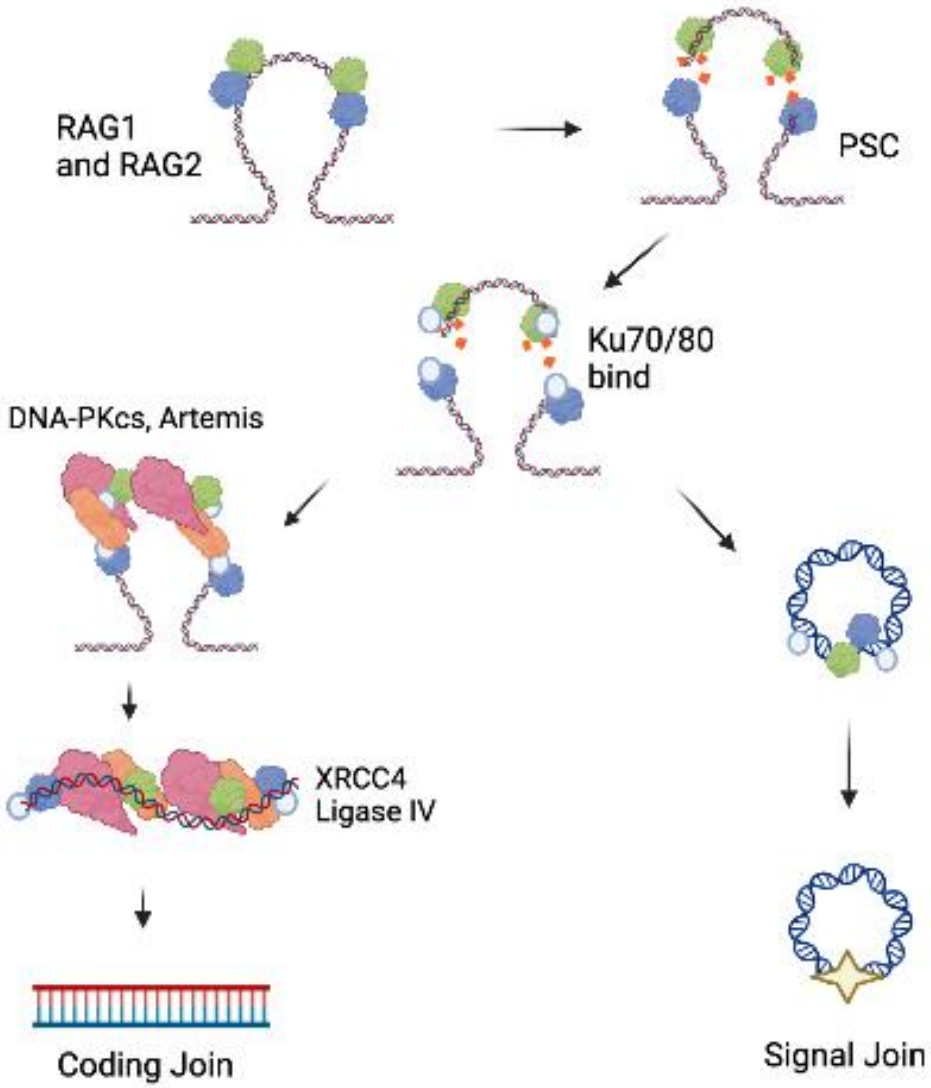

Figure 1.5. Double stranded base repair by the NHEJ (Non-homologous end-joining) pathway is initiated by RAG1/2 during CSR (Class switch recombination).. Ku70 and Ku80 proteins heterodimerize to form the Ku complex. The Ku proteins detect and bind to double stranded breaks of DNA, protecting the exposed and vulnerable ends and facilitate a short resection of the DNA. They then recruit and activate DNA PKc's and other binding proteins that allow for accumulation of phosphorylation of Ser139 of Histone 2AX (γ-H2AX), a marker of DNA damage. XRCC4 directs DNA ligase IV to ligate the DNA and polymerization of new DNA. (Images created using Biorender.)

in a severe phenotype, as T and B cell development is arrested at early progenitor stages and there is deficiency in V(D)J rearrangement in mice (Nussenzweig et al., 1996). Furthermore, Ig and TCR provide antigen-binding specificity for an immune response, and the proteins encoded by the recombination activating genes 1 and 2 (RAG1,2) that form an endonuclease (RAG). RAG is required to initiate V(D)J and detects recombination signal sequences (RSSs) neighboring the V, D and J gene segments (Deriano et al., 2011). B cell and T cell development are blocked in RAG 1 and 2 deficient mice (Mombaerts et al. 1992; Shinkai et al. 1992). This further supports the insinuation of Ku80's role in V(D)J recombination, class switch recombination and DNA damage response.

Immunoglobulins, or antibodies, play a crucial role in immune response through their effector functions. Class switch recombination (CSR) takes place in mature B cells, when constant regions of immunoglobulins switch from IgM to IgG, IgA or IgE. CSR is initiated by activation-induced cytidine deaminase (AID), causing DNA deamination producing an abasic (apyrimidinic/apurinic [AP]) site subsequently cut by AP endonuclease (APE) 1 or 2. (Xu et al., 2012). DNA single-strand breaks (SSB) are produced, and two SSBs on opposite DNA strands form DSBs, initiating the CSR (Xu et al., 2012). The joining of DSBs during the CSR is performed both by the classical NHEJ (C-NHEJ) and alternative end joining (A-EJ) (Yan et al., 2007). This further supports the role of NHEJ in early B and T cell development.

Histones.

The organization of DNA, the material that allows for the inheritance of genetic information, is packaged as 147 bp of DNA wrapped around an octamer of core histones known as nucleosomes, and forms increasingly more complex structures to form chromatin (Rogakou et al., 1997). This nucleosome includes DNA and eight core histone proteins, two from each of four

histone protein families, known as H4, H3, H2B, and H2A (Peterson et al., 2004). The histone octamer is composed of a central heterotetramer of histones H3 and H4, flanked by two heterodimers of histones H2A and H2B. Each nucleosome is separated by 10–60 bp of 'linker' DNA, and the resulting nucleosome array constitutes a chromatin fiber of ∼10 nm in diameter. This simple 'beads-on-a-string' arrangement is folded into more condensed, ∼30 nm thick fibers that are stabilized by binding of a linker histone to each nucleosome core (note that linker histones are not related in sequence to the core histones). This organization of DNA into chromatin hinders its accessibility to proteins that must bind or transcriptionally activate the DNA. Therefore, such structures must be dynamic and capable of regulated remodeling transitions by remodeling proteins to allow for temporally and spatially activation, and subsequent silencing, if necessary (Peterson et al., 2004). The three H2A subfamilies are the: H2A1-H2A2 family; the H2AZ family; and the H2AX family (Rogakou et al., 1998). H2AX is known to associate with CDCA7 and is therefore a protein of interest (Unoki et al., 2018).

γ-H2AX and DNA Damage.

H2AX is a variant of the H2A protein family, which is a component of the histone octamer in nucleosomes. γ-H2AX, (pronounced "gamma-H2AX", also known as Serine 139-phosphorylated H2AX), facilitates the concentration of DNA damage repair machinery and simultaneously serves as a DNA damage signal and biomarker (Hunt et al., 2013; Rogakou et al., 1998; Celeste et al., 2003). H2AX is defined as distinct from the other two H2A subfamilies since it has the distinctive motif SQ(D/E)(I/L/Y)-(end) at its C-terminal end, and this motif includes the site of γ-phosphorylation at residue serine 139 (Rogakou et al., 1998).

In response to DNA damage, H2AX is phosphorylated by ATM, (ataxia telangiectasia mutated), a PI3K family member. Ataxia telangiectasia mutated (ATM) is a DDR regulator

protein kinase that phosphorylates multiple substrates in response to the DSBs, including histone H2AX, modulator of DNA damage checkpoint 1 (MDC1) and p53-binding protein 1 (53BP1) (Kumar et al., 2014). Following the activation of Really Interesting New Gene (RING), Finger Protein 8 (RNF8), and RNF168, which are ubiquitin ligases, y-H2AX recruits MDC1. Phosphorylated and ubiquitinated H2AX recruits p53, which in turn mediates recruitment of RIF1 and interacts with Rev7. Accumulation of DSBs results in ATM-dependent activation of checkpoint kinases 1 and 2 (CHK1 and CHK2), arresting the cell cycle, followed by phosphorylation and stabilization of p53, triggering apoptosis.

The H2AX protein is always phosphorylated at Ser 139 in the presence of DNA damage. This creates a platform to allow for the recruitment of other important DDR proteins. These foci represent DSBs in a 1:1 manner, resulting in a close correlation of phosphorylated foci and DNA damage (Rogakou et al., 1998). This phosphorylation triggers the NHEJ pathway ending in ligation and ultimately repair of the double stranded break (Stiff et al., 2004).

γ-H2AX has been shown to have various functions in different cell regulatory capacities such as DSB processing and correlation with growth deficiencies. Mice and yeast lacking the conserved serine residue demonstrate a variety of defects in DNA DSB processing (Pilch et al., 2003). 2AX Delta/Delta mice are smaller, sensitive to ionizing radiation, defective in class switch recombination and spermatogenesis while cells from the mice demonstrate substantially increased numbers of genomic defects (Pilch et al., 2003). As the most highly conserved of the three H2A subfamilies in eukaryotes, H2AX comprises 2–10% of the H2A proportion in mammalian tissues and H2AX constitutes almost all of the H2A in budding yeast (Baxevanis et al., 1996; Rogakou et al., 1998).

Doxorubicin and DNA Damage.

Activation of the PI3K-AKT pathway is an important requirement of cancer cells to escape cell death upon exposure to toxic stimuli, and many chemotherapy drugs commonly in use, including doxorubicin, face the barrier of patients becoming "chemoresistant" (Bezler et al., 2012). Doxorubicin is a natural anthracycline drug originally extracted from *Streptomyces peucetius var. caesius*, and is one of the most effective chemotherapy drugs used against solid tumors in the treatment of several cancer types (Arcamone et al., 1969). It is known to cause DNA double-strand breaks in rapidly dividing cells however its mechanism is not fully understood (Yang et al., 2013).

One proposed model in which doxorubicin induces DNA damage, is doxorubicin intercalates within DNA and inhibits topoisomerase II. This results in overwinding of DNA during transcription, thereby preventing the recombination of the DNA double strand and impeding DNA replication. Additionally, when doxorubicin intercalates in promoter sequences, it hinders topoisomerase II activity. Subsequently, the dynamics of nucleosomes are affected by the resulting torsional stress, resulting in an increased rate of nucleosome turnover, eviction and replacement. This culminates in exposure of vulnerable DNA susceptible to double stranded breaks, resulting in cell death (Yang et al., 2013; Pommier et al., 2010; Pang et al., 2013; Taymaz-Nikerel, et al., 2018). This was supported by a study that used a genome wide method to map DSB's in cancer cells. They found spontaneous DSB's occur preferentially around promoters of active genes, and that anthracyclines increase DSB's around promoters (Yang et al., 2015).

However, this method was not identified in all cell types and tissues, such as heart and liver, as doxorubicin has been shown to cause histone eviction and nucleosome turnover despite

no evidence of double stranded breaks (Pang et al., 2013). Three possible consequences of histone eviction were described as diminished DDR, epigenetic alterations, and stimulation of apoptosis (Pang et al., 2013). Additionally, 14-3-3 signaling was seen as upregulated in the heart after treatment with doxorubicin, potentially related to the cardiotoxicity side affect of doxorubicin (Pang et al., 2013).

A second model proposes doxorubicin causes the generation of free radicals and oxidative damage to biomolecules, causing DNA damage and ultimately cell death (Kim et al., 2006; Li et al., 2005; Lepos et al, 2008).

One of the major disadvantages of long-term cancer treatments is resistance to chemotherapy reagents. Repeated administration of doxorubicin has been shown to lead to drug-resistant cancer cells and increased cytotoxicity, the most common side effect of doxorubicin (Taymaz-Nikerel, et al., 2018; Ferreira et al., 2017).

AKT has been shown to suppress apoptosis induced by chemotherapy or radiotherapy through interaction with critical apoptosis pathway regulatory proteins, leading to conference of resistance by AKT to multiple types of chemotherapy reagents in a plethora of cancers (Li et al., 2005). Overactive AKT has been shown to confer resistance to multiple types of chemotherapy reagents including doxorubicin in breast cancer (Knuefermann et al., 2003). Additionally, phosphorylation of AKT was observed to be significantly higher in patients with esophageal squamous cell carcinoma who received chemotherapy. This increase was correlated with poor prognosis (Yoshioka et al., 2018). Another study showed in a radiation-resistant versus a radiation-sensitive group, significantly increased levels of phosphorylated AKT in cervical cancer (Kim et al., 2006). In ovarian cancer cells doxorubicin induces activation of the HER3-PI3K-AKT signaling cascade, and results in chemotherapy resistance. This was successfully

inhibited by specific kinase inhibitors, and inhibition of this signaling cascade significantly induced apoptosis (Bezler et al., 2012).

When doxorubicin was introduced in a panel of breast cancer cell lines, the results showed differential responses in the baseline levels of Akt phosphorylation and kinase activity, indicating their possible connection to similar cellular regulatory processes. Using Western Blot analysis, doxorubicin was observed as requiring a minimum of 24 hours for peak kinase activity by AKT, and exhibited a dose-dependent response with a peak in detected AKT intensity at 1 uM when compared with a range of doses in breast cancer cell lines (Li et al., 2005). Overall, this accumulation of studies shows the significant correlation of the PI3K pathway and DNA damage by doxorubicin in multiple cancer types.

Furthermore, 293T cells showed significant cell damage when incubated in the presence of doxorubicin. The serine/threonine protein kinase ATM, a member of the PI3K pathway family of proteins, was found to be activated by doxorubicin, partially through the generation of reactive oxygen species (ROS) and was necessary for the initial response for phosphorylation of H2AX, a DNA damage biomarker (Kurz et al., 2004).

This indicates a possible method by which doxorubicin causes DNA damage, and by upregulating the PI3K pathway by overstimulation of AKT and the increased upregulation of DNA damage repair components such as γ-H2AX, may possibly cause overstimulation of CDCA7 and associated proteins. This may allow us to fully elucidate the role of CDCA7 and HELLS in mediating DNA damage response through the Ku complex.

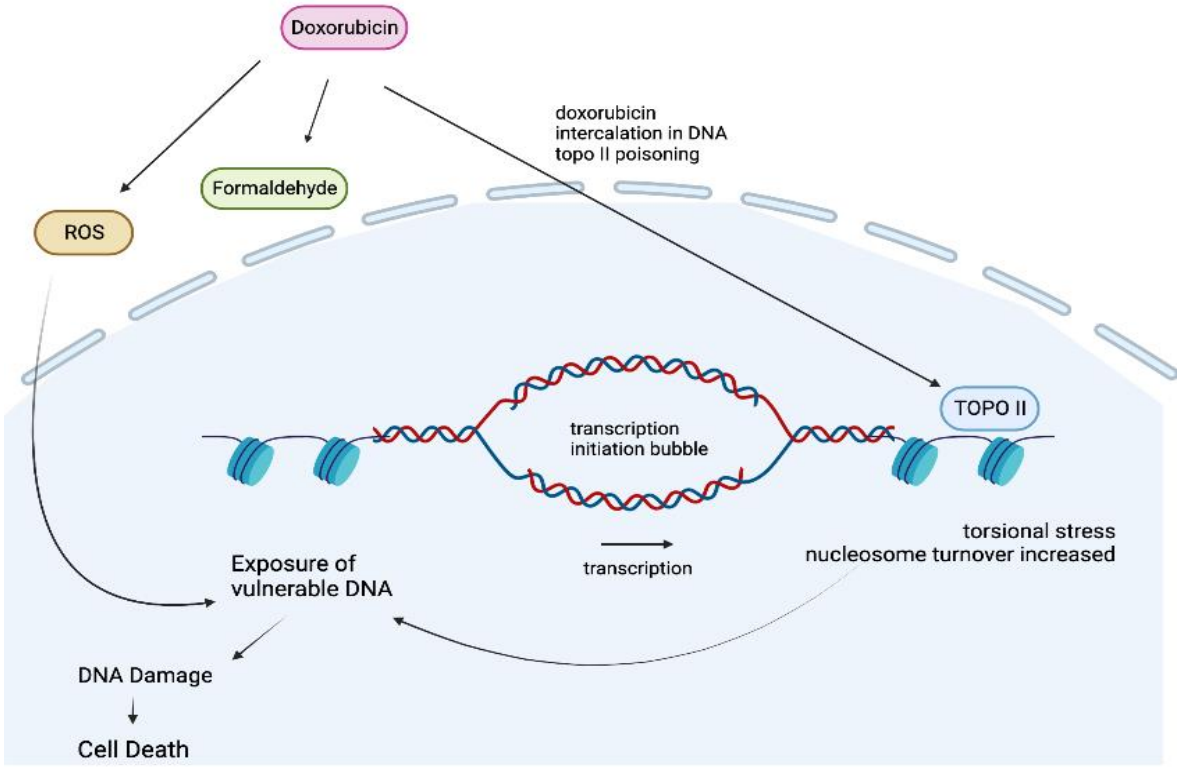

Figure 1.6. Doxorubicin causes DNA damage via 1 of 3 proposed mechanisms. One method is through topoisomerase II, critical in preventing twisting that would stress and prevent proper transcription and maintenance of the transcription initiation bubble. This causes subsequent torsional stress and nucleosome turnover is increased. This causes exposure of vulnerable DNA resulting in DNA damage leading to cell death. Other pathways include formaldehyde and ROS (reactive oxygen species).

Hypothesis.

I hypothesize that CDCA7 interaction with HELLS requires a conserved region of amino acids, and loss of these amino acids will disrupt CDCA7-HELLs interaction. My approach was to evaluate the interaction between CDCA7 and HELLs after altering regions of CDCA7. Within the CDCA7 protein, there are several regions that are commonly known to mediate protein interaction. These include a leucine rich region near the N-terminus, a phosphorylation site at the mid-point of the amino acid sequence that we have previously discovered interacts with 14-3-3, an acidic region closer to the C-terminus, and a C-terminal cysteine rich Zinc Finger domain (Figure 2.1).

The literature reports the association of CDCA7 with Ku80 (Unoki et al., 2018). Therefore, my goal was to map the region of CDCA7 critical for their interaction. It is likely Ku80 will require a conserved sequence of amino acids to interact with CDCA7.

Additionally, the association of CDCA7 with γ-H2AX is documented (Unoki et al., 2018). Therefore, my goal was to map the region of CDCA7 critical for their interaction. It is likely γ-H2AX will require a conserved sequence of amino acids to interact with CDCA7.

Finally, to investigate the functional effect on CDCA7's role in DNA damage via Ku80 and γ-H2AX, when doxorubicin is added to HEK293Ta cells, significant DNA damage should be indicated by an upregulation of Ku80 and γ-H2AX.

Chapter 2: Procedures, Protocols, and Methodology

DNA Related Procedures:

Some plasmid constructs were obtained by other members of the Scheid lab produced for a previous publication (Gill et al, 2013), while I generated the remaining constructs. Constructs were made using site-directed mutagenesis using the NEBaseChanger Q5 kit (NEB Catalog # E0554S).

All constructs contain a carbenicillin resistance gene under control of a bacterial promoter. *Escherichia coli* cells were grown in Lennox Luria Broth (LB) from Sigma Aldrich (Stock Keeping Unit/SKU L3022). The carbenicillin (100 μg/ml) from Sigma Aldrich (SKU C1613) was added to the LB media. Cells were plated on LB-agar (1.5% w/v; Bacto Agar from Difco & BBL, Catalog no. 214010) with carbenicillin (100 μg /ml). Cells are NEB 5-alpha (DH5alpha strain) competent *E. coli* (subcoloning efficiency) cells (NEB Catalog# C2988). All cultures were incubated at 37℃, 220 rpm on a VWR S-500 Orbital Shaker.

Transformation.

DH5α *E. coli* cells (50 µl) were thawed on ice and mixed with 1-5 µL of plasmid DNA with gentle agitation. The mix was placed on ice for 30 minutes, followed by immersing in the Eppendorf Thermomixer 5436 for 45 seconds at 42°C (heat shock) and then placed back on ice for 5 minutes. The cells were resuspended in SOC Outgrowth Medium (NEB Catalog# B9020; 2% Vegetable Peptone, 0.5% Yeast Extract, 10 mM NaCl, 2.5 mM KCl, 10 mM $MgCl_2$, 10 mM $MgSO_4$, 20 mM Glucose), incubated at 37°C for 1 hour, resuspended again and plated onto an LB-agar plate and incubated overnight at 37°C inverted. Plates were stored at -4°C if colonies successfully formed after 24 hours.

DNA Preparation.

After DNA was transformed onto LB-agar plates, a colony was picked and grown overnight in 100 mL of media. DNA was purified from the overnight cultures of DH5α *E. coli* cells with PureLink™ HiPure Plasmid Filter Miniprep kit or Midiprep kit according to the manufacturer's protocol. All kits were from ThermoFisher Scientific.

Sequence Verification.

After DNA is prepared, plasmid DNA was sent for sequencing at TCGA Facilities (Sick Kids Hospital) along with associated sequencing primers for the construct. The sequence reads were compared to the sequence of the gene insertion with the Nation Center for Biotechnology Information (NCBI) tool called Align Sequences Nucleotide BLAST (Basic Local Alignment Search Tool).

Cell Lines and Cell Culture.

HEK 293T cells were obtained from the American Type Culture Collection and maintained in Dulbecco's modified Eagle's medium (DMEM) supplemented with 10% fetal bovine serum (FBS) and antibiotics (Penicillin Streptavidin) at 37°C and 5% CO_2.

Thawing.

Cells in a cryogenic vial were placed in a water bath at 37°C until nearly thawed. 1 mL of DMEM was added drop wise to the cells and then cells are plated in a 100 mm dish with 8 mL of media. A second 100 mm dish, diluted ten-fold, is plated from the first dish. After 24 hours incubation and allowing cells to adhere, media was aspirated and replaced with fresh cell culture media DMEM.

Transfections.

For transient expression of FLAG tagged vector DNA in HEK 293T cells, cells were plated on 100 m diameter dishes at 80% confluency and transfected with 15 μg of total plasmid DNA using polyethylenimine (PEI) (Sigma-Aldrich #408727). 15 μg of DNA was diluted with 750 μl of sterile serum free OPTIMEM (ThermoFisher scientific #31985062) and incubated at room temperature for 5 minutes. Simultaneously, 45 μl of PEI (volume is 3x the amount of DNA utilized) diluted with 750 μl of sterile serum free OPTIMEM. The two diluted solutions of DNA and PEI are combined and incubated at room temperature for 15 minutes and within 30 minutes were added dropwise in 500 μl increments indirectly to plated HEK 293T cells. Cells were incubated at 37°C and 5% CO_2 overnight. DMEM media was removed, and fresh DMEM supplemented with 10% fetal bovine serum and antibiotics were replaced. After 24 hours of incubation, cells were rinsed with sterile PBS (Phosphate Buffered Saline), and harvested.

Harvest and Immunoprecipitation Assay with FLAG Beads.

Plated 293T cells were kept on ice. 1 ml of cold Lysis Buffer that included phosphatase and protease inhibitors was added to each plate, and cells were collected into centrifuge tubes. Each sample was sonicated 3 times for 5 seconds, then centrifuged at 21,100 rpm for 5 minutes at 4°C. Supernatant was retained while pellet discarded. 20 μl of each sample supernatant was aliquoted as a "lysate" protein loading control sample to be combined with SDS PAGE (Sodium dodecyl-sulfate polyacrylamide gel electrophoresis) sample loading buffer, boiled at 95°C for 5 minutes and then stored at -20°C until use. The remaining supernatant was incubated and rotated gently at 4°C with precleaned M2 FLAG agarose beads (Sigma-Aldrich) for 1 hour to overnight ("IP samples"). IP beads samples were washed as follows: samples were centrifuged at 4°C for 12 seconds at 12000 rpm, supernatant removed, and washed with 350-700 μl lysis buffer

containing protease and phosphatase inhibitors. This process of washing the beads was repeated 3 times.

FLAG Elution.

After washing the IP samples, to elute the bound FLAG tagged proteins and associated proteins from the beads, the samples were incubated with a 5 μg FLAG elution peptide (Sigma) suspended in lysis buffer containing protease and phosphatase inhibitors with a final concentration of 150 μg. The beads were flicked to resuspend in the solution, allowed to settle for 15 minutes, then pelleted via centrifugation; this process was repeated 3 times in the span of 45 minutes to 1 hour at 4℃. After, the bead samples were centrifuged for 1 minute at 4℃ at 21,100 rpm. 90 μl of the supernatant was aliquoted and combined with 30 μl of 4x SDS PAGE sample loading buffer and boiled at 95℃ for 5 minutes. These samples were then stored at -20℃ until use.

Antibodies.

Mouse monoclonal anti-Flag M2 (A2220) antibodies were purchased from Sigma-Aldrich. Mouse monoclonal anti-14-3-3β (catalog no. SC-1657) and mouse monoclonal anti-MYC (9E10; catalog no. SC-40) antibodies were purchased from Santa Cruz. Rabbit polyclonal anti-Ku80 (C48E7), rabbit polyclonal anti-14-3-3, rabbit polyclonal anti-γ-H2AX (S139), and mouse monoclonal anti-P-Ser473 AKT (4051) antibodies were purchased from Cell Signaling Technology. An anti-P-Thr163 CDCA7 rabbit polyclonal antibody was generated by GenScript Corporation (CA).

Western Blot.

Criterion TM XT Precast 4-12% Bis-Tris gels were used for a portion of the western blotting procedures. The rest used either 10% or 15% aa/bis acrylamide percentage gels following the NuPAGE gel casting protocol.

NuPAGE Gel Casting Protocol.

Gels were cast in either 1mm or 1.5 mm spacers (BIORAD). Resolving gels were cast (10%/10 ml) by mixing in a 50 mL conical tube 30% acrylamide from BioShop Canada (Catalog no. ACR010), 7x BisTris Buffer, *dd*H_2O, Tetramethylethylenediamine (TEMED) from Bioshop Canada (Catalog no. TEM001), and 0.1% ammonium persulfate (APS). Every gel was then overlayed with 500 ml ethanol. Acrylamide was allowed to polymerize for at least 25 minutes. Ethanol was drained and rinse thoroughly several times with deionized water. Stacking gel was cast (4%/10 ml) in a 50 mL conical tube, 30% AA/bis (4ºC), 7x BisTris Puffer (4ºC), H_2O , TEMED (RT), APS (4ºC) and mixed by inverting the tube. 2-3 ml was poured onto each gel and combs inserted. Gels were allowed to set for 25 minutes, then covered with a wet paper towel and parafilm to let completely polymerize overnight at 4℃ (fridge) or used straight away once leftover gel solution fully polymerized in tube.

After gels were produced, they were assembled on the MiniPROTEAN® Tetra vertical electrophoresis cell from BioRad. The unit was filled to the required volume with running buffer, 1xXTMOPS (BioRad). After samples were loaded, the gel was run at constant voltage (130 Volts) for 80 minutes. Current was provided through a VWR AccuPower Model 300 electrophoresis power supply unit.

Transfer.

Immobilon-P (PVDF) Membrane (Millipore Sigma Catalog no. IPVH00010) and FisherbrandTM Pure Cellulose Chromatography Paper (transfer paper) from Fisher Scientific (Catalog no. 05-714-4) were cut out into rectangle pieces, based on the dimensions of the gel to be transferred. The polyvinylidene fluoride (PVDF) membrane was activated by completely immersing the membrane in 100% methanol for 10 minutes. The membrane is then soaked in transfer buffer, pH 7.2 (bicine 25 mM, Bis-Tris 25 mM, EDTA 1 mM, 10% methanol). Once the gel finished running, the gel and transfer paper were soaked entirely in transfer buffer for 10 minutes. The components for transfer were assembled on a Semiphor Semi-dry transfer unit from Amersham Pharmacia Biotech. The order of the components were as follows: four pieces of transfer paper, PVDF membrane, gel and four more pieces of transfer paper. The transfer apparatus was run at constant current (50 milliamps/gel) for 60 minutes.

Blocking.

Blocking buffer depended on the type of secondary antibody (fluorescent vs. horse radish peroxidase (HRP)). For fluorescent secondary antibodies, membranes were incubated in Odyssey® Blocking Buffer (TBS) from LI-COR (Product Number 927-50000) for at least 1 hour prior to incubation with primary antibody. If commercial blocking buffer was unavailable, 3% powdered skim milk dissolved in 1X PBS (BIORAD) was used instead.

Blotting.

All antibody mixtures were made in phosphate-buffered saline (PBS) with 50% blocking buffer or 50% of 3% skim milk dissolved in 1X PBS. Primary antibodies were added to the antibody mixture with 0.1% Tween®-20 from BioShop Canada (Catalog no. TWN510) and

0.01% SDS. The primary antibodies were incubated with the membrane in a glass tray for 1-2 hours at room temperature or overnight at 4°C. Next, membranes were washed 3 times, 5 minutes per wash, with 0.1% Tween-20 and 0.01% SDS in 1xPBS (Western Wash). Secondary antibodies were added to the antibody mixture with 0.1% Tween®-20 and 0.01% SDS in 1xPBS (Western Wash). Secondary antibodies were incubated in the dark for 30-45 minutes at room temperature. Membranes were again washed 3 times, 5 minutes per wash, with 0.1% Tween-20 and 0.01% SDS in 1xPBS (Western Wash) before being imaged.

Odyssey Imaging.

Fluorescent secondary antibodies were used so membranes were scanned on the Odyssey® Infrared Imaging System, Model 9120. The system detects emission wavelengths at 700 nm and 800 nm.

Cell Viability Assay: Trypan Blue Exclusion.

Cells were seeded with 50,000-500,000 cells and allowed to adhere while incubated at 37℃ with 5% CO_2. After 24 hours, various concentrations (25 μM, 10 μM, 5 μM, and 1 μM) of doxorubicin was added to each well. Water was used as a vehicle control. Cells were incubated at 37℃ for 48 hours. Media supernatant was collected, cells were rinsed with PBS and PBS collected, cells trypsinized, trypsin deactivated by addition of DMEM media and DMEM collected. Collected solution was pelleted for 5 minutes at 1200 rpm. The supernatant was removed, and cells resuspended in 1-2 ml of fresh DMEM media. Following the addition of trypan blue solution (0.4%, Invitrogen), the stained cells were counted using a hematocytometer.

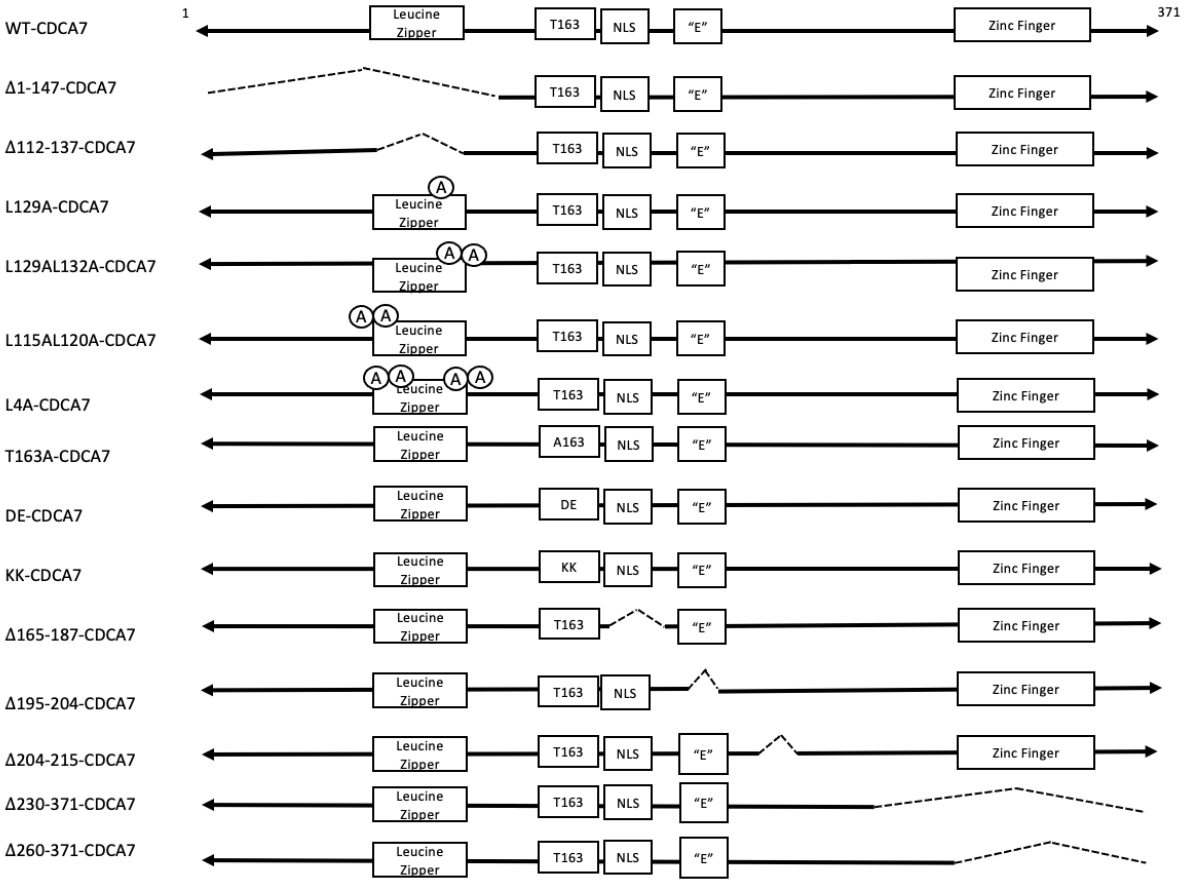

Figure 2.1. Mutant constructs of WT-CDCA7 (371 amino acids) created by site directed mutagenesis. **"**Delta260-371-CDCA7" and "Delta230-260-CDCA7" is the removal of the C-terminal end. "Delta1-147-CDCA7" is the removal of the 147 amino acids from the N-terminus. "Delta112-137-CDCA7" is the removal of the 25 amino acids within the "putative Leucine Zipper region". "4LA-CDCA7" is the substitution mutations of 4 leucines to alanines within the 112-137 putative leucine zipper region. "T163A-CDCA7" is the substitution mutation of Threonine 163 to Alanine, and the abolishing of phosphorylation by p-AKT at T163 and subsequent binding of 14-3-3 of CDCA7 and sequestering it to the cytoplasm. "DE-CDCA7" is the replacement of the 20 amino acids surrounding the T163 site with an R18 peptide (PHCVPRDLSWLDLEANMCLP). The "KK-CDCA7" construct is the replacement of the D and E residues that form contacts with 14-3-3 and are substituted for phospho-amino acids, resulting in complete prevention of 14-3-3 binding.

Chapter 3: Discoveries, Findings, and Results

HELLS Requires the N-terminal Leucine Zipper for Interaction with CDCA7

The schematic in Figure 2.1. shows the various regions of CDCA7 and their proposed roles, including a C-terminal zinc finger DNA binding domain (amino acids 262-371), a putative coiled coil leucine zipper (Lz) region (amino acids 112-137) with the potential to promote homo- or hetero- dimerization, a highly acidic "E" region (amino acids 195-204) critical for interaction with TPX2, a mitotic spindle assembly protein, highly conserved in mammals (Figure 3.1B), an NLS (nuclear localization signal) domain (amino acids 165-187), and a threonine at position 163 that is critical for binding to 14-3-3 phospho-adapter protein (Gill et al., 2013).

First, I asked whether HELLS associated with CDCA7 in cells. HA-HELLS was detected following the immunoprecipitation of FLAG-epitope tagged CDCA7 when each were cotransfected in HEK293Ta cells (Figure 3.1). Next, I used various internal deletions with CDCA7 to test whether the 14-3-3 binding site, the NLS domain, and the acidic region were required for interaction with HELLS. HELLS coimmunoprecipitated with "wildtype" (WT)-CDCA7, the 14-3-3-binding site mutation (T163A-CDCA7), the acidic region (delta195-204-CDCA7, and the 11 amino acids immediately C-terminal to the acidic region (delta204-215-CDCA7; Figure 3.1) that could include a second 14-3-3 binding site based on sequence analysis (Gabor and Scheid, unpublished observations). Furthermore, I found that deletion of the NLS region from 165-187 also did not prevent HELLS-CDCA7 interaction (Figure 3.6) This indicates that neither the T163/AKT phosphorylation site, the NLS region, nor the acidic E region are critical for interaction of HELLS and CDCA7.

To find the site required for HELLS interaction, I performed further co-immunoprecipitation experiments using deletions of both N-terminal and C-terminal segments of CDCA7. Deletions of 230-371 and 260-371 each remove the Zn-Finger domain that has been shown to harbour mutations implicated in ICF3 (Thjissen et al., 2015). Experiments depicted in Figures 3.2, 3.3 and 3.4 showed that the loss of the C-terminal Zn-finger domain led to a reduced, but not complete loss of interaction of HELLS with CDCA7, while they revealed the N-terminal region of amino acids 1-147 to be critical for this interaction (Figure 3.3).

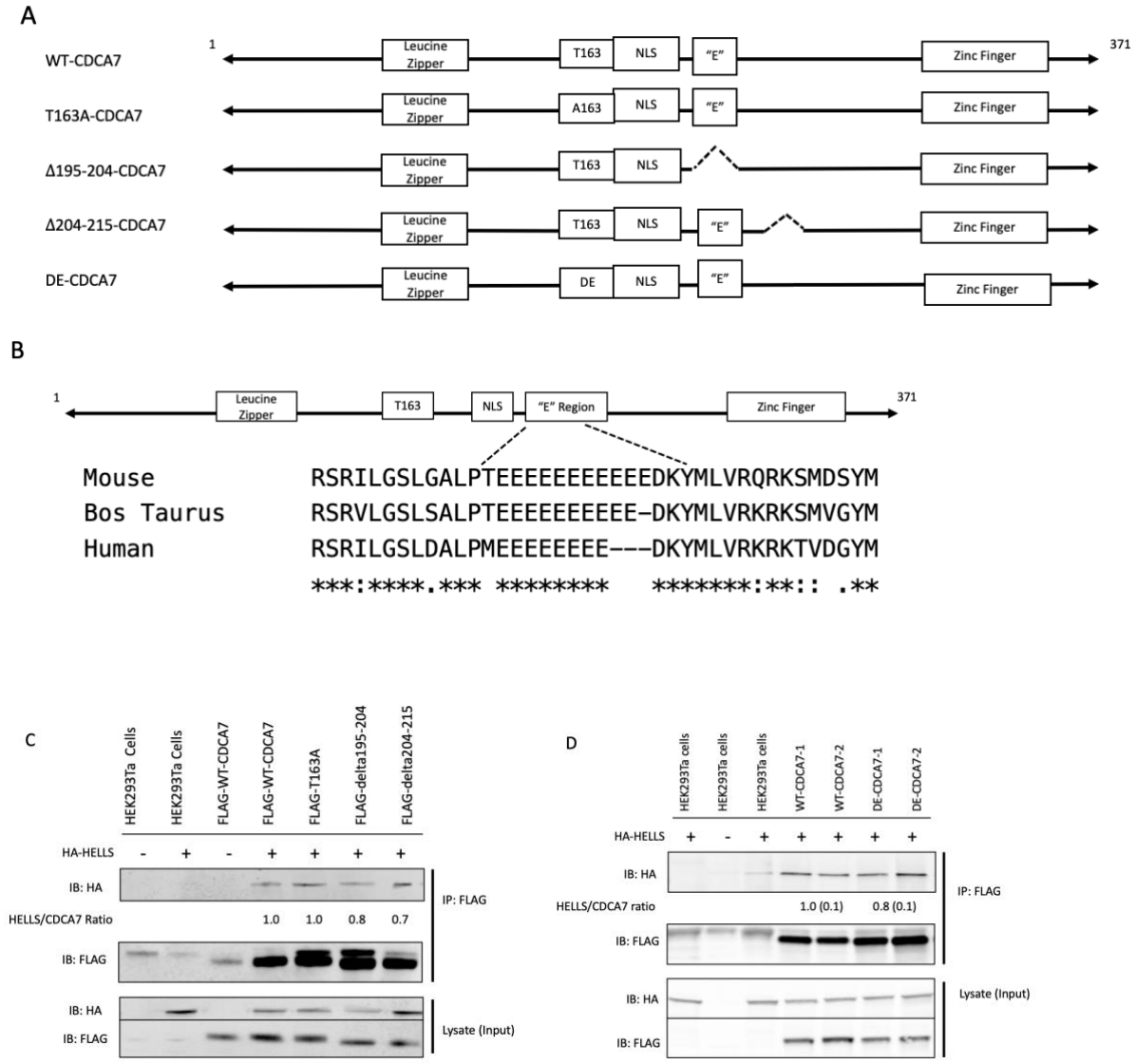

Figure 3.1. 14-3-3 binding of CDCA7 does not significantly regulate HELLS binding with CDCA7. A) Schematics of WT and mutant constructs of 3xFLAG-tagged CDCA7 used in the experiments in this figure. Mutant constructs used in this figure include T163A-CDCA7, delta 195-204-CDCA7, and delta204-215-CDCA7, and DE-CDCA7. DE-CDCA7 is the replacement of the 20 amino acids surrounding the T163 site with an R18 peptide (PHCVPRDLSWLDLEANMCLP). B) Sequence alignment of CDCA7 amino acids 204-215 indicate a highly conserved "E" region. Asterisks (*) denote identical matches while a colon (:) indicates similar matches. C) CDCA7 or various truncated versions including WT-CDCA7, T163A-CDCA7, delta195-204-CDCA7, and delta204-215-CDCA7 were transfected into cells together with HA-HELLS and subjected to pulldown by FLAG immunoprecipitation followed by immunoblotting with an anti-FLAG and anti-HA antibody. A reserved portion of the input CDCA7 and HA-HELLS was also immunoblotted. D) CDCA7 or various truncated versions including WT-CDCA7 and DE-CDCA7 were transfected into cells together with HA-HELLS and subjected to pulldown by FLAG immunoprecipitation followed by immunoblotting with an anti-FLAG and anti-HA antibody. A reserved portion of the input CDCA7 and HA-HELLS was also immunoblotted. The HELLS/CDCA7 Ratio numbers were generated determining relative enrichment. This was determined by detected HA background subtracted from the HA cotransfected with the sample of interest, normalized to WT-FLAG. Numbers within brackets (#) indicate the range of samples 1 and 2.

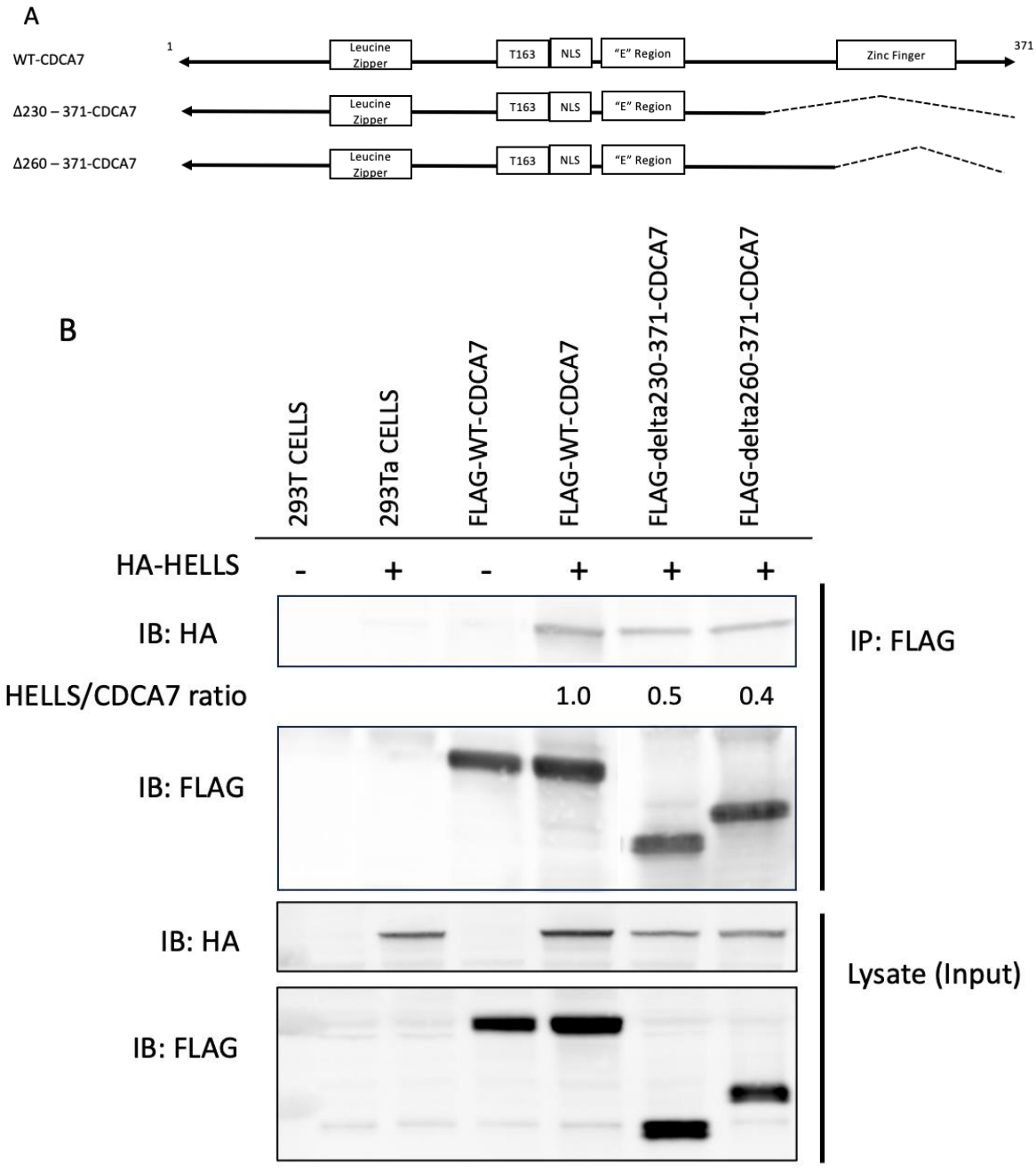

Figure 3.2. Zinc Finger DNA binding region of CDCA7 is not critical for interaction with HELLS. A) Schematics of WT-CDCA7 , delta230-371-CDCA7, and delta260-371-CDCA7 constructs used in the experiments in this figure. B) CDCA7 or various truncated versions including WT-CDCA7, delta230-371-CDCA7, and delta260-371-CDCA7 were transfected into cells together with HA-HELLS and subjected to pulldown by FLAG immunoprecipitation followed by immunoblotting with an anti-FLAG and anti-HA antibody. A reserved portion of the input CDCA7 and HA-HELLS was also immunoblotted.

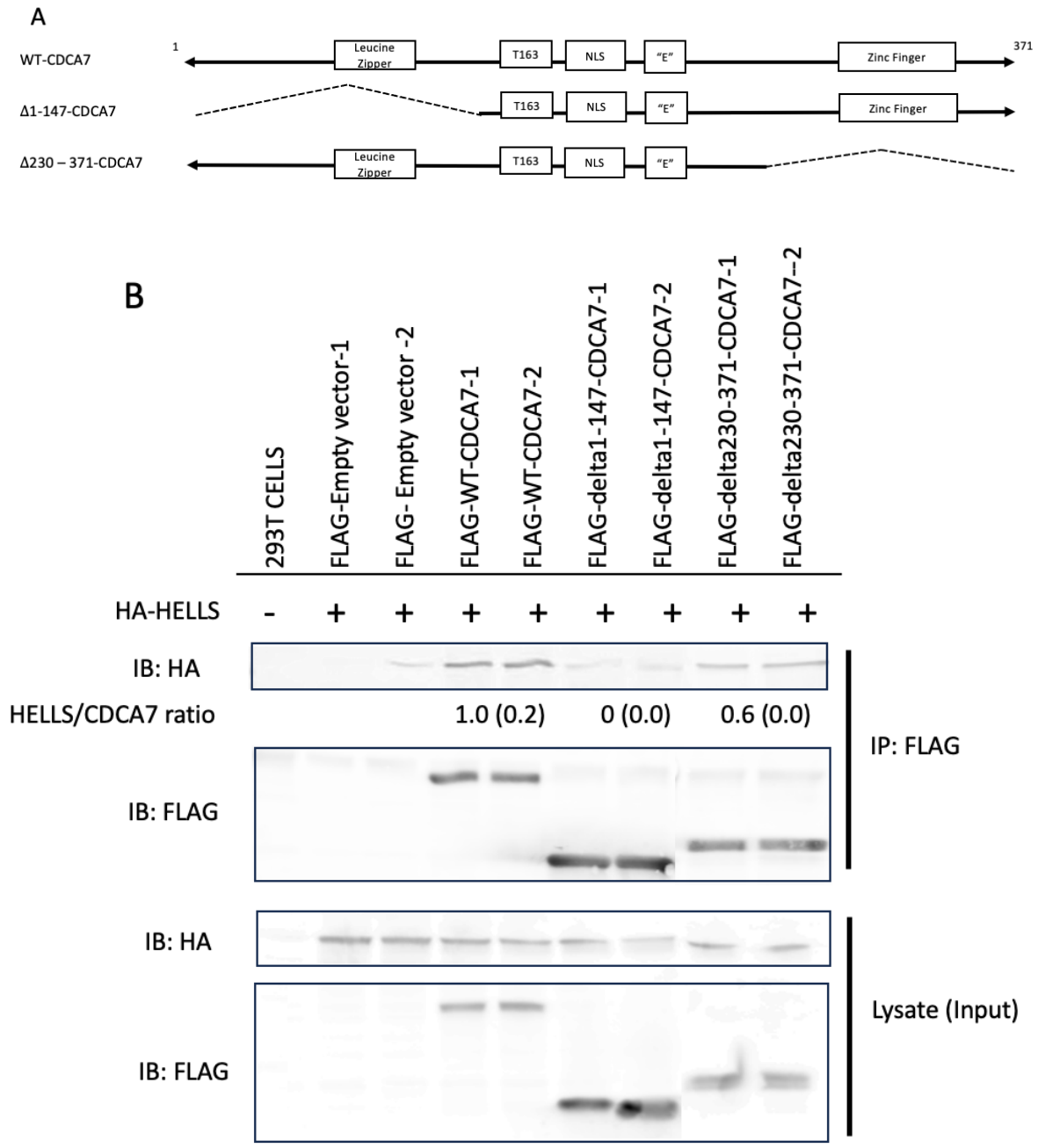

Figure 3.3. HELLS pulled down by the N-terminal region of CDCA7 but *not* by the C terminal region. A) Schematics WT-CDCA7, delta230-371-CDCA7, and delta1-147-CDCA7 constructs used in the experiments in this figure. B) CDCA7 or various truncated versions including WT-CDCA7, delta230-371-CDCA7, and delta1-147-CDCA7 were transfected into cells together with HA-HELLS and subjected to pulldown by FLAG immunoprecipitation followed by immunoblotting with an anti-FLAG, anti-PT163-CDCA7 and anti-HA antibody. A reserved portion of the input CDCA7 and HA-HELLS was also immunoblotted.

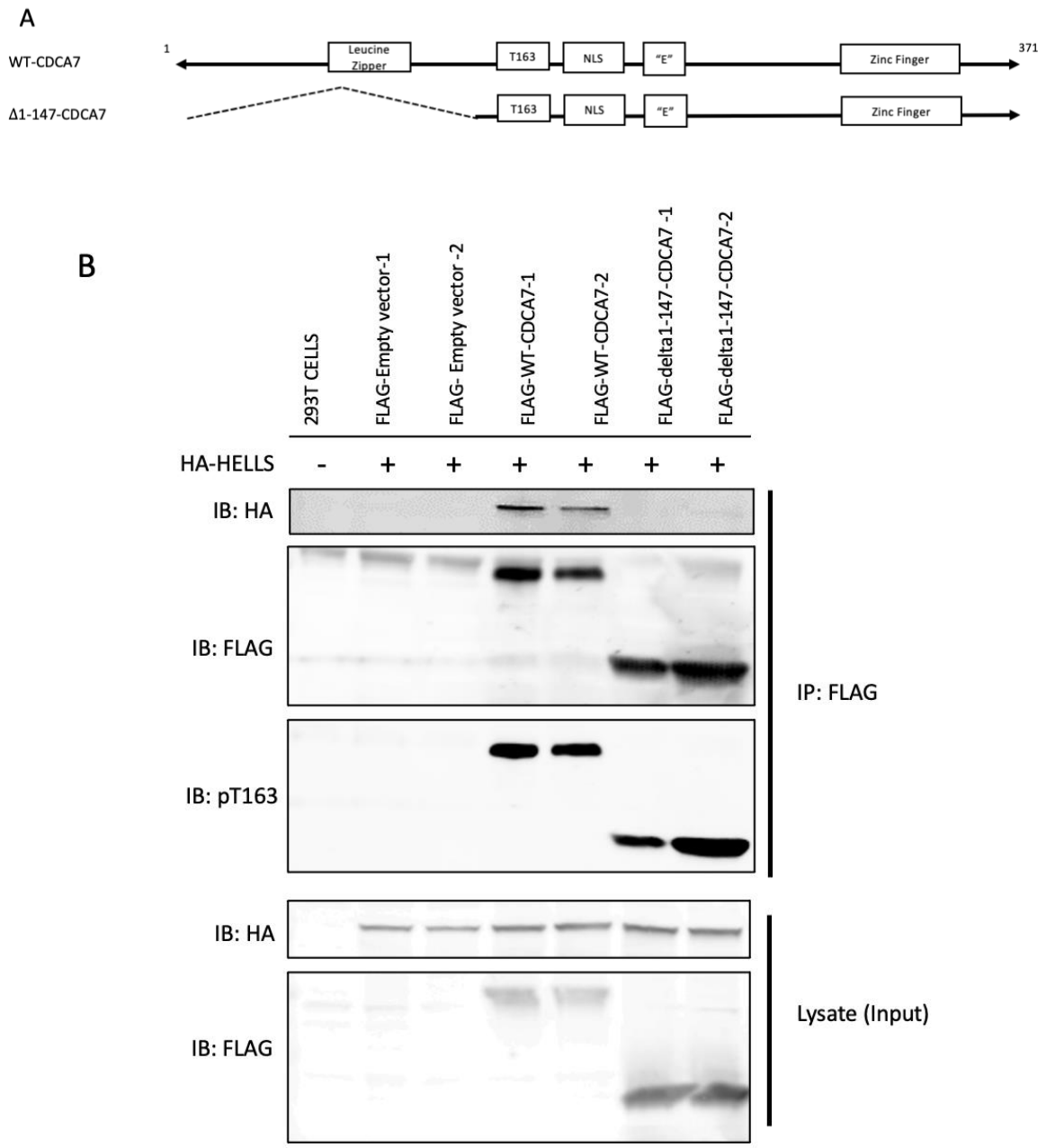

Figure 3.4. HELLS pulled down by the N-terminal region of CDCA7. A) Schematics of WT-CDCA7 and delta1-147-CDCA7 constructs used in the experiments in this figure. B) CDCA7 or various truncated versions including WT-CDCA7 delta1-147-CDCA7 were transfected into cells together with HA-HELLS and subjected to pulldown by FLAG immunoprecipitation followed by immunoblotting with an anti-FLAG, anti-PT163-CDCA7 and anti-HA antibody. A reserved portion of the input CDCA7 and HA-HELLS was also immunoblotted.

HELLS Requires CDCA7- Leucine Zipper Region for Interaction.

The N-terminal region is interesting since it contains a postulated leucine zipper region at amino acids 112-137. Leucine zippers are a protein-protein interaction domain and tend to be formed classically by two proteins each with a region of approximately 4 or more leucines or isoleucines spaced approximately 7 amino acids apart, forming a coiled-coil (Krylov et al., 2001) (Figure 3.5). Additionally, when the amino acid sequence of CDCA7 was analyzed by Alpha fold and Rosetta fold software and reconciled using Pymol, this region of amino acids predicts an alpha helical coiled coil structure (Figure 3.5). Additionally, approximately every ~7 amino acids are a leucine or isoleucine that is reported by the literature to be typical of the structure of the distinctive "leucine zipper" alpha helix (Figure 3.5). Therefore, I formed the hypothesis that this region is a putative leucine zipper, and set out to test if it is necessary for CDCA7 interaction with HELLS.

To test this hypothesis, I expressed a truncated form of CDCA7 with the amino acids 112-137 removed by site directed mutagenesis. Compared to wildtype CDCA7, loss of the putative Lz completely abolished HELLS association (Figure 3.6). This suggested that the 112-137 region was critical for HELLS and CDCA7 interaction.

To further investigate the role of the leucine rich region of 112-137 in association with HELLS, the specific leucines between amino acids 112-137 were mutated to alanine. First, I investigated this with a single mutation of leucine 129 to alanine and compared this with the loss of the entire region (Figure 3.7). While loss of the 112-137 amino acids showed a complete loss of HELLS interaction with CDCA7, the L129 to alanine mutation resulted a significant decrease but not complete loss of HELLS interaction.

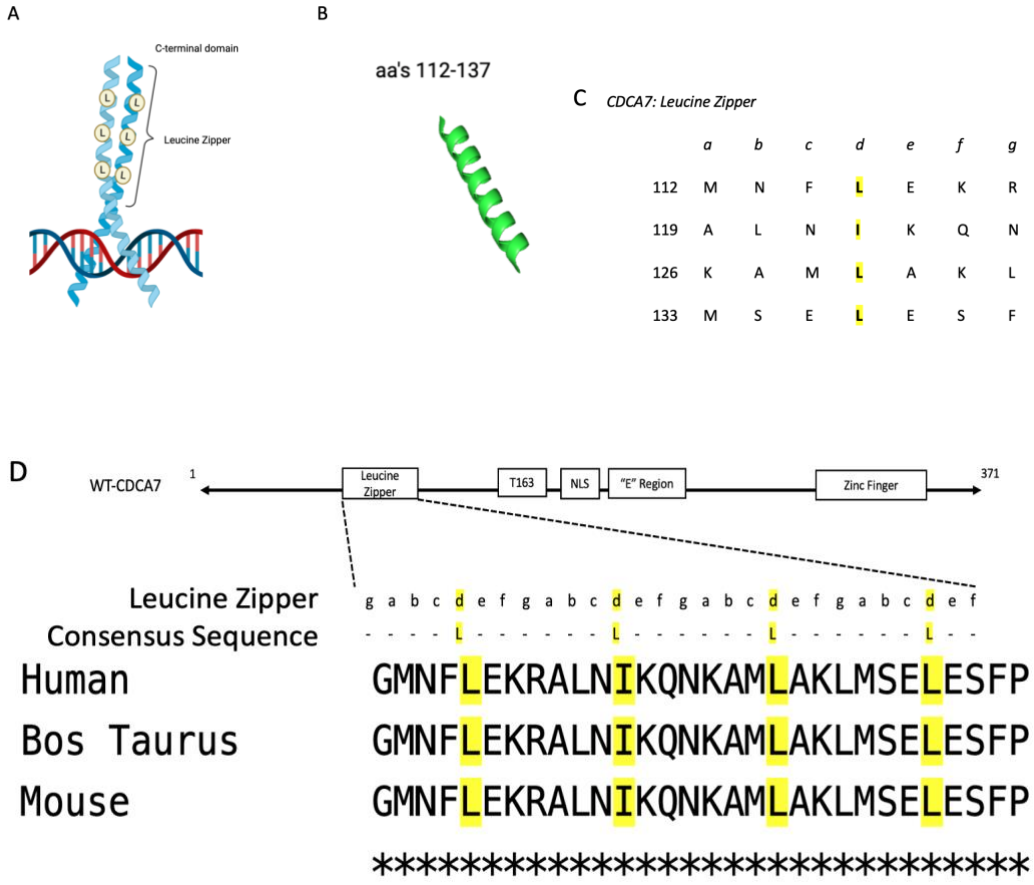

Figure 3.5. A) Leucine zippers are a protein-protein interaction domain and tend to be formed classically by two proteins each with a region of approximately 4 or more leucines or isoleucines spaced approximately 7 amino acids apart, forming a coiled-coil (Krylov et al., 2001). Image created using Biorender.com. B) Pymol computer programming software generates a coiled coil alpha helix structure based on the amino acids 112-137 sequence input of CDCA7 using alphafold and rosettafold software DeLano, W. L. (2002). The PyMOL Molecular Graphics System. Retrieved from https://pymol.org/. C) CDCA7 amino acid sequence from 111-138 shows the repeating sequence of leucines or isoleucines in the same position (Uniprot.org). D) Construct of WT-CDCA7 showing the amino acid sequence of aa's 112-137 compared with the leucine zipper consensus sequence. This sequence is highly conserved among mammals.

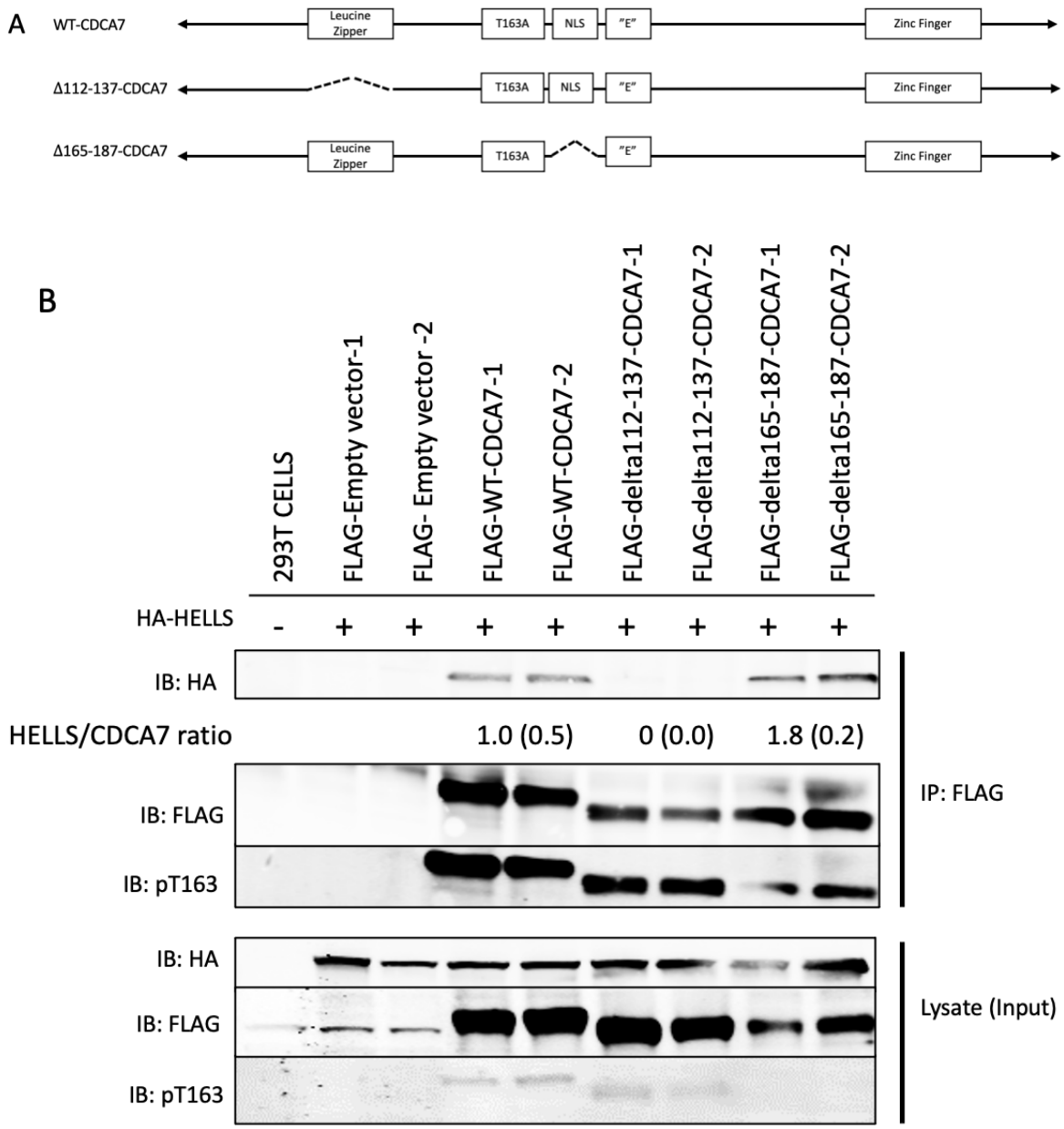

Figure 3.6. HELLS associates with the putative Leucine Zipper region (aa's 112-137) of CDCA7. A) Schematics of WT-CDCA7, delta112-137-CDCA7, and delta165-187-CDCA7 (containing a nuclear localization signal) constructs used in the experiments in this figure. B) CDCA7 or various truncated versions including WT-CDCA7, delta112-137-CDCA7, and delta165-187-CDCA7 were transfected into cells together with HA-HELLS and subjected to pulldown by FLAG immunoprecipitation followed by immunoblotting with an anti-FLAG, anti-PT163-CDCA7 and anti-HA antibody. A reserved portion of the input CDCA7 and HA-HELLS was also immunoblotted.

Next, I introduced compound mutations of various Leucines within the Lz region. While loss of the 112-137 amino acids showed a complete loss of HELLS interaction with CDCA7, the double compound mutations of L115A:L120A and the L129A:L132A mutations resulted in a significant decrease but not complete loss of HELLS interaction (Figure 3.8).

Finally, I generated a construct containing four mutations, and which included two leucines within row "e" of the consensus leucine zipper sequence (L115, L129) and two adjacent leucines (L120, L132) (Figure 3.5, 3.9). Mutation of these four leucines resulted in a complete loss of HELLS interaction with CDCA7.

Taken together, these results indicate a leucine zipper region with a coiled coil alpha helical structure exists at this region of amino acids between 112-137 within CDCA7 and this structure is required for successful CDCA7 and HELLS interaction.

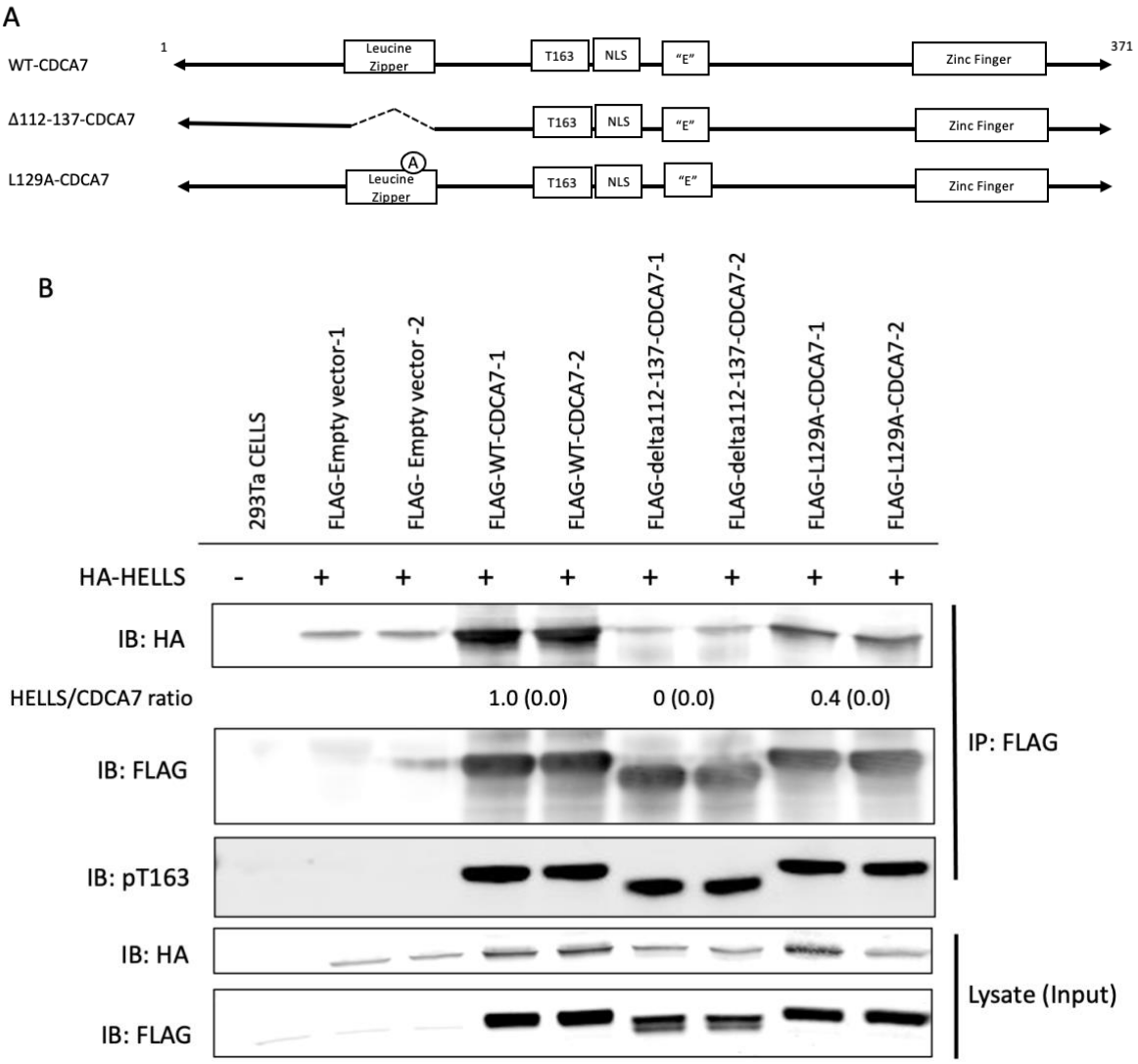

Figure 3.7. **HELLS association with CDCA7 regulated by the Leucines within the Leucine Zipper region (aa's 112-137).** A) Schematics of WT-CDCA7, delta112-137-CDCA7, and deltaL129A CDCA7 constructs used in the experiments in this figure. B) CDCA7 or various truncated versions including WT-CDCA7, delta112-137-CDCA7, and deltaL129A-CDCA7 were transfected into cells together with HA-HELLS and subjected to pulldown by FLAG immunoprecipitation followed by immunoblotting with an anti-FLAG, anti-PT163-CDCA7 and anti-HA antibody. A reserved portion of the input CDCA7 and HA-HELLS was also immunoblotted.

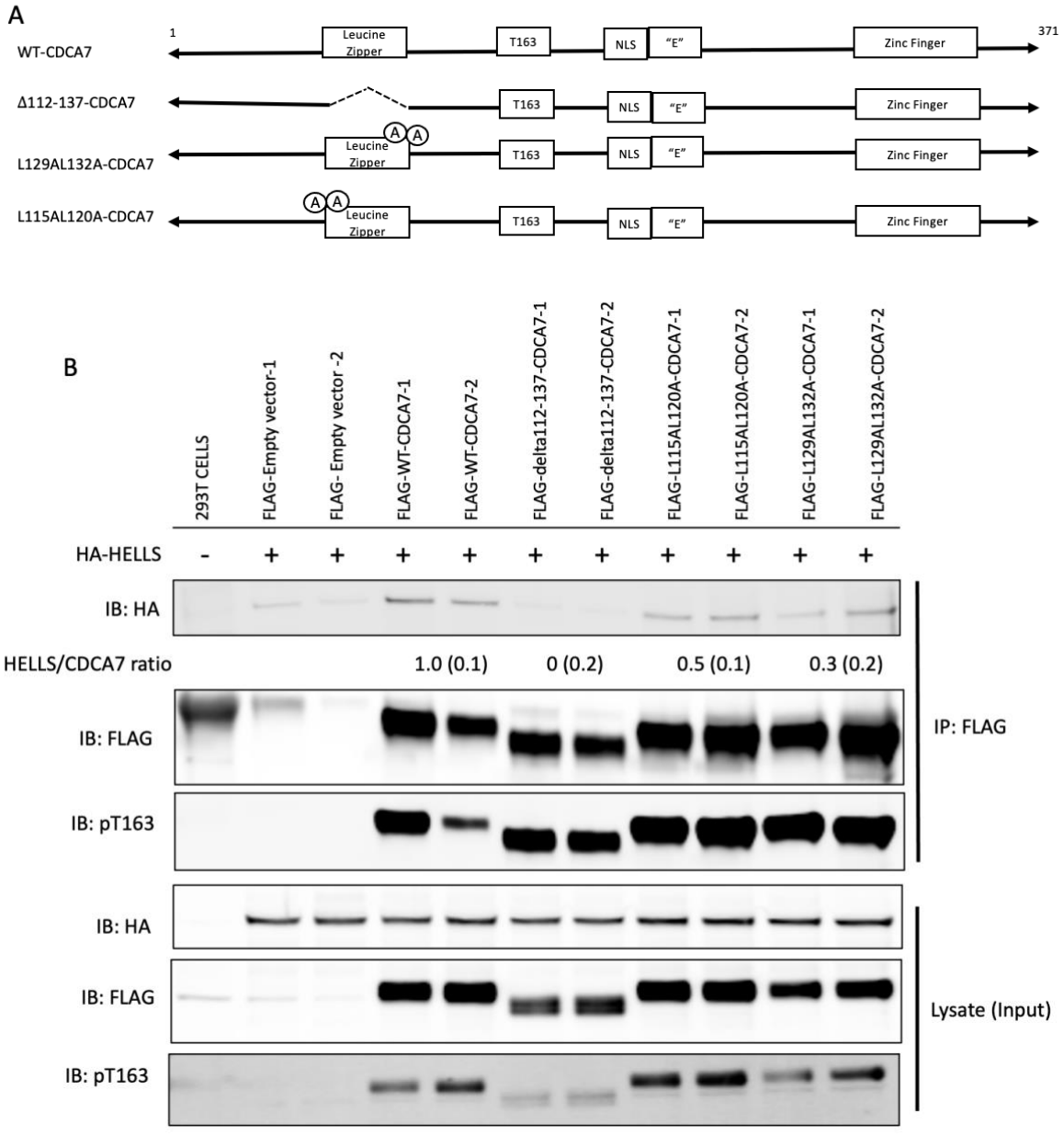

Figure 3.8. **HELLS association with CDCA7 regulated by the Leucines within the Leucine Zipper region (aa's 112-137).** A) Schematics of WT-CDCA7, delta112-137-CDCA7, L115AL120A-CDCA7 and L129AL132A-CDCA7 constructs used in the experiments in this figure. B) CDCA7 or various truncated versions including WT-CDCA7, delta112-137-CDCA7, L115AL120A-CDCA7 and L129AL132A-CDCA7 were transfected into cells together with HA-HELLS and subjected to pulldown by FLAG immunoprecipitation followed by immunoblotting with an anti-FLAG, anti-PT163-CDCA7 and anti-HA antibody. A reserved portion of the input CDCA7 and HA-HELLS was also immunoblotted.

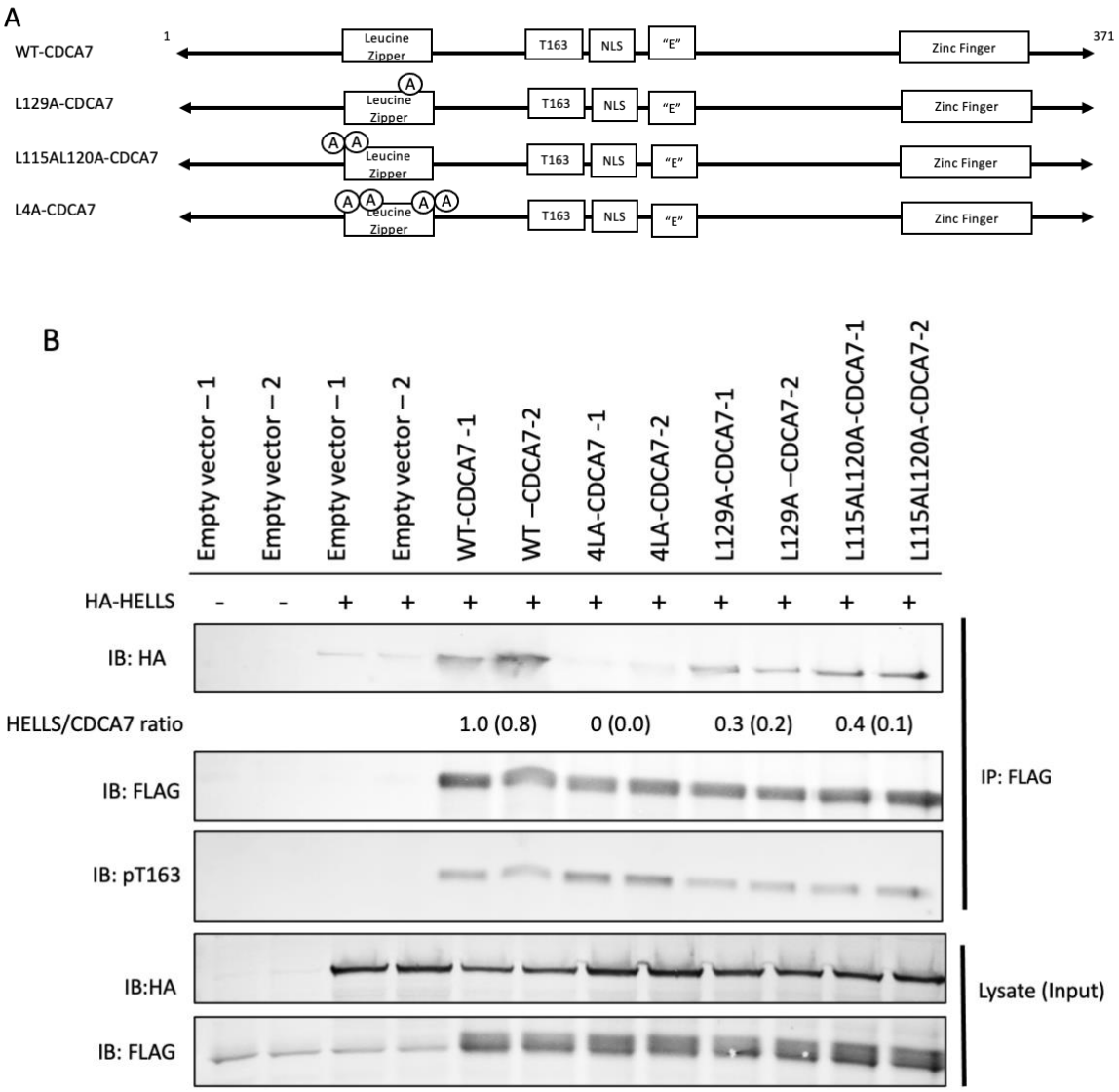

Figure 3.9. HELLS association with CDCA7 regulated by the Leucines within the Leucine Zipper region (aa's 112-137).A) Schematics of WT-CDCA7, 4LA-CDCA7, L129A-CDCA7 and L115AL120A-CDCA7 constructs used in the experiments in this figure. B) CDCA7 or various truncated versions including WT-CDCA7, 4LA-CDCA7, L129A-CDCA7 and L115AL120A-CDCA7 were transfected into cells together with HA-HELLS and subjected to pulldown by FLAG immunoprecipitation followed by immunoblotting with an anti-FLAG, anti-PT163-CDCA7 and anti-HA antibody. A reserved portion of the input CDCA7 and HA-HELLS was also immunoblotted.

NHEJ protein Ku80 and DNA damage marker γ--H2AX interaction with CDCA7 is regulated by 14-3-3.

Previous work by others have shown that the NHEJ and DNA damage repair proteins Ku80, Ku70 and γ-H2AX interact with CDCA7 (Unoki et al., 2019). As I have shown that HELLs interaction requires the Lz region, I was curious if Ku70/80 and γ-H2AX association also requires the leucine rich region of 112-137 of CDCA7.

To test this, I immunoprecipitated CDCA7 from cells and found that endogenous Ku80 and Ku70 associated with CDCA7 (Figure 3.10). Since Ku80 is considered the more significant protein involved in recruiting PKcs (Protein Kinase catalytic subunit) and allowing for NHEJ activity (Nussenzweig et al.,1996), I focused on investigating the Ku80 and CDCA7 interaction.

Next, I tested whether the leucine-rich region of 112-137 was required for association with Ku80, as it was for HELLs. So, I transfected cells with CDCA7 or CDCA7 with the 112-137 deletion. Surprisingly, more Ku80 was co-immunoprecipitated with Delta-112-137 CDCA7 than wildtype CDCA7 (Figure 3.11), indicating that this region negatively regulates association with CDCA7. Similarly, γ-H2AX was also enriched following CDCA7 immunoprecipitation when the 112-137 region was deleted (Figure 3.11).

Since 14-3-3 regulates the interaction of CDCA7 with other proteins such as MYC, I asked if threonine 163 phosphorylation, or constitutive 14-3-3 binding independent of threonine 163 phosphorylation versus prevention of 14-3-3 binding could regulate this interaction of Ku80 and γ-H2AX with CDCA7. To do this, I employed various mutations within CDCA7: The T163A substitutes alanine for the threonine and prevents 14-3-3 binding, as work from our group

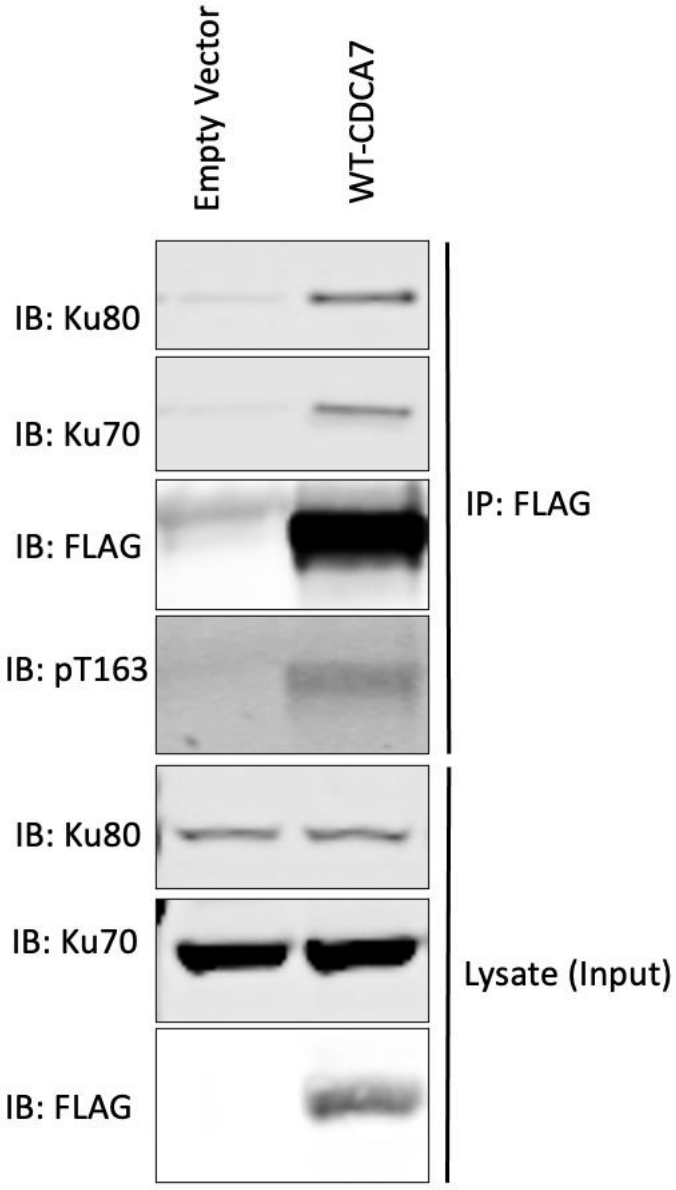

Figure 3.10. Ku80 and Ku70 associates with CDCA7. A) CDCA7 or Empty Vector were transfected into cells and subjected to pulldown by FLAG immunoprecipitation followed by immunoblotting with an anti-FLAG, anti-Ku80 (Sigma), anti-Ku70 (Sigma) and anti-pT163 antibody. A reserved portion of the input CDCA7 and HA-HELLS was also immunoblotted.

have previously demonstrated (Gill et al, 2013). To promote constitutive 14-3-3 binding, I used a version of CDCA7 where the region around T163 was replaced with a 20 amino acids sequence call the R18 peptide (PHCVPRDLSWLDLEANMCLP). This peptide was isolated from a phage display screen for peptides that bind strongly to 14-3-3, and this construct version in this thesis is referred to as "DE-CDCA7".

I expressed WT-CDCA7, T163A-CDCA7 and DE-CDCA7, and performed co-immunoprecipitation of Ku80. In Figures 3.11, 3.12, and 3.13, I found that T163A mutation, which abolishes 14-3-3 binding, increased the association of Ku80. Constitutive 14-3-3 binding to DE-CDCA7 significantly reduced Ku80 binding. Therefore, 14-3-3 binding negatively regulates Ku80 association.

Next, I examined another protein known to associate with CDCA7 in the DNA damage repair pathway complex, γ-H2AX. In Figures 3.11, 3.12, and 3.13, I found that endogenous γ-H2AX immunoprecipitated with WT-CDCA7, T163A-CDCA7 but not with DE-CDCA7. To confirm that the R18 peptide substitution within CDCA7 as not preventing association independent of 14-3-3 binding, I used a loss-of-14-3-3 binding version, termed KK, which substitutes the D and E amino acids in the R18 peptide and completely prevents 14-3-3 binding. Expression of KK-CDCA7 rescued the γ-H2AX association with CDCA7. Therefore, 14-3-3 binding negatively regulates γ-H2AX association. Additionally, like Ku80, loss of 112-137 led to increased association of γ-H2AX (Figure 3.11).

I next asked if HELLs, when bound to the Lz region of 112-137, influences the association of Ku80, as I found earlier (Fig 3.11) that this region negatively regulates Ku80/γ-H2AX association. It is possible that HELLS, when bound to the Lz, may compete with Ku80 for binding with CDCA7. To test this, HELLS or empty vector control was cotransfected with

CDCA7 and immunoprecipitated. Figure 3.14 shows that while there was an increase in Ku80 detection when the 112-137 region was removed, there was no statistically significant decrease in Ku80 detected when HELLS was cotransfected, indicating HELLS does not regulate this interaction.

In summary, the constitutive 14-3-3 binding of CDCA7 (DE-CDCA7) resulted in a significant decrease in interaction of Ku80 and γ-H2AX with CDCA7, and this interaction is rescued to WT-CDCA7 level by the removal of the D and E residues critical for 14-3-3 interaction with CDCA7 (KK-CDCA7). Similarly, the loss of the Lz region of CDCA7 showed a twofold enhanced interaction with Ku80, and the loss of Threonine 163 phosphorylation (T163A-CDCA7) showed a five-fold increase in interaction of Ku80 with CDCA7. These results show for the first time that 14-3-3 is a modulator of CDCA7 interaction with NHEJ proteins Ku80 and DNA damage protein γ-H2AX, indicating 14-3-3's role in mediating CDCA7 participation in NHEJ and DNA damage repair.

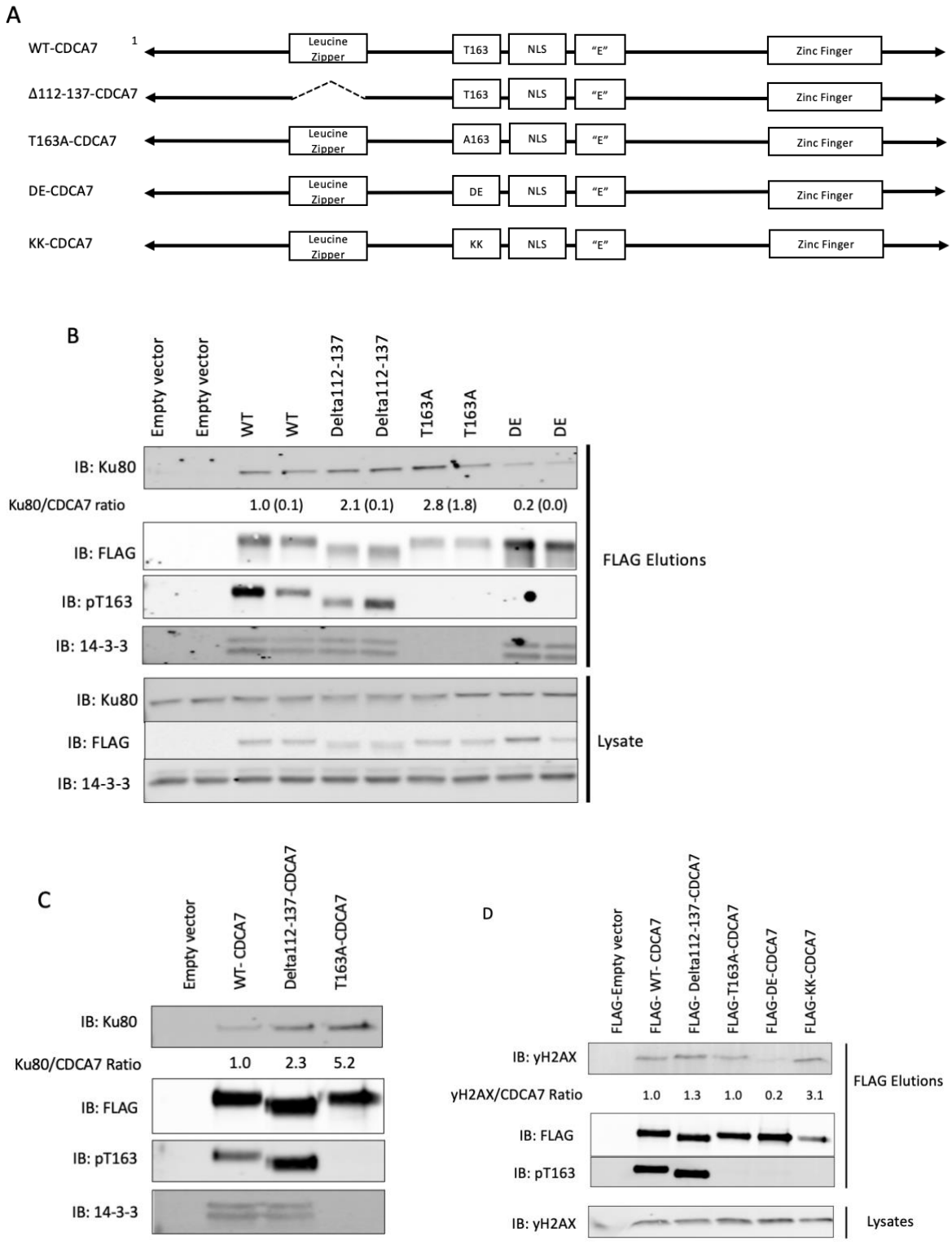

Figure 3.11. Ku80, Ku70 and γ-H2AX interact with WT-CDCA7, and this interaction is enhanced by prevention of 14-3-3 binding. A) Schematics of WT-CDCA7, T163A-CDCA7, DE-CDCA7 and KK-CDCA7 constructs used in the experiments in this figure. T163A prevents phosphorylation of CDCA7 by AKT, , anti-14-3-3, anti-FLAG, and anti-PT163 antibody. A reserved portion of the input was also immunoblotted.

preventing 14-3-3 from binding CDCA7. DE-CDCA7 is the replacement of the 20 amino acids surrounding the T163 site with an R18 peptide (PHCVPRDLSWLDLEANMCLP). The "KK-CDCA7" construct is the replacement of the D and E residues that form contacts with 14-3-3 and are substituted for phospho-amino acids, resulting in complete prevention of 14-3-3 binding. B) CDCA7 or various truncated versions including WT-CDCA7, delta112-137, T163A-CDCA7, DE-CDCA7 were transfected into cells and subjected to pulldown by FLAG immunoprecipitation followed by immunoblotting with an anti-Ku80, anti-γ-H2AX, anti-14-3-3, anti-FLAG, and anti-PT163 antibody. A reserved portion of the input was also immunoblotted. C) CDCA7 or various truncated versions including WT-CDCA7, delta112-137, and T163A-CDCA7 were transfected into cells and subjected to pulldown by FLAG immunoprecipitation followed by immunoblotting with an anti-Ku80, anti-14-3-3, anti-FLAG, and anti-PT163 antibody. A reserved portion of the input was also immunoblotted. D) CDCA7 or various truncated versions including WT-CDCA7, delta112-137, T163A-CDCA7, DE-CDCA7 and KK-CDCA7 were transfected into cells and subjected to pulldown by FLAG immunoprecipitation followed by immunoblotting with an anti-γ-H2AX

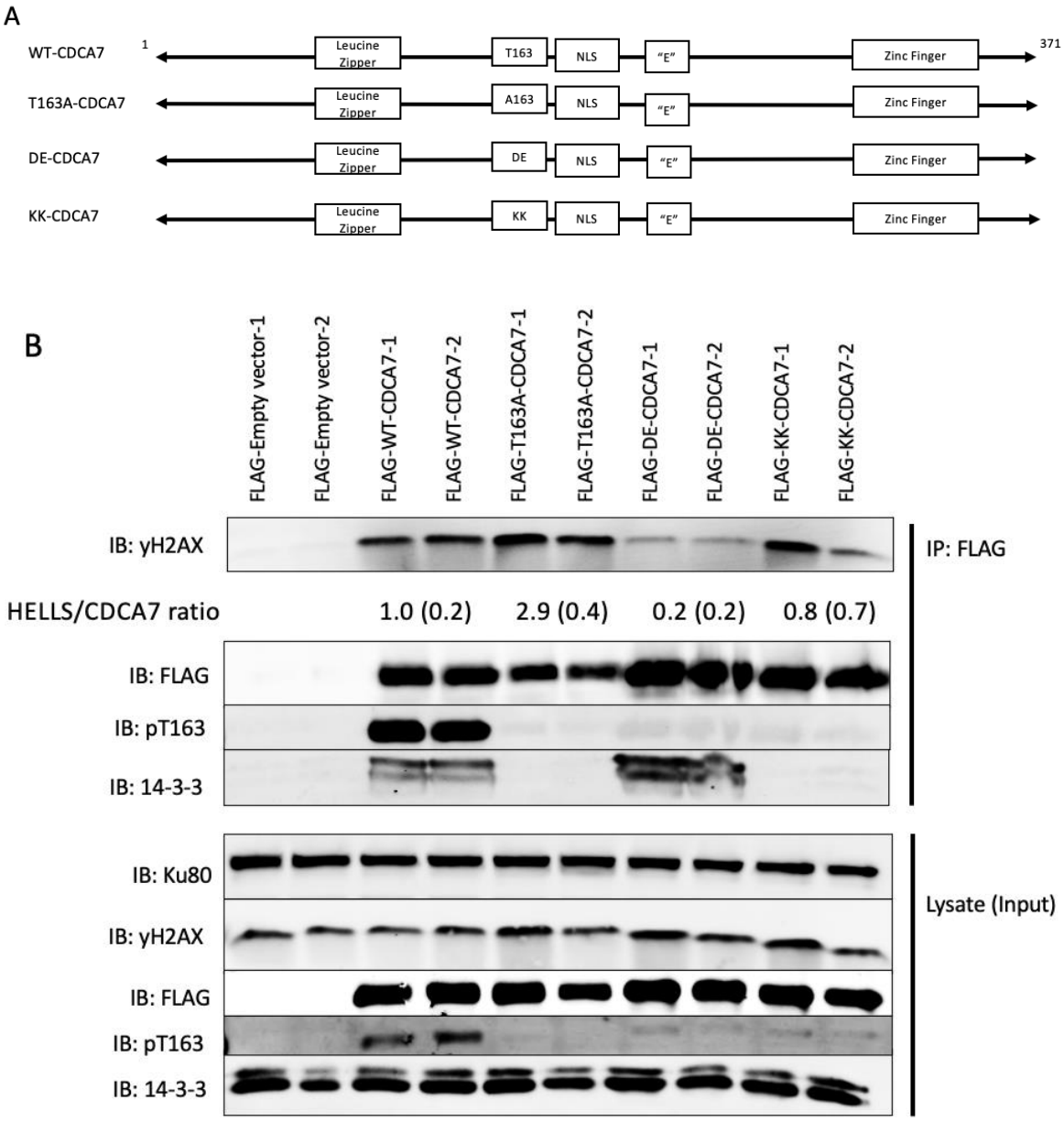

Figure 3.12. γ-H2AX interaction with CDCA7 is regulated by 14-3-3. A) Schematics of WT-CDCA7, T163A-CDCA7, DE-CDCA7 and KK-CDCA7 constructs used in the experiments in this figure. T163A prevents phosphorylation of CDCA7 by AKT, preventing 14-3-3 from binding CDCA7. DE is the replacement of the NLS signal of CDCA7 with a sequence that constitutively binds 14-3-3, while KK replaces the D and E residues within that sequence causing 14-3-3 to not bind at all. B) Duplicate samples of CDCA7 or various truncated versions including WT-CDCA7, T163A-CDCA7, DE-CDCA7 and KK-CDCA7 were transfected into cells and subjected to pulldown by FLAG immunoprecipitation followed by immunoblotting with an anti-γ-H2AX, anti-14-3-3, anti-FLAG, and anti-PT163 antibody. A reserved portion of the input was also immunoblotted.

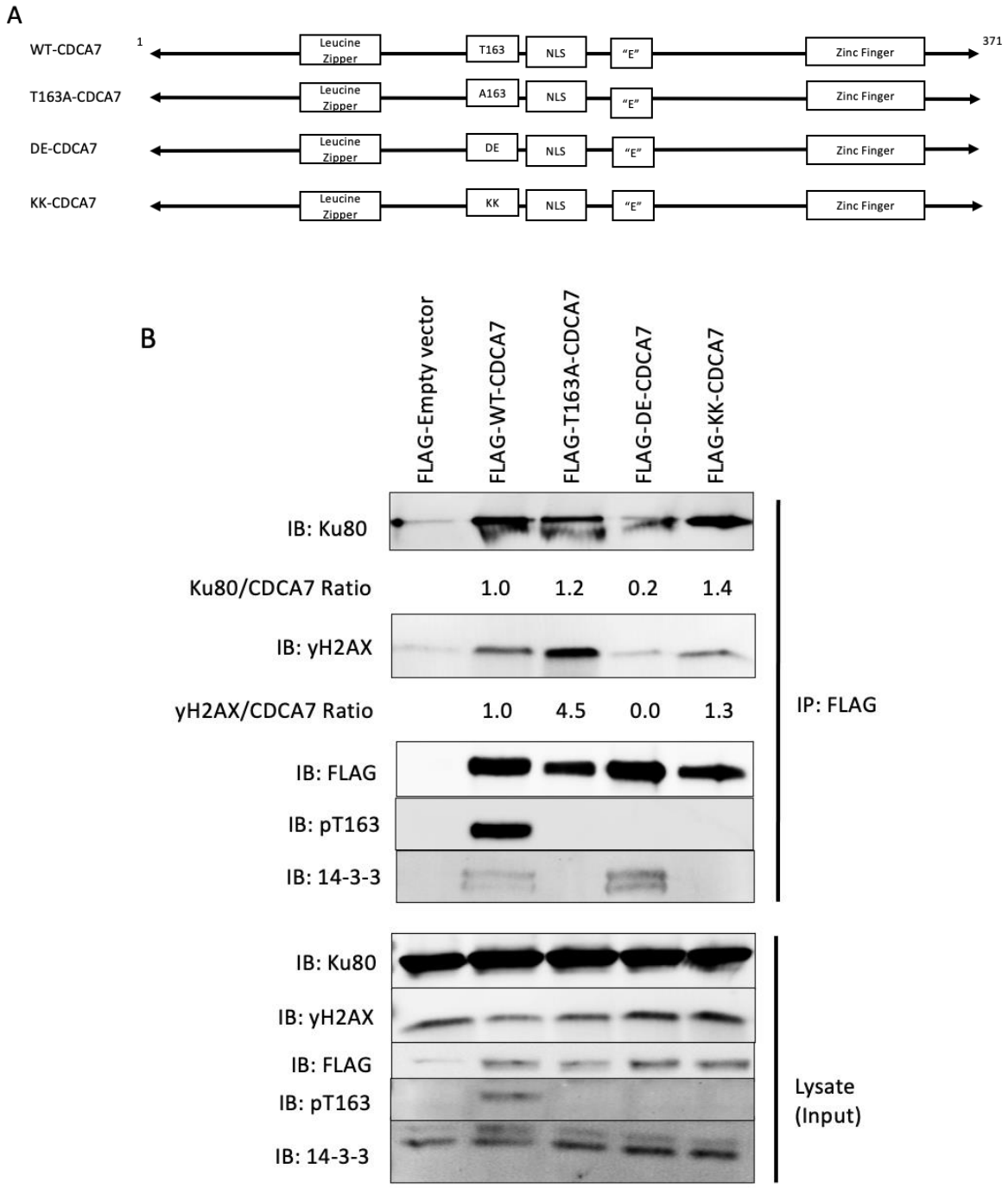

Figure 3.13. Ku80, Ku70 and γ-H2AX interaction with CDCA7 is regulated by 14-3-3. A) Schematics of WT-CDCA7, T163A-CDCA7, DE-CDCA7 and KK-CDCA7 constructs used in the experiments in this figure. T163A prevents phosphorylation of CDCA7 by AKT, preventing 14-3-3 from binding CDCA7. DE is the replacement of the NLS signal of CDCA7 with a sequence that constitutively binds 14-3-3, while KK replaces the D and E residues within that sequence causing 14-3-3 to not bind at all. B) CDCA7 or various truncated versions including WT-CDCA7, T163A-CDCA7, DE-CDCA7 and KK-CDCA7 were transfected into cells and subjected to pulldown by FLAG immunoprecipitation followed by immunoblotting with an anti-Ku80, anti-γ-H2AX, anti-14-3-3, anti-FLAG, and anti-PT163 antibody. A reserved portion of the input was also immunoblotted.

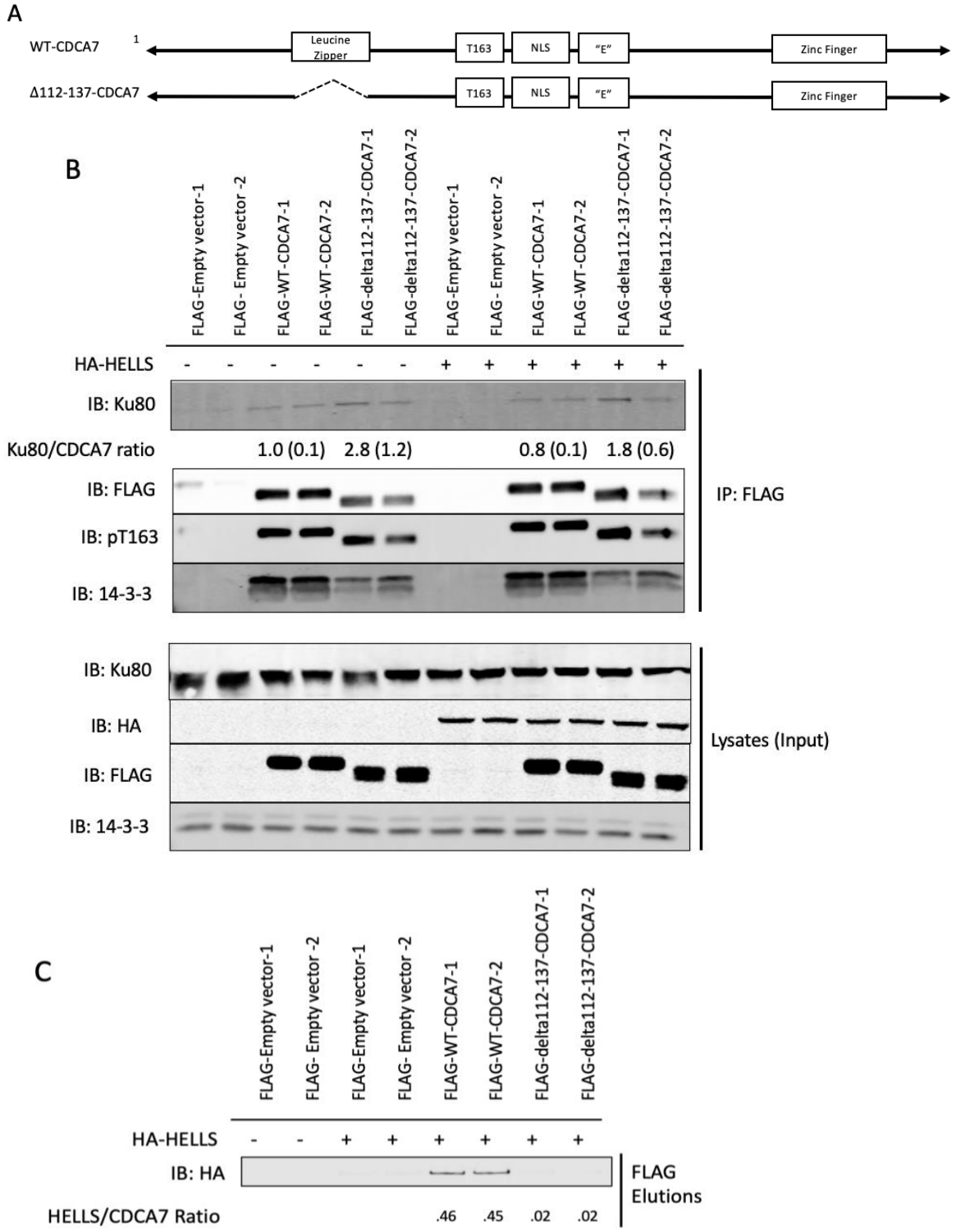

Figure 3.14. Ku80 interaction with CDCA7 is enhanced by 112-137 deletion and is not regulated by HELLS. A) Schematics of WT-CDCA7 and delta112-137-CDCA7 constructs used in this experiment. B) CDCA7 or various truncated versions including WT-CDCA7 and delta112-137-CDCA7 were cotransfected with HA-HELLS. Lysates were subjected to pulldown by FLAG immunoprecipitation followed by immunoblotting with an anti-Ku80, anti-HA, anti-14-3-3, anti-FLAG, and anti-PT163 antibody. A reserved portion of the input was also immunoblotted.

No Effect by Doxorubicin on CDCA7 association with NHEJ proteins was Detected.

Doxorubicin causes DNA damage and has previously been shown to initiate DNA damage repair that involves the DNA damage proteins Ku80 and γ-H2AX (Kurz et al., 2004). Further, others have shown that doxorubicin leads to increased AKT activation and phosphorylation of DNA damage targets (Bezler et al., 2012), which could include CDCA7. Therefore, my hypothesis is that doxorubicin-induced DNA damage could initiate a change in association between CDCA7 and Ku80/γ-H2AX.

To first confirm the efficacy of the drug, I performed a cell proliferation assay (Figure 3.16). HEK293T cells were seeded, and various concentrations of doxorubicin was added. After 48 hours, cells were counted. Figure 3.16 shows that doxorubicin inhibited HEK293Ta cell proliferation at all concentrations from 0.1 to 1.0 uM.

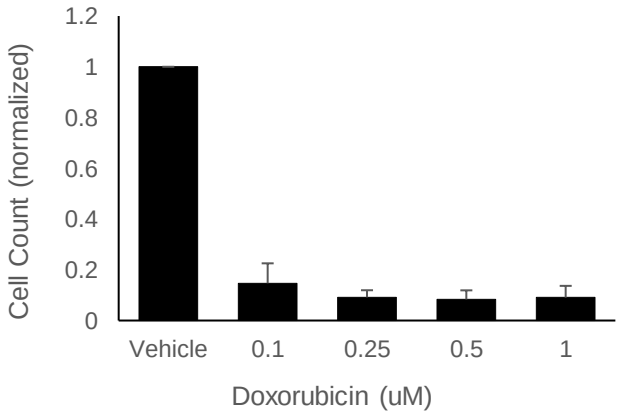

Figure 3.15. Doxorubicin causes decrease in proliferation in HEK293Ta cells. 50,000 HEK293T cells were seeded in 6 well plates. After 24 hours, various concentrations **(0.1, 0.25, 0.5 and 1 uM)** of doxorubicin was added to each well vs Water as a vehicle control and allowed to incubate at 37 degrees incubator for 48 hours. Supernatant was collected, cells rinsed with PBS, cells trypsinized, trypsin deactivated by addition of DMEM media, collected, and pelleted for 5 minutes at 1200 rpm. The supernatant was removed, and cells resuspended in 1-2 ml of DMEM media. Cell suspension was mixed 50:50 with 0.25% trypan blue, and 15 ul mounted on a hemocytometer and counted the number of viable cells. Multiple trials (>3) were conducted to confirm results.

Next, I wanted to see if there would be an effect of doxorubicin on CDCA7 association with NHEJ proteins Ku80 and γ-H2AX. Figure 3.17 shows how no effect was detected in the relationship of transiently transfected WT-CDCA7 and endogenous Ku80 and γ-H2AX for response to doxorubicin, or proposed DNA damage. Water or 1uM doxorubicin was added to HEK293T cells transfected with FLAG epitope tagged WT-CDCA7 or FLAG epitope tagged Empty Vector at 24 hours. Ku80 and γ-H2AX was detected evenly indicating no significant effect by doxorubicin versus water. This suggested no functional change in this relationship caused by doxorubicin in HEK293Ta cells.

Finally, I investigated the possibility of a dose dependency of doxorubicin effect on CDCA7 function. Figure 3.18 shows an experiment where either Empty vector or WT-CDCA7 was subjected to 0.1, 0.25, 0.5, or 1 uM of doxorubicin. Water or doxorubicin was added to Empty Vector or WT-CDCA7 at 24 hours before harvest. Lysate was incubated with FLAG beads. Samples were immunoblotted for anti-FLAG, anti-pT163, anti-14-3-3, and anti-γ-H2AX. γ-H2AX, 14-3-3, and FLAG and pT163 was detected evenly in all transfected samples, indicating no significant effect by doxorubicin versus water. This suggested no functional change in this relationship caused by doxorubicin in HEK293Ta cells.

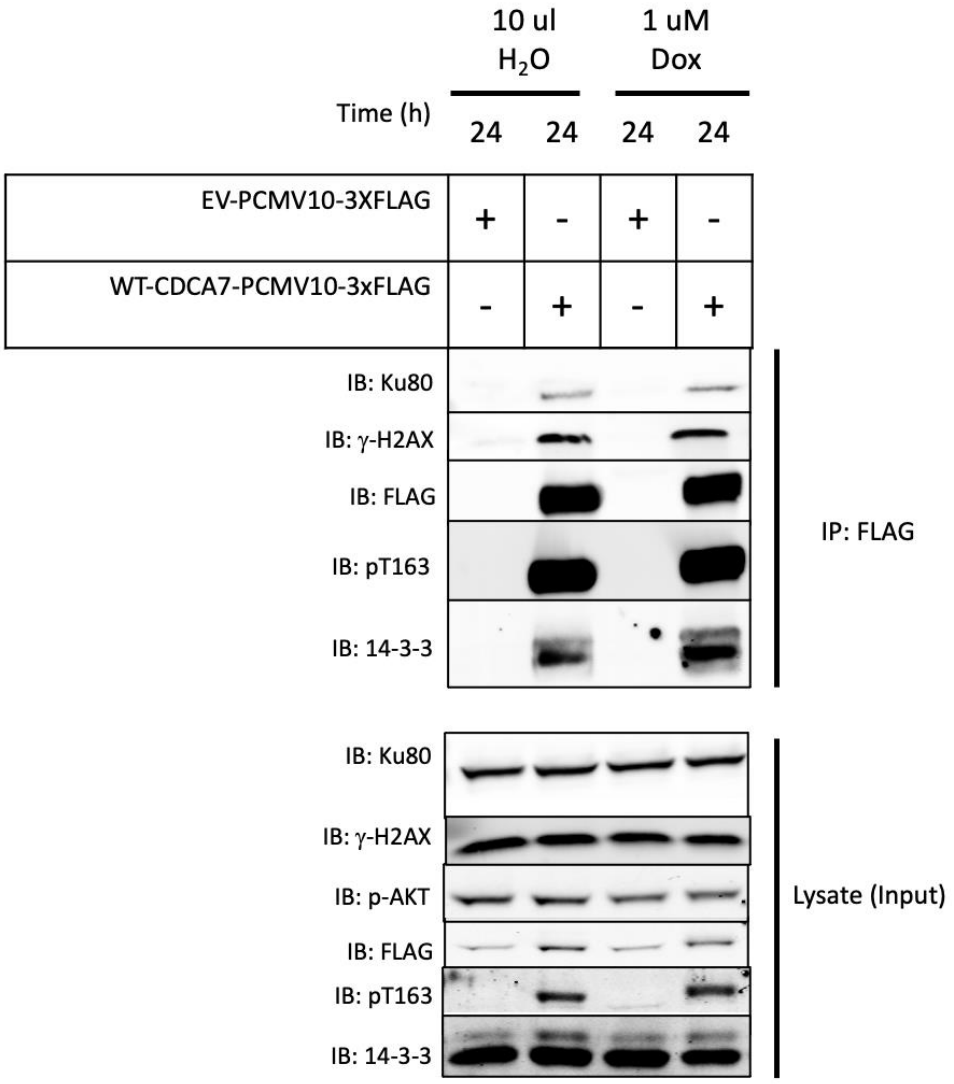

Figure 3.16. No effect of doxorubicin on CDCA7 interaction with DNA damage associated proteins Ku80 and γ-H2AX. Water or 1uM doxorubicin was added to HEK293T cells transfected with FLAG tagged WT-CDCA7 or FLAG tagged Empty Vector 24 hours before harvest. Cells were lysed, sonicated, and immunoprecipitated with FLAG beads. Samples were western blotted for anti-ku80, anti-FLAG, anti-pT163, anti-14-3-3, and anti-γ-H2AX, and anti-pAKT. A portion of the input used for IP was reserved and blotted. Anti-pAKT was detected in the lysate but not in the immunoprecipitated samples.

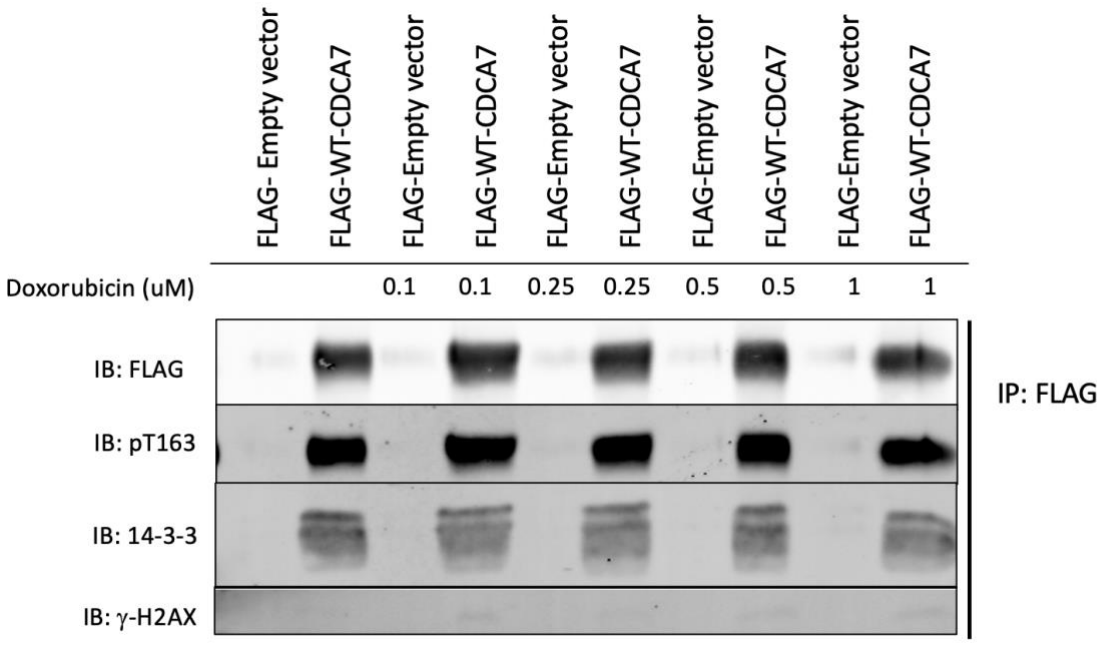

Figure 3.17. No difference detected between various doses of doxorubicin on CDCA7 interactions with DNA damage biomarker γ-H2AX in HEK293Ta cells. Water was used as a vehicle control where doxorubicin was not added. Doxorubicin was added to HEK293T cells transfected with FLAG tagged WT-CDCA7 or FLAG tagged Empty Vector. Doxorubicin at concentrations of 0.1 uM, 0.25 uM, 0.5 uM, and 1 uM were added to samples 24 hours before harvest. Cells were lysed, sonicated, and immunoprecipitated with FLAG beads. Samples were western blotted for anti-FLAG, anti-pT163, anti-14-3-3, and anti-γ-H2AX. Membrane was blotted for anti-Ku80 however none was successfully detected.

Chapter 4: Discussion, Future Directions, and Conclusion

Discussion.

CDCA7 is a transcription factor protein that plays a role in facilitating methylation, NHEJ repair of DNA damage, apoptosis, cell proliferation, and cell cycle processes. It is overexpressed in numerous cancers and plays a part in neoplastic growth. MYC, an important tumour suppressor, requires interaction with CDCA7 for apoptosis to occur under stress. This CDCA7-Myc interaction is regulated by Akt phosphorylation and 14-3-3 binding (Gill et al., 2013). Understanding the critical regions of CDCA7 for interaction of various proteins with CDCA7 within the cell may shed light on its oncogenic properties and its function. This study focused on identifying the critical regions of CDCA7 through immunoprecipitation experiments.

Various candidates for interaction with CDCA7 are reported in the literature (Unoki et al., 2019). HELLS, helicase lymphoid specific, was determined as a high interactor with CDCA7, and are both implicated in causing ICF syndrome (Unoki et al., 2019; Jenness et al., 2018). Using truncation mutations and immunoprecipitation experiments, the region of interaction with HELLS was mapped to amino acids 112-137 on CDCA7. This was interesting since analysis of this region contains a putative leucine zipper domain (Figure 3.5) (Osthus et al. 2005). The 4 leucine residues of Leucine-115, Isoleucine-122, Leucine-129, and Leucine-136 all perfectly space 7 amino acids apart are predicted in Pymol to form a coiled coil motif and together conform to the classical Leucine Zipper consensus sequence (Figure 3.5). As well, it is interesting to note that in clinical examples of ICF syndrome 3, the ICF3 (CDCA7) familial mutations recorded are within the C-terminal Zinc Finger DNA binding region and *not* yet found within the putative N-terminal Leucine Zipper domain. This theoretically could be due to a

mechanism where the Leucine Zipper region is necessary for binding and recruitment of HELLS, but the R274H and other ICF mutations (Thijssen et al., 2015) are necessary for the bipartite nucleosome remodeling activity HELLS and CDCA7 perform to allow for methylation by DNMT3b. Alternatively, since ICF3 a very rare syndrome, and only a limited number of cases have undergone genetic analysis for the involvement of CDCA7, my work suggests that homozygous mutations of the *cdca7* allele in ICF3 patients may uncover mutations within the Lz region. This work potentially provides insight into epigenetic control of methylation by DNMT3 proteins, the necessity of complex DNA binding procedures and recruitment of necessary proteins, and how such pathologies such as ICF and cancers occur when this process is disrupted.

The study of epigenetics in the context of cancer is one method researchers are pursuing in the quest of potential treatment. Methylation and phosphorylation are two types of epigenetic post translational modifications that are either directly or indirectly experienced or caused by various proteins. Inhibition of methylation via DNA methyltransferases and PKI's (Protein Kinase Inhibitors) have been demonstrated by the literature to be a promising approach for cancer therapy. While CDCA7 is shown to be mutated and therefore inhibited in ICF syndrome resulting in hypomethylation of critical satellite repeats resulting in instability of chromosomes. Investigating this pathology may not only allow for therapeutic benefits for pathologies and cancers caused by hypomethylation but may also uncover a method of therapeutic benefit for other pathologies such as cancers of the colon, ovaries, etc. where there is hypermethylation and overstimulation of the PI3K pathway as evidenced by overstimulation of downstream targets such as AKT (Giri et al., 2019). Additionally, the main hindrance of current DDR-associated therapies is tumor resistance mediated by compensatory survival signaling after DNA damage, permitting cancer cells to escape cell death (Alemi et al., 2022).

AKT, a kinase involved in many cell signaling processes such as apoptosis and cell cycle arrest, has been shown be directly involved in DNA damage repair. DNA damage-induced AKT activation mechanisms remain to be fully understood. DNA-PK (DNA-protein kinase) and other PIKKs, such as ATM and ATR, critical for DNA damage repair, also promote activation of the kinase AKT, a critical mediator of cell survival under stress conditions. In cancer cells, DNA DSBs induced by radiation and chemotherapeutic drugs, such as topoisomerase inhibitors such as doxorubicin, mainly induce DNA-PK–dependent phosphorylation of AKT, activating downstream targets involved in DNA damage repair. This provides cancer cells with an increased ability to repair DSBs and escape cell death. Thus, an extensive understanding of AKT activation mechanisms and the identification of target proteins, such as CDCA7, are pivotal to the success of future cancer therapies.

AKT phosphorylates CDCA7 in the nucleus and causes the sequestration of CDCA7 by 14-3-3 to the cytoplasm, regulating its location and capabilities in the cell (Gill et al., 2013). In this study, I showed how Ku and γ-H2AX, DNA damage response proteins, interaction with CDCA7 is regulated by 14-3-3. I have not shown here that when AKT was prevented from phosphorylating CDCA7, the interaction with Ku/γ-H2AX is altered. A future experiment could test this by either pharmacological inhibition of AKT, or mRNA knockdown. This is interesting since the ku80/ku70 complex is critical for the stabilization of exposed double stranded DNA broken ends to allow for repair by the NHEJ (Non-homologous end-joining pathway), and it facilitates the accumulation of phosphorylation of histone 2 AX (γ-H2AX) foci, and these foci are direct 1:1 indicators of DNA damage (Kinashi et al., 2011). This interaction of NHEJ protein Ku80 and DNA damage marker with CDCA7 thus could be regulated by phosphorylation of

AKT, promoting 14-3-3 binding, and provide a potential connection between AKT and the DNA damage response.

Consequently, the dysregulation of CDCA7 is thought to play a significant role in the manifestation of various phenotypes, such as the ICF3 phenotypes characterized by multiradial chromosomal configurations resulting from genomic instability, as well as the development of diverse types of cancers. A fascinating observation is the connection between the involvement of repair proteins in the non-homologous end joining (NHEJ) pathway and V(D)J recombination during immune cell development, particularly in the processing of heavy chains critical for B cell maturation (Blanco-Betancourt et al., 2004; Dai et al., 2003).

Consistently observed in both ICF3 (CDCA7 mutant) and ICF4 (HELLS mutant) patients is a phenotype associated with agammaglobulinemia, where naive B cells are present, but memory and gut plasma cells are absent (Blanco-Betancourt et al., 2004). It is plausible that this phenotype arises due to the misregulation of CDCA7 and HELLS, as they are involved in NHEJ processes. The mutation of CDCA7 potentially leads to NHEJ dysfunction, resulting in the deficiency of mature B cells, as manifested in individuals with ICF syndrome.

Additionally, it is possible that the consensus phosphorylation site of T163, even though it is a known AKT target, could also be targeted by other AGC kinases that are present in a complex. For example, Pariel et al. showed that Aurora B kinase may phosphorylate CDCA7 and regulates its role in providing mitotic spindle activity and stability, and it is also shown to be highly poly(ADP-ribosyl)ated in response to DNA damage, inhibiting its intrinsic kinase function (Monaco et al., 2005; Pariel et al., 2018). Furthermore, it is possible that phosphorylation of CDCA7 by AKT or another AGC kinase could regulate Ku/γ-H2AX

association, while HELLS is only dependent on the presence of the Leucine Zipper region. This shows the different ways CDCA7 could be the hypothetical target of multiple possible kinases.

Several caveats need to be addressed regarding this study's findings on the relationship between CDCA7 and HELLS. Although the immunoprecipitation experiments demonstrated a clear interaction between HELLS and CDCA7, it is important to note that these experiments relied on the detection of an overexpression of FLAG epitope tagged CDCA7 and HA epitope tagged HELLS through immunoblotting. Consequently, the detection of CDCA7 and HELLS was only indirect, achieved via immunoprecipitation. Moreover, it is crucial to acknowledge that co-immunoprecipitation alone does not provide conclusive evidence of direct binding; it merely suggests that CDCA7 and HELLS may potentially be present together in a complex. Therefore, caution should be exercised in interpreting the results as definitive proof of a direct binding interaction between CDCA7 and HELLS. Furthermore, an enhanced presentation of these findings would include a control group of exclusively agarose beads, serving as a baseline to account for potential background binding with the beads.

Since the Lz is necessary for precipitation of HELLS with CDCA7, this could mean that the Lz potentially interacts with Lz within HELLS to promote heterodimerization, however HELLS does not contain an apparent Lz motif (L-X6-L) motif. Another possibility is that HELLS only interacts with CDCA7 when CDCA7 as a dimer, and the Lz is necessary for CDCA7 to homodimerize. However, this is unlikely since Gabor et al. showed that deletion of amino acids 112-137 does not disrupt CDCA7-CDCA7 association by co-expressing HA-CDCA7 with FLAG-delta (112-137), and showed their precipitation was equivalent to wildtype with wildtype. Thus, at present, we do not know how CDCA7 and HELLS interact, and even if it is direct interaction (Gabor et al., 2018).

Future Directions.

Future experiments would investigate direct interaction between endogenous proteins. These experiments would include demonstrating endogenous proteins interact by in vitro association studies such as purified GST-CDCA7 precipitating recombinant purified HELLS. To further investigate the interaction of CDCA7 and HELLS, a cell line of knockout CDCA7 or delta112-137-CDCA7 could be generated in mouse embryonic fibroblasts. Transiently co-expressing HELLS or staining for endogenous Ku80 or γ-H2AX should show an affect on interaction with CDCA7 by precipitation.

The doxorubicin experiments showed no significant effect on CDCA7 and associated proteins. Since doxorubicin has the capacity to stop the cell cycle since it is a topoisomerase inhibitor preventing DNA replication, it is possible there is no affect due to cell proliferation being halted. Additionally, it may due to the nature of HEK293Ta cells requiring a significantly higher or lower dose, and the growth assay and the immunopreciptiation assay varying components such as varying in numbers of cells seeded, the number of days after seeding doxorubicin was added, and the time of doxorubicin incubation. These results generated could be due to a flaw in the experiment design or perhaps there is no significant effect on CDCA7 by doxorubicin to be determined.

Future experiments would require several improvements in the protocol on utilizing doxorubicin as a DNA damage inducing reagent. These include decreasing the number of cells to allow for space to proliferate in the presence of the DNA damage reagent and increasing the incubation time of the cells in the presence of the DNA damage reagent. Additionally, attempting the experiment in other types of cell lines such as ovarian cancer or breast cancer cell lines would perhaps allow for a more significant affect on Ku80, γ-H2AX and CDCA7 interaction. To

further investigate the functional effect of CDCA7 role in DNA damage, a cell line of knockout CDCA7 or delta112-137-CDCA7 could be generated in a breast cancer cell line or in mouse embryonic fibroblasts and incubating in the presence of doxorubicin. Transiently co expressing HELLS or staining for endogenous Ku80 or γ-H2AX should show an affect on interaction with CDCA7 by immunoprecipitation and high levels of DNA damage when conducting a dose dependent or time dependent experiment.

To explore the possibility of HELLS regulation of DNA damage repair by NHEJ through CDCA7, mutant constructs of CDCA7 with various versions of the Lz could be incorporated. Additionally, to explore the involvement of 14-3-3, the T163A, DE, and KK constructs of CDCA7 could be included to investigate its relationship with Ku80, γ-H2AX, and CDCA7.

Conclusion.

In conclusion, CDCA7 plays a crucial role in maintaining genomic stability by participating in various DNA repair processes and DNA methylation. Its interactions with HELLS, Ku70, Ku80, and γ-H2AX highlight its multifunctional nature in coordinating nucleosome remodeling, DNA damage repair, and support of DNA methylation. The identification of a putative leucine zipper motif for CDCA7's association with HELLS and the regulatory role of phosphorylation-mediated 14-3-3 binding in CDCA7's interactions with Ku70/80 and γ-H2AX further elucidate the intricate mechanisms underlying its functional versatility. Understanding the intricate network of interactions involving CDCA7 provides valuable insights into the pathogenesis of ICF syndrome as well as various cancers and contributes to overall understanding of the maintenance of genome integrity.

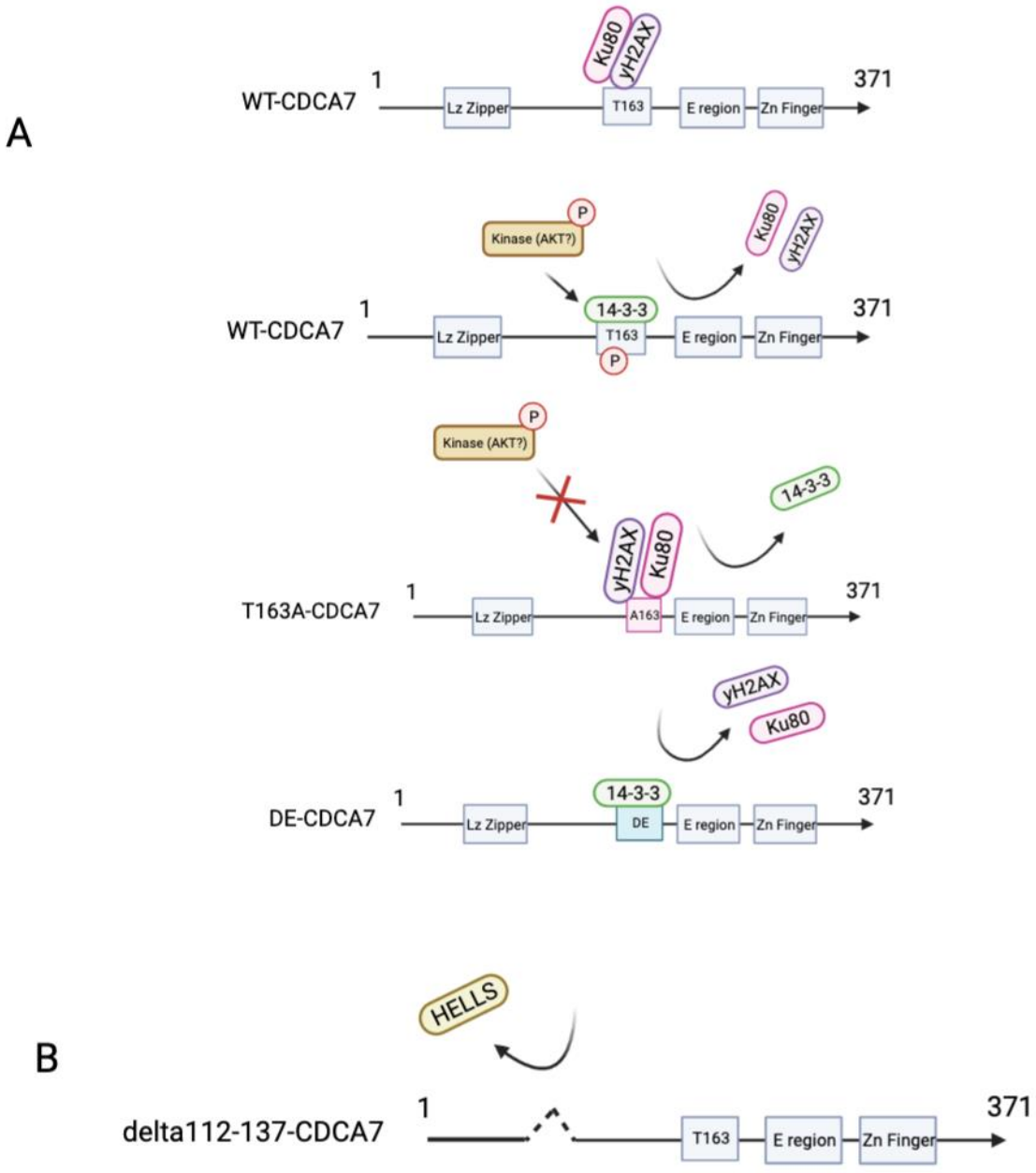

Figure 4.1 A) DNA damage biomarkers Ku80 and yH2AX, and this interaction is regulated by 14-3-3. 14-3-3 binds to the phosphorylated Threonine 163 site of CDCA7. When this phosphorylation is prevented by the mutation of Threonine to Alanine, this causes the interaction of γ-H2AX and ku80 with CDCA7 to be enhanced. **B) CDCA7 interacts with HELLS via the postulated leucine zipper region** HELLS binds to the putative leucine zipper region of CDCA7, amino acids 112-137. When this region is removed, association with HELLS is prevented.

Appendix:

Site Directed Mutagenesis of HELLS Coiled-Coil Region.

I attempted to create HELLS truncation mutations and used Eurofins primer design tool to generate primers. A forward primer F'-GTTATATCATGGAACCCAGGAGG to create an N-terminal stop codon single base pair mutation was designed for Sanger Sequencing to confirm successful mutagenesis. A forward primer F'-GAAAAGGCTCGCATGTCTTGG and reverse primer R'-GGCCGGGGTAATCACAGC were created to delete the amino acids 30-50 within the "coiled coil" region amino acids 30-115 of HELLS. Annealing temperatures were adjusted +/- 5 degrees Celsius of 67 degrees Celsius. However, all attempts to create any mutations despite changing the annealing temperature, timing, etc. were to no avail. The project was subsequently abandoned.

Antibodies.

Table A.1. Antibodies used for Immunostaining during Western blotting.

Primary Antibody	**Concentration**	**Secondary Antibody**	**Concentration**
Anti-Mouse monoclonal Anti-FLAG	1:10,000	800CW	1:10,000
Anti-rabbit Anti-Pt163	1:1000	680LT	1:20,000
		680 RD	1:10,000
Anti-mouse anti-HA	1:1000	800CW	1:10,000
Anti-rabbit Anti-14-3-3	1:1000	680LT	1:20,000
		680 RD	1:10,000
Anti-rabbit anti-γ-H2AX serine 139	1:1000	680LT	1:20,000
		680 RD	1:10,000
Ku80	1:1000	680LT	1:20,000
		680 RD	1:10,000

List of Common Reagents.

All aqueous acids, bases, and alcohols were purchased from the store in Petrie Science and Engineering building at York University.

Table A.2. Common reagents purchased from BioShop Canada.

Name	**Catalog No.**
Ethylenediaminetetraacetic acid (EDTA)	EDT002
Sodium Acetate (NaCH2COOH)	SAA304
Sodium Chloride (NaCl)	SOD004
Sodium Dodecyl Sulfate (SDS)	SDS001
Tris (tris(hydroxymethyl)aminomethane)	TRS001
Tris-hydrochloride (HCl)	TRS004

Table A.3. Common reagents purchased from BioRad.

Name	**Catalog No.**
Ammonium persulfate	1610700
Precision Plus Protein Dual Color Standards, 500 ul	1610374
20x XT MOPS Running Buffer	1610788
10x PBS (Phosphate Buffered Saline)	1610780

References:

Ahnesorg, P., Smith, P., & Jackson, S. P. (2006). XLF interacts with the XRCC4–DNA ligase IV complex to promote nonhomologous end-joining. Cell, 124(2), 301–313. https://doi.org/10.1016/j.cell.2005.12.031

Alemi F, Raei Sadigh A, Malakoti F, Elhaei Y, Ghaffari SH, Maleki M, Asemi Z, Yousefi B, Targhazeh N, Majidinia M. (2022). Molecular mechanisms involved in DNA repair in human cancers: An overview of PI3k/Akt signaling and PIKKs crosstalk. J Cell Physiol 237, 313–328

Alessi, D. R., James, S. R., Downes, C. P., Holmes, A. B., Gaffney, P. R., Reese, C. B., & Cohen, P. (1997). Characterization of a 3-phosphoinositide-dependent protein kinase which phosphorylates and activates protein kinase balpha. Current Biology, 7(4), 261–269. https://doi.org/10.1016/s0960-9822(06)00122-9

Alt, F. W., Zhang, Y., Meng, F. L., Guo, C., & Schwer, B. (2013). Mechanisms of programmed DNA lesions and genomic instability in the immune system. Cell, 152(3), 417–429. https://doi.org/10.1016/j.cell.2013.01.007

Amati, B., Littlewood, T. D., Evan, G. I., & Land, H. (1993). The c-Myc protein induces cell cycle progression and apoptosis through dimerization with Max. The EMBO journal, 12(13), 5083–5087. https://doi.org/10.1002/j.1460-2075.1993.tb06202.x

Aravind, L., & Koonin, E. V. (2001). Prokaryotic homologs of the eukaryotic DNA-end-binding protein Ku, novel domains in the Ku protein and prediction of a prokaryotic double-strand break repair system. Genome research, 11(8), 1365–1374. https://doi.org/10.1101/gr.181001

Arcamone, F., Cassinelli, G., Fantini, G., Grein, A., Orezzi, P., Pol, C., ... Zunino, F. (1969). Adriamycin, 14-hydroxydaunomycin: A new antitumor antibiotic from S. peucetius var. caesius. Biotechnology and Bioengineering, 11, 1101–1110.

Avery, A., Alden, J., Kramish, C., Caballero, C., Wright-Void, C., & Bruner, E. T. (2022). The pathologic diagnosis of carcinoma in various tissues. *Advances in cancer research*, *154*, 1–14. https://doi.org/10.1016/bs.acr.2022.03.001

Bae, H., Viennet, T., Park, E., Chu, N., Salguero, A., Eck, M. J., Arthanari, H., & Cole, P. A. (2022). PH domain-mediated autoinhibition and oncogenic activation of Akt. *eLife*, *11*, e80148. https://doi.org/10.7554/eLife.80148

Ballone, A., Centorrino, F., & Ottmann, C. (2018). 14-3-3: A case study in PPI modulation. Molecules, 23, 1386.

Barletta, J.A., (2014). Surgical Pathology of Carcinomas, Pathobiology of Human Disease, Academic Press, 3526-3545, 9780123864574,

Bassing, C. H., Swat, W., & Alt, F. W. (2002). The mechanism and regulation of chromosomal V(D)J recombination. Cell, 109(2), S45-S55. https://doi.org/10.1016/S0092-8674(02)00675-X

Baxevanis, A. D., and Landsman, D. (1996) Histone Sequence Database: A Compilation of Highly-Conserved Nucleoprotein Sequences. Nucleic Acids Res. 24, 245–247

Bebenek, K., Pedersen, L. C., & Kunkel, T. A. (2014). Structure-function studies of DNA polymerase lambda. Biochemistry, 53, 2781-2792.

Bezler, M., Hengstler, J. G., & Ullrich, A. (2012). Inhibition of doxorubicin-induced HER3-PI3K-AKT signalling enhances apoptosis of ovarian cancer cells. *Molecular oncology*, *6*(5), 516–529. https://doi.org/10.1016/j.molonc.2012.07.001

Blanco-Betancourt, C. E., Moncla, A., Milili, M., Jiang, Y. L., Viegas-Péquignot, E. M., Roquelaure, B., Thuret, I., & Schiff, C. (2004). Defective B-cell-negative selection and terminal differentiation in the ICF syndrome. Blood, 103(7), 2683–2690. https://doi.org/10.1182/blood-2003-08-2632

Blier, P. R., Griffith, A. J., Craft, J., & Hardin, J. A. (1993). Binding of Ku protein to DNA. Measurement of affinity for ends and demonstration of binding to nicks. Journal of Biological Chemistry, 268, 7594–7601.

Bosma, M. J., & Carroll, A. M. (1991). The SCID Mouse Mutant: Definition, Characterization, and Potential Uses. Annual Review of Immunology, 9(1), 323-350.

Brouwer I et al. (2016). Sliding sleeves of XRCC4–XLF bridge DNA and connect fragments of broken DNA. Nature 535, 566–569

Burrage, J., Termanis, A., Geissner, A., Myant, K., Gordon, K., & Stancheva, I. (2012). The SNF2 family ATPase LSH promotes phosphorylation of H2AX and efficient repair of DNA double-strand breaks in mammalian cells. Journal of Cell Science, 125(Pt 22), 5524–5534.

E.M. Blackwood, R.N. Eisenman. (1991). Max: A Helix-Loop-Helix Zipper Protein That Forms a Sequence-Specific DNA-Binding Complex with Myc. *Science*, 251 pp. 1211-1217

Cai, C., Peng, X., & Zhang, Y. (2021). Downregulation of cell division cycle-associated protein 7 (CDCA7) suppresses cell proliferation, arrests cell cycle of ovarian cancer, and restrains angiogenesis by modulating enhancer of zeste homolog 2 (EZH2) expression. *Bioengineered*, *12*(1), 7007–7019. https://doi.org/10.1080/21655979.2021.1965441

Carriaga, M. T., & Henson, D. E. (1995). The histologic grading of cancer. Cancer, 75(1 Suppl), 406–421.https://doi.org/10.1002/1097-0142(19950101)75:1+<406::aid-cncr2820751322>3.0.co;2-w

Chang, H. H. Y., Pannunzio, N. R., Adachi, N., & Lieber, M. R. (2017). Non-homologous DNA end joining and alternative pathways to double-strand break repair. Nature reviews. Molecular cell biology, 18(8), 495–506. https://doi.org/10.1038/nrm.2017.48

Chaudhri, M., Scarabel, M., & Aitken, A. (2003). Mammalian and yeast 14-3-3 isoforms form distinct patterns of dimers in vivo. Biochemical and Biophysical Research Communications, 300, 679-685.

Chen, F., Peterson, S. R., Story, M. D., & Chen, D. J. (1996). Disruption of DNA-PK in Ku80 mutant xrs-6 and the implications in DNA double-strand break repair. Mutation Research, 362(1), 9-19. https://doi.org/10.1016/0921-8777(95)00026-7

Coblitz, B., Wu, M., Shikano, S., & Li, M. (2006). C-terminal binding: An expanded repertoire and function of 14-3-3 proteins. FEBS Letters, 580, 1531-1535.

Coller, H. A., Grandori, C., Tamayo, P., Colbert, T., Lander, E. S., Eisenman, R. N., & Golub, T. R. (2000). Expression analysis with oligonucleotide microarrays reveals that MYC regulates genes involved in growth, cell cycle, signaling, and adhesion. Proceedings of the National Academy of Sciences of the United States of America, 97(7), 3260–3265. https://doi.org/10.1073/pnas.97.7.3260

Compere, S. J., & Palmiter, R. D. (1981). DNA methylation controls the inducibility of the mouse metallothionein-I gene lymphoid cells. Cell, 25(1), 233–240. https://doi.org/10.1016/0092-8674(81)90248-8m

Dai, Y., Kysela, B., Hanakahi, L. A., Manolis, K., Riballo, E., Stumm, M., & Jeggo, P. A. (2003). Nonhomologous end joining and V(D)J recombination require an additional factor. Proceedings of the National Academy of Sciences of the United States of America, 100, 2462-2467.

Dang C. V. (2012). MYC on the path to cancer. Cell, 149(1), 22–35. https://doi.org/10.1016/j.cell.2012.03.003

de Greef, J. C., Wang, J., Balog, J., den Dunnen, J. T., Frants, R. R., Straasheijm, K. R., Aytekin, C., van der Burg, M., Duprez, L., Ferster, A., Gennery, A. R., Gimelli, G., Reisli, I., Schuetz, C., Schulz, A., Smeets, D. F. C. M., Sznajer, Y., Wijmenga, C., van Eggermond, M. C., van Ostaijen-Ten Dam, M. M., … van der Maarel, S. M. (2011). Mutations in ZBTB24 are associated with immunodeficiency, centromeric instability, and facial anomalies syndrome type 2. American journal of human genetics, 88(6), 796–804. https://doi.org/10.1016/j.ajhg.2011.04.018

Dennis, K., Fan, T., Geiman, T.M., Yan, Q.S., Muegge, K. (2001). Lsh, a member of the SNF2 family, is required for genome wide methylation. Genes Dev. *15*, 2940–2944

Deriano, L., Chaumeil, J., Coussens, M., Multani, A., Chou, Y., Alekseyenko, A., ... & Roth, D. B. (2011). The RAG2 C terminus suppresses genomic instability and lymphomagenesis. Nature, 471(7336), 119-123..

Ehrlich, M., Jackson, K., Weemaes, C. (2006). Immunodeficiency, centromeric region instability, facial anomalies syndrome (ICF). Orphanet J. Rare Dis. 1, 2.

Fan, T., Schmidtmann, A., Xi, S., et al. (2003). Lsh-deficient murine embryonal fibroblasts show reduced proliferation with signs of abnormal mitosis. Cancer Res, 63(15), 4677-4683.

Ferreira, A. *et al*. (2017). Altered mitochondrial epigenetics associated with subchronic Doxorubicin cardiotoxicity. *Toxicology* **390**, 63–73, https://doi.org/10.1016/j.tox.2017.08.011

Fu, H., Subramanian, R. R., & Masters, S. C. (2000). 14-3-3 proteins: Structure, function, and regulation. Annual Review of Pharmacology and Toxicology, 40, 617-647.

Furnari, B., Rhind, N., & Russell, P. (1997). CDC25 mitotic inducer targeted by Chk1 DNA damage checkpoint kinase. Science, 277, 1495-1497.

Galy, V., Olivo-Marin, J. C., Scherthan, H., Doye, V., Rascalou, N., & Nehrbass, U. (2000). Nuclear pore complexes in the organization of silent telomeric chromatin. Nature, 403, 108-112.

Gao, T., Furnari, F., & Newton, A. C. (2005). PHLPP: A phosphatase that directly dephosphorylates Akt, promotes apoptosis, and suppresses tumor growth. Molecular Cell, 18, 13-24. https://doi.org/10.1016/j.molcel.2005.03.008

Geiman, T. M., Tessarollo, L., Anver, M. R., Kopp, J. B., Ward, J. M., & Muegge, K. (2001). Lsh, a SNF2 family member, is required for normal murine development. Biochimica et Biophysica Acta, 1526(2), 211-220.

Gilbertson, R. J. (2011). Mapping cancer origins. Cell, 145(1), 25-29. doi: 10.1016/j.cell.2011.03.019

Gill, R.M., Gabor, T.V., Couzens, A.L., Scheid, M.P. (2013). The MYC-associated protein CDCA7 is phosphorylated by AKT to regulate MYC-dependent apoptosis and transformation. Mol Cell Biol. *33*, 498–513.

Giri AK, Aittokallio T. (2019). DNMT Inhibitors Increase Methylation in the Cancer Genome. Front Pharmacol. Apr 24;10:385. doi: 10.3389/fphar.2019.00385. PMID: 31068808; PMCID: PMC6491738.

Gottlieb, T. M., & Jackson, S. P. (1993). The DNA-dependent protein kinase: Requirement for DNA ends and association with Ku antigen. Cell, 72, 131-142.

Hemmings, B.A., Restuccia, D.F. (2012). PI3K-PKB/Akt pathway. Cold Spring Harb Perspect Biol. *4(9)*, a011189. https://doi.org/10.1101/cshperspect.a011189

Hornbeck, P. V., Zhang, B., Murray, B., Kornhauser, J. M., Latham, V., & Skrzypek, E. (2015). PhosphoSitePlus, 2014: Mutations, PTMs and recalibrations. Nucleic Acids Research, 43, D512-D520. https://doi.org/10.1093/nar/gku1267

Hsu, H. L., Gilley, D., Blackburn, E. H., & Chen, D. J. (1999). Ku is associated with the telomere in mammals. Proceedings of the National Academy of Sciences, 96, 12454-12458.

Jenness, C., Giunta, S., Müller, M. M., Kimura, H., Muir, T. W., Funabiki, H. (2018). HELLS and CDCA7 comprise a bipartite nucleosome remodeling complex defective in ICF syndrome. Proc. Natl. Acad. Sci. U.S.A. *115*(5), E876–E885. doi:10.1073/pnas.1717509115

Jiang, Y. L., et al. (2005). DNMT3B mutations and DNA methylation defect define two types of ICF syndrome. Human Mutation, 25(1), 56-63. https://doi.org/10.1002/humu.20113

Kim, S., et al. (2006). Doxorubicin-induced reactive oxygen species generation and intracellular Ca2+ increase are reciprocally modulated in rat cardiomyocytes. Experimental and Molecular Medicine, 38, 535-545. https://doi.org/10.1038/emm.2006.63

Kim, T. J., Lee, J. W., Song, S. Y., Choi, J. J., Choi, C. H., Kim, B. G., Lee, J. H., & Bae, D. S. (2006). Increased expression of pAKT is associated with radiation resistance in cervical cancer. British Journal of Cancer, 94, 1678-1682.

Kinashi, Y., Takahashi, S., Kashino, G., Okayasu, R., Masunaga, S., Suzuki, M., & Ono, K. (2011). DNA double-strand break induction in Ku80-deficient CHO cells following boron neutron capture reaction. *Radiation oncology (London, England)*, *6*, 106. https://doi.org/10.1186/1748-717X-6-106

Kinner, A., Wu, W., Staudt, C., & Iliakis, G. (2008). Gamma-H2AX in recognition and signaling of DNA double-strand breaks in the context of chromatin. Nucleic acids research, 36(17), 5678–5694. https://doi.org/10.1093/nar/gkn550

Kloet, D. E., Polderman, P. E., Eijkelenboom, A., et al. (2015). FOXO target gene CTDSP2 regulates cell cycle progression through Ras and p21(Cip1/Waf1). Biochemical Journal, 469, 289-298.

Khanna, K. K. & Jackson, S. P. (2001). DNA double-strand breaks: signalling, repair and the cancer connection. Nature Genet. 27, 247–254

Knuefermann, C., Lu, Y., Liu, B., Jin, W., Liang, K., Wu, L., Schmidt, M., Mills, G. B., Mendelsohn, J., & Fan, Z. (2003). HER2/PI-3K/Akt activation leads to a multidrug resistance in human breast adenocarcinoma cells. Oncogene, 22(21), 3205–3212. https://doi.org/10.1038/sj.onc.1206394

Kollárovič, G., Topping, C. E., Shaw, E. P., & Chambers, A. L. (2020). The human HELLS chromatin remodelling protein promotes end resection to facilitate homologous recombination and contributes to DSB repair within heterochromatin. Nucleic acids research, 48(4), 1872–1885. https://doi.org/10.1093/nar/gkz1146

Krylov, D., Vinson, C.R. (2001). Leucine Zipper. In eLS, (Ed.). https://doi.org/10.1038/npg.els.0003001

Kumar V, Alt FW, Oksenych V. Functional overlaps between XLF and the ATM-dependent DNA double strand break response. DNA Repair (Amst). 2014; 16: 11- 22.

Kuo, Y. C., Huang, K. Y., Yang, C. H., Yang, Y. S., Lee, W. Y., & Chiang, C. W. (2008). Regulation of phosphorylation of Thr-308 of Akt, cell proliferation, and survival by the B55α regulatory subunit targeting of the protein phosphatase 2A holoenzyme to Akt. The Journal of Biological Chemistry, 283, 1882-1892. https://doi.org/10.1074/jbc.M709585200

Kurz, E. U., Douglas, P., & Lees-Miller, S. P. (2004). Doxorubicin activates ATM-dependent

phosphorylation of multiple downstream targets in part through the generation of reactive oxygen species. The Journal of biological chemistry, 279(51), 53272–53281. https://doi.org/10.1074/jbc.M406879200

Laity, J. L., Lee, B. M., & Wright, P. E. (2001). Zinc finger proteins: New insights into structural and functional diversity. Current Opinion in Structural Biology, 11(1), 39–46. https://citeseerx.ist.psu.edu/document?repid=rep1&type=pdf&doi=33a262a7186e1c17ce2bf2bced02ed39fa251ec3

Lakshminarasimhan, R., & Liang, G. (2016). The Role of DNA Methylation in Cancer. Advances in experimental medicine and biology, 945, 151–172. https://doi.org/10.1007/978-3-319-43624-1_7

Li, Q., Li, Z., Luo, T., & Shi, H. (2022). Targeting the PI3K/AKT/mTOR and RAF/MEK/ERK pathways for cancer therapy. *Molecular biomedicine*, *3*(1), 47. https://doi.org/10.1186/s43556-022-00110-2

Li, X., Lu, Y., Liang, K. et al. (2005). Differential responses to doxorubicin-induced phosphorylation and activation of Akt in human breast cancer cells. Breast Cancer Res 7, R589. https://doi.org/10.1186/bcr1259

Liang, J., Slingerland, J. (2003) Multiple Roles of the PI3K/PKB (Akt) Pathway in Cell Cycle Progression, Cell Cycle, 2:4, 336-342, DOI: 10.4161/cc.2.4.433

Lieber, M. R. (2016). Mechanisms of human lymphoid chromosomal translocations. Nature Reviews Cancer, 16, 387-398. https://doi.org/10.1038/nrc.2016.47

Lieber, M. R. (2010). The mechanism of double-strand DNA break repair by the nonhomologous DNA end-joining pathway. Annual Review of Biochemistry, 79, 181-211. https://doi.org/10.1146/annurev.biochem.052308.093131

Lindahl, T., & Barnes, D. E. (2000). Repair of endogenous DNA damage. Cold Spring Harbor Symposia on Quantitative Biology, 65, 127-134.

Liu, J., Cao, S., Ding, G., Wang, B., Li, Y., Zhao, Y., ... & Xiao, Y. (2021). The role of 14-3-3 proteins in cell signalling pathways and virus infection. Journal of Cellular and Molecular Medicine, 25(9), 4173-4182. https://doi.org/10.1111/jcmm.16490

Lopes, M. A., Meisel, A., Dirnagl, U., Carvalho, F. D., & Bastos, M. L. (2008). Doxorubicin induces biphasic neurotoxicity to rat cortical neurons. Neurotoxicology, 29(2), 286-293. https://doi.org/10.1016/j.neuro.2007.12.003

Ma, Y., Pannicke, U., Schwarz, K., & Lieber, M. R. (2002). Hairpin opening and overhang processing by an Artemis/DNA-dependent protein kinase complex in nonhomologous end joining and V(D)J recombination. Cell, 108, 781-794.

Ma Y et al. (2004). A biochemically defined system for mammalian nonhomologous DNA end joining. Mol. Cell 16, 701–713

Malone, E. R., Oliva, M., Sabatini, P. J. B., et al. (2020). Molecular profiling for precision cancer therapies. Genome Medicine, 12, 8. https://doi.org/10.1186/s13073-019-0703-1

Manning BD, Toker A. (2017). AKT/PKB signaling: navigating the network. Cell.;169:381–405. doi: 10.1016/j.cell.2017.04.001.

Maraschio, P., Zuffardi, O., Dalla Fior, T., & Tiepolo, L. (1988). Immunodeficiency, centromeric heterochromatin instability of chromosomes 1, 9, and 16, and facial anomalies: the ICF syndrome. Journal of Medical Genetics, 25(3), 173-180. https://doi.org/10.1136/jmg.25.3.173

Mattiuzzi, C., & Lippi, G. (2019). Current Cancer Epidemiology. Journal of epidemiology and global health, 9(4), 217–222. https://doi.org/10.2991/jegh.k.191008.001

Monaco, L., Kolthur-Seetharam, U., Loury, R., Murcia, J. M., de Murcia, G., & Sassone-Corsi, P. (2005). Inhibition of Aurora-B kinase activity by poly(ADP-ribosyl)ation in response to DNA damage. Proceedings of the National Academy of Sciences of the United States of America, 102(40), 14244–14248. https://doi.org/10.1073/pnas.0506252102

Milburn, C. C., Deak, M., Kelly, S. M., Price, N. C., Alessi, D. R., & Van Aalten, D. M. F. (2003). Binding of phosphatidylinositol 3,4,5-trisphosphate to the pleckstrin homology domain of protein kinase B induces a conformational change. The Biochemical Journal, 375, 531-538. https://doi.org/10.1042/BJ20031229

Mishra K, Shore D. (1999). Yeast Ku protein plays a direct role in telomeric silencing and counteracts inhibition by rif proteins. Curr Biol. 9:1123–1126.

Miwa, S., Yamamoto, N., & Tsuchiya, H. (2023). Sarcoma: Molecular Pathology, Diagnostics, and Therapeutics. International Journal of Molecular Sciences, 24(6), 5833. https://doi.org/10.3390/ijms24065833

Mobadersany, P., Yousefi, S., Amgad, M., Gutman, D. A., Barnholtz-Sloan, J. S., Velázquez Vega, J. E., Brat, D. J., & Cooper, L. A. D. (2018). Predicting cancer outcomes from histology and genomics using convolutional networks. Proceedings of the National Academy of Sciences of the United States of America, 115(13), E2970-E2979. https://doi.org/10.1073/pnas.1717139115

Moshous, D., Callebaut, I., de Chasseval, R., Corneo, B., Cavazzana-Calvo, M., Le Deist, F., ... & Fischer, A. (2001). Artemis, a novel DNA double-strand break repair/V(D)J recombination protein, is mutated in human severe combined immune deficiency. Cell, 105, 177-186. https://doi.org/10.1016/S0092-8674(01)00309-9

Moon, A. F., Pryor, J. M., Ramsden, D. A., Kunkel, T. A., & Bebenek, K. (2014). Sustained active site rigidity during synthesis by human DNA polymerase μ. Nature Structural & Molecular Biology, 21, 253-260. https://doi.org/10.1038/nsmb.2785

Moore, L. D., Le, T., & Fan, G. (2013). DNA methylation and its basic function. Neuropsychopharmacology : official publication of the American College of Neuropsychopharmacology, 38(1), 23–38. https://doi.org/10.1038/npp.2012.112

Nussenzweig, A., Chen, C., da Costa Soares, V., Sanchez, M., Sokol, K., Nussenzweig, M. C., & Li, G. C. (1996). Requirement for Ku80 in growth and immunoglobulin V(D)J recombination. *Nature*, *382*(6591), 551–555. https://doi.org/10.1038/382551a0

Ochi, T., Blackford, A. N., Coates, J., Jhujh, S., Mehmood, S., Tamura, N., ... & Niedzwiedz, W. (2015). DNA repair. PAXX, a paralog of XRCC4 and XLF, interacts with Ku to promote DNA double-strand break repair. Science, 347, 185-188. https://doi.org/10.1126/science.1261971

Okano, M., Bell, D. W., Haber, D. A., & Li, E. (1999). DNA methyltransferases Dnmt3a and Dnmt3b are essential for de novo methylation and mammalian development. Cell, 98(2), 247-257.

O'Neil, K. T., Hoess, R. H., & DeGrado, W. F. (1990). Design of DNA-binding peptides based on the leucine zipper motif. Science (New York, N.Y.), 249(4970), 774–778. https://doi.org/10.1126/science.2389143

Osthus, R. C., Karim, B., Prescott, J. E., Smith, B. D., McDevitt, M., Huso, D. L., & Dang, C. V. (2005). The Myc target gene JPO1/CDCA7 is frequently overexpressed in human tumors and has limited transforming activity in vivo. *Cancer research*, *65*(13), 5620–5627. https://doi.org/10.1158/0008-5472.CAN-05-0536

Pang, B., X. Qiao, L. Janssen, A. Velds, T. Groothuis, R. Kerkhoven, M. Nieuwland, H. Ovaa, S. Rottenberg, O. van Tellingen, J. Janssen, P. Huijgens, W. Zwart, J. Neefjes. (2013). Drug-induced histone eviction from open chromatin contributes to the chemotherapeutic effects of doxorubicin. Nat. Commun., 4 p. 1908

Pariel, S. (2018). Novel interaction, regulation of phosphorylation and mitotic localization of cell division cycle associated protein 7 (CDCA7) (dissertation). Toronto, Ontario. Retrieved from http://hdl.handle.net/10315/35017.

Peterson, C. L., & Laniel, M. A. (2004). Histones and histone modifications. *Current biology : CB*, *14*(14), R546–R551. https://doi.org/10.1016/j.cub.2004.07.007

Pilch, D. R., Sedelnikova, O. A., Redon, C., Celeste, A., Nussenzweig, A., & Bonner, W. M. (2003). Characteristics of gamma-H2AX foci at DNA double-strand breaks sites. Biochemistry and cell biology = Biochimie et biologie cellulaire, 81(3), 123–129. https://doi.org/10.1139/o03-042

Pommier, Y., Leo, E., Zhang, H., & Marchand, C. (2010). DNA Topoisomerases and Their Poisoning by Anticancer and Antibacterial Drugs. Chemistry & Biology, 17, 421-433. https://doi.org/10.1016/j.chembiol.2010.04.012

Prescott, J.E., Osthus, R.C., Lee, L.A., Lewis, B.C., Shim, H., Barrett, J.F., Guo, Q., Hawkins, A.L., Griffin, C.A., Dang CV. (2001). A novel c-Myc-responsive gene, JPO1, participates in neoplastic transformation. J. Biol. Chem. *276*, 48276–48284

Ramsden, D. A., & Gellert, M. (1998). Ku protein stimulates DNA end joining by mammalian DNA ligases: A direct role for Ku in repair of DNA double-strand breaks. The EMBO Journal, 17, 609-614.

Ren, R., Hardikar, S., Horton, J. R., Lu, Y., Zeng, Y., Singh, A. K., Lin, K., Coletta, L. D., Shen, J., Lin Kong, C. S., Hashimoto, H., Zhang, X., Chen, T., & Cheng, X. (2019). Structural basis of specific DNA binding by the transcription factor ZBTB24. *Nucleic acids research*, *47*(16), 8388–8398. https://doi.org/10.1093/nar/gkz557

Rodriguez, J., Frigola, J., Vendrell, E., Risques, R. A., Fraga, M. F., Morales, C., ... & Esteller, M. (2006). Chromosomal instability correlates with genome-wide DNA demethylation in human primary colorectal cancers. Cancer Research, 66, 8462-8468.

Rogakou, E. P., Pilch, D. R., Orr, A. H., Ivanova, V. S., & Bonner, W. M. (1998). DNA double-stranded breaks induce histone H2AX phosphorylation on serine 139. The Journal of biological chemistry, 273(10), 5858–5868. https://doi.org/10.1074/jbc.273.10.5858

Sagie, S., Toubiana, S., Hartono, S. R., Katzir, H., Tzur-Gilat, A., Havazelet, S., ... & Selig, S. (2017). Telomeres in ICF syndrome cells are vulnerable to DNA damage due to elevated DNA:RNA hybrids. Nature Communications, 8, 14015. https://doi.org/10.1038/ncomms14015

Sharma, S., Kelly, T. K., & Jones, P. A. (2010). Epigenetics in cancer. Carcinogenesis, 31, 27-36. https://doi.org/10.1093/carcin/bgp220

Shen, H., & Laird, P. W. (2013). Interplay between the cancer genome and epigenome. Cell, 153, 38-55. https://doi.org/10.1016/j.cell.2013.03.008

Smeets, D. F., Hamel, B. C., van Oost, B. A., & van den Ouweland, A. M. (1994). ICF syndrome: A new case and review of the literature. Human Genetics, 94(3), 240-246. https://doi.org/10.1007/BF00211062

Stewart, G. S., Wang, B., Bignell, C. R., Taylor, A. M., & Elledge, S. J. (2003). MDC1 is a mediator of the mammalian DNA damage checkpoint. Nature, 421(6926), 961-966. https://doi.org/10.1038/nature01446

Taymaz-Nikerel, H., Karabekmez, M. E., Eraslan, S., et al. (2018). Doxorubicin induces an extensive transcriptional and metabolic rewiring in yeast cells. Scientific Reports, 8, 13672. https://doi.org/10.1038/s41598-018-31939-9

Thijssen, P.E., Ito, Y., Grillo, G., Wang, J., Velasco, G., Nitta, H., Unoki, M., Yoshihara, M., Suyama, M., Sun, Y., Lemmers, R.J., de Greef, J.C., Gennery, A., Picco, P., Kloeckener-Gruissem, B., Güngör, T., Reisli, I., Picard, C., Kebaili, K., Roquelaure, B., Iwai, T., Kondo, I., Kubota, T., van Ostaijen-Ten Dam, M.M., van Tol, M.J., Weemaes, C., Francastel, C., van der Maarel, S.M., Sasaki, H. (2015). Mutations in CDCA7 and HELLS cause immunodeficiency-centromeric instability-facial anomalies syndrome. Nat Commun. *6*, 7870

Toubiana, S., Velasco, G., Chityat, A., Kaindl, A.M., Hershtig, N., Tzur-Gilat, A., Francastel, C., Selig, S. (2018). Subtelomeric methylation distinguishes between subtypes of Immunodeficiency, Centromeric instability and Facial anomalies syndrome. Hum Mol. 27(20), 3568-3581. doi: 10.1093/hmg/ddy265.

Tuck-Muller, C. M., Narayan, A., Tsien, F., Smeets, D. F., Sawyer, J., Fiala, E. S., Sohn, O. S., & Ehrlich, M. (2000). DNA hypomethylation and unusual chromosome instability in cell lines from ICF syndrome patients. Cytogenetics and cell genetics, 89(1-2), 121–128. https://doi.org/10.1159/000015590

Stiff, T., O'Driscoll, M., Rief, N., Iwabuchi, K., Lobrich, M., & Jeggo, P. A. (2004). ATM and DNA-PK function redundantly to phosphorylate H2AX after exposure to ionizing

radiation. Cancer Research, 64, 2390-2396. https://doi.org/10.1158/0008-5472.CAN-03-3207

Tian, Y., Han, W., Fu, L., Lv, K., & Wu, S. (2023). CDCA7 serves as a novel prognostic marker in human hepatocellular carcinoma. Biotechnology & genetic engineering reviews, 1–17. Advance online publication. https://doi.org/10.1080/02648725.2023.2216072

Tomoka, T., Montgomery, N. D., Powers, E., Dhungel, B. M., Morgan, E. A., Mulenga, M., Gopal, S., & Fedoriw, Y. (2018). Lymphoma and Pathology in Sub-Saharan Africa: Current Approaches and Future Directions. Clinical Laboratory Medicine, 38(1), 91-100. https://doi.org/10.1016/j.cll.2017.10.007Tonegawa, S. (1983). Somatic generation of antibody diversity. Nature, 302, 575-581.

Tzivion, G., Dobson, M., & Ramakrishnan, G. (2011). FoxO transcription factors; regulation by AKT and 14-3-3 proteins. Biochimica et Biophysica Acta, 1813, 1938-1945. https://doi.org/10.1016/j.bbamcr.2011.06.002

Unoki, M., Funabiki, H., Velasco, G., Francastel, C., Sasaki, H. (2019) CDCA7 and HELLS mutations undermine nonhomologous end joining in centromeric instability syndrome. J Clin Invest. 129(1):78-92. https://doi.org/10.1172/JCI99751.

Valko, M., Rhodes, C. J., Moncol, J., Izakovic, M., & Mazur, M. (2006). Free radicals, metals and antioxidants in oxidative stress-induced cancer. Chemical Biology & Interactions, 160, 1-40. https://doi.org/10.1016/j.cbi.2005.12.009

Van den Berg, J., et al. (2018). A limited number of double-strand DNA breaks is sufficient to delay cell cycle progression. Nucleic Acids Research, 46(19), 10132-10144. https://doi.org/10.1093/nar/gky786

Wang, Q., Ross, K. E., Huang, H., Ren, J., Li, G., Vijay-Shanker, K., Wu, C. H., & Arighi, C. N. (2017). Analysis of Protein Phosphorylation and Its Functional Impact on Protein-Protein Interactions via Text Mining of the Scientific Literature. Methods in molecular biology (Clifton, N.J.), 1558, 213–232. https://doi.org/10.1007/978-1-4939-6783-4_10

Trakarnphornsombat, W., & Kimura, H. (2023). Live-cell tracking of γ-H2AX kinetics reveals the distinct modes of ATM and DNA-PK in the immediate response to DNA damage. Journal of Cell Science, 136(8), jcs260698. https://doi.org/10.1242/jcs.260698

Whitfield, M.L., Sherlock, G., Saldanha A.J., Murray, J.I., Ball, C.A., Alexander, K.E., Matese, J.C., Perou, C.M., Hurt, M.M., Brown, P.O., Botstein, D. (2002). Identification of genes periodically expressed in the human cell cycle and their expression in tumors. Mol. Cell. Biol. 13(6):1977-2000.

Williams, G., Williams, R. S., & Williams, J. S. (2014). Structural insights into NHEJ: Building up an integrated picture of the dynamic DSB repair super complex, one component and interaction at a time. DNA Repair, 17, 110-120. https://doi.org/10.1016/j.dnarep.2014.01.011

Wilson, A. S., Power, B. E., & Molloy, P. L. (2007). DNA hypomethylation and human diseases. Biochimica et Biophysica Acta, 1775, 138-162. https://doi.org/10.1016/j.bbcan.2006.08.007

Woo, C. G., Son, S. M., Lee, H. C., Han, H. S., Lee, K. H., Kim, D., Kim, E. G., & Lee, O. J. (2022). Histologic Changes in Non-Small Cell Lung Cancer under Various Treatments: A Comparison of Histology and Mutation Status in Serial Samples. Cancer research and treatment, 54(3), 737–743. https://doi.org/10.4143/crt.2021.773

Wu, H., et al. (2016). Converging disease genes in ICF syndrome: ZBTB24 controls expression of

CDCA7 in mammals. Human Molecular Genetics, 25(18), 4041-4051. https://doi.org/10.1093/hmg/ddw243

Xing, M., Yang, M., Huo, W., Feng, F., Wei, L., Jiang, W., ... & Xu, B. (2015). Interactome analysis identifies a new paralogue of XRCC4 in non-homologous end joining DNA repair pathway. Nature Communications, 6, 6233. https://doi.org/10.1038/ncomms7233

Xu, Z., Zan, H., Pone, E. J., Mai, T., & Casali, P. (2012). Immunoglobulin class-switch DNA recombination: induction, targeting and beyond. Nature Reviews Immunology, 12(7), 517-531. https://doi.org/10.1038/nri3216

Yan, C. T., Boboila, C., Souza, E. K., et al. (2007). IgH class switching and translocations use a robust non-classical end-joining pathway. Nature, 449(7161), 478-482. https://doi.org/10.1038/nature06020

Yang, F., Kemp, C. & Henikoff, S. (2013). Doxorubicin Enhances Nucleosome Turnover around Promoters. Current Biology 23, 782–787, https://doi.org/10.1016/j.cub.2013.03.043

Yang, F., Kemp, C. & Henikoff, S. (2015). Anthracyclines induce double-strand DNA breaks at active gene promoters. *Mutation Research-Fundamental and Molecular Mechanisms of Mutagenesis* **773**, 9–15, https://doi.org/10.1016/j.mrfmmm.2015.01.007

Yoshioka, A., Miyata, H., Doki, Y., Yasuda, T., Yamasaki, M., Motoori, M., Okada, K., Matsuyama, J., Makari, Y., Sohma, I., Takiguchi, S., Fujiwara, Y., & Monden, M. (2008). The activation of Akt during preoperative chemotherapy for esophageal cancer correlates with poor prognosis. Oncology Reports, 19, 1099-1107.

Zhu, H., Geiman, T. M., Xi, S., Jiang, Q., Schmidtmann, A., Chen, T., En, Li., Muegge, K. (2006). Lsh is involved in de novo methylation of DNA. Embo J. 25(2), 335–345. doi:10.1038/sj.emboj.7600925